

Investigation For Study Of Complex Chemical Equilibrium Of Combustion Products Gas Mixture

A thesis

Submitted to the College of Engineering of
Al-Nahrain University in partial fulfillment
of the requirements for the degree of
Doctor of Philosophy in Chemical Engineering

by

FAIQ HUSSAM SIRRI

B.Sc. 1997

M.Sc. 2000

Jumada I
June

1425
2004

Certification

We certify that this thesis entitled “Investigation for Study of Complex Chemical Equilibrium of Combustion Products Gas Mixture” was prepared under our supervision at Al-Nahrain University, College of Engineering in partial fulfillment of the requirements for the degree of Doctor of Philosophy in Chemical Engineering.

Signature: *H.S. Majdi*

Supervisor: Dr. **H.S. Majdi**

Date: *7/4/2004*

Signature:

Mahmoud Omar Abdulllah

Supervisor: Prof. **M.O. Abdullah**

Date: *7/4/2004*

Signature:


Prof. Dr. **Qasim J. Sliman**


Head of the Chemical Engineering Department

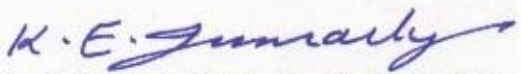
Date: *7/4/2004*

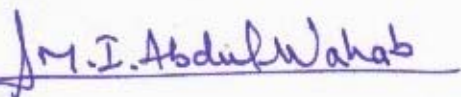
Certificate


We certify that we have read this thesis, entitled “*Investigation for Study of Complex Chemical Equilibrium of Combustion Products Gas Mixture*”, and as Examining Committee examined the student **FAIQ HUSSAM SIRRI** on its content, and that in our opinion it is adequate as a thesis for the degree of Doctor of Philosophy in Chemical Engineering.

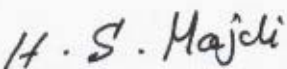
Signature: 
Prof. Dr. **Jabir Shanshool**
(Chairman)
Date: 24/ 7 / 2004


Signature: 
Prof. Dr. **Esam K. Halabia**
(Member)
Date: 24/ 07 / 2004

Signature: 
Assistant Prof. Dr. **khalil E. J. Al-Jumaily**
(Member)
Date: 24/ 7 / 2004

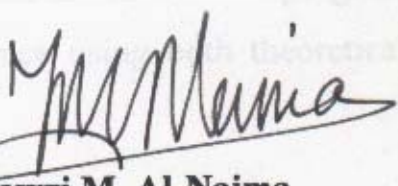
Signature: 
Assistant Prof. Dr. **Majid I. Abdul Wahab**
(Member)
Date: 29/ 7 / 2004

Signature: 
Assistant Prof. Dr. **Neeran K. Ibrahim**
(Member)
Date: 24/ 7 / 2004

Signature: 
Assistant Prof. Dr. **Hasan S. Majdy**
(Member, Supervisor)
Date: 3 / 8 / 2004


Signature:
Prof. Dr. **Mahmoud Omar Abdullah**
(Member, Supervisor)
Date: 24/ 7 / 2004

Approved to the College of Engineering

Signature: 
Prof. Dr. **Fawzi M. Al-Naima**
Dean of the College of Engineering
Date: 18/ 8 / 2004

Abstract

Prediction of equilibrium condition in complex system is very important in process design calculation and other industrial applications. Complex chemical equilibrium usually occurs at severe conditions in which experimental measurements are very difficult. Therefore, in order to obtain accurate theoretical results, attention had been directed to investigate the existing methods, and to modify the most suitable one to give accurate results. This work included both theoretical analysis and experimental work.

In the theoretical analysis, an adequate method for calculating chemical equilibrium in a predominantly gaseous, multi-component reactive mixture was investigated and successfully applied. This method involved the minimization of Gibbs free energy, in which the expected reaction products are stated. First the formation of chemical species, of which concentrations prevail in the mixture, then the formation of the gaseous atomic species by dissociation of previous ones, and finally, the formation of complex chemical species from the atomic species. A computer program, which permits calculation of equilibrium compositions by the Newton-Raphson iteration procedure, and Gauss elimination technique, has been developed. The program contains a data base file, in which the newer thermodynamic properties of reactants and all expected products are listed. The program also calculates theoretical rocket motor performance using both theoretical and recent empirical equations.

An experimental solid propellant rocket motor was designed and subjected to static testing. Two types of propellants, double base propellant and composite propellant, were examined with different compositions for each type. A set of fourteen experiments was successfully conducted (nine experiments using double base propellants, and five using composite propellants).

The Results of the calculations have been compared with those obtained from the experiments and with those published by NASA. The comparison gave satisfactory agreement (Average deviation = 5% for the experiments, and = 4% for NASA). Thus, the program can be used, with confidence, to obtain either complex chemical equilibrium composition and/or rocket motor performance.

Contents

Nomenclature	viii
1. Introduction and Literature Review	1
1.1. Complex Chemical Equilibrium	2
1.2. Background of Previous Studies	4
1.2-1. Previous Studies on Complex Chemical Equilibrium	4
1.2-1-1. Brinkly, S.R., 1947	4
1.2-1-2. White, W.B., et.al., 1958	4
1.2-1-3. Zeleznik and Gordon, 1968	4
1.2-1-4. Van Zeggern and Storey, 1970	5
1.2-1-5. Smith, W.R., 1978, 1980, 1982, 1998	5
1.2-2. Previous Computer Program for Calculation of Complex Chemical Equilibrium	6
1.2-2-1. NASA Computer Program	6
1.2-2-2. STANJAN	6
1.2-2-3. CHEPP	7
1.2-2-4. VTEC	7
1.2-2-5. SCORES	7
1.2-2-6. PHATCAT	8
1.3. Importance and Application of Chemical Equilibrium	8
1.4. The Aim of This Work	11
2. Theoretical Analysis of Chemical Equilibrium in Complex System	13
2.1. Thermodynamic Potential Function and Criteria of Equilibrium	14

2.2. The Element Abundance Equations	15
2.2-1 Equation of State	16
2.3. Thermodynamic Description of a Chemical System	18
2.4. Formulations of the Equilibrium Conditions	20
2.4-1. The Stoichiometric Formulation	21
2.4-2. The Non-Stoichiometric Formulation	22
2.5. The Chemical Potential	23
2.5-1. Pure Species	24
2.5-2. Species in Solution	24
2.6. Methods for Obtaining Standard Free Energy	25
2.6-1. Use of Free Energy of Formation	26
2.6-2. Use of the Free Energy Function	26
2.6-3. Use of Conventional Absolute Entropies	27
2.6-4. Use of Standard Electrode Potentials	28
2.7. Minimization of Gibbs Energy	28
2.8. Minimization of Helmholtz Energy	31
2.9. Thermodynamic Derivatives from Matrix Solution	33
2.9-1. Derivative with Respect to Temperature	34
2.9-2. Derivative with Respect to Pressure	36
2.9-3. Other Thermodynamic Derivatives	37
3. Theoretical Analysis of Solid Rocket Motor	39
3.1. Introduction	40
3.2. Chemical Rocket Motor	40
3.3. Basic Assumptions	42
3.4. Propellants	43
3.4-1. Liquid Propellants	44
3.4-2. Solid Propellants	44

3.4-2-1. Double-Base Propellants	45
3.4-2-2. Composite Propellants	47
3.4-2-3. Composite-Double-Base Propellants	49
3.4-3. Propellant Grain	49
3.4-4. Propellant Combustion	55
3.5. Nozzle Theory	57
3.6. Rocket Motor Thrust and the Thrust Coefficient	66
3.7. Total Impulse	70
3.8. Characteristics Velocity	72
3.9. Specific Impulse	72
3.10. Chamber Pressure	74
3.11. Correction for Actual Rocket Motors	80
3.11-1. Chamber Conditions	80
3.11-2. Nozzle Correlations	81
3.11-3. Corrections for Specific Impulse	83
4. Analysis and Models for Computation of Chemical Equilibrium in Complex Systems	84
4.1 Introduction	85
4.2. Thermodynamic Analysis	85
4.3. Input and Output Data	86
4.4. Gibbs Iteration Equations	88
4.4-1. Reduced Gibbs Iteration Equations	89
4.5. Procedure for Obtaining Equilibrium Compositions	90
4.5-1. Initial Estimates	91
4.5-2. Magnitude of Species Used During Iteration	91
4.5-3. Convergence	93
4.5-4. Tests for Condensed Phases	96

4.5-5. Iteration Procedure and Tests for Ions	97
4.6. Procedure for Obtaining Equilibrium Rocket Performance	98
4.6-1. Combustion Conditions	98
4.6-2. Exit Conditions	98
4.6-3. Throat Conditions	99
4.6-4. Discontinuities at Throat	100
4.6-5. Empirical Formulas for Initial Estimates of P_c/P_e	100
4.6-6. Analytic Expression for Improved Estimates of P_c/P_e	101
4.7. Procedure for Obtaining Frozen Rocket Performance	102
4.7-1. Exit Conditions	103
4.7-2. Throat Conditions	104
4.7-3. Thermodynamic Derivatives for Frozen Composition	104
4.8. Algorithms	105
4.8-1. Algorithm for Chemical Equilibrium Calculations	105
4.8-2. Algorithm for Calculating Rocket Performance	106
5. Experimental Work, Rocket Motor Static Testing	107
5.1. Introduction	108
5.2. Experimental System	108
5.2-1. The Testing Rig	108
5.2-2. The Room of Measuring Apparatus	108
5.3. Determination of Total and Specific Impulse from Test Data	110
5.4. Cases Studied	110
5.4-1. The Test Rocket Motor	110
5.4-2. The Solid Propellant	113
5.5. Preparation of the Experiments	115
5.6. Executing the Experiment	115

6. Results and Discussion	116
6.1. Experimental Results	117
6.2. Combustion Simulation and Motor Performance Prediction	131
6.2-1. Results of Double Base Propellants	131
6.2-2. Results of Composite Propellants	153
6.3. Output Data from Experiment	169
6.4. Comparison Between Experimental and Theoretical Results	170
6.5. Discussion	171
6.6. Conclusion	180
6.7. Recommendation	181
References	182
Appendix A:	(A-1)
Appendix B	(B-1)

Nomenclature

Symbol	Definition	Units
A	Helmholtz function	J/mol K
A_t	Throat area	m^2
A_p	Flow area	m^2
a_s	Velocity of sound	M/s
a	Acceleration	m/s^2
b	Fixed number of moles	
C_f	Thrust coefficient	
c^*	Characteristics velocity	m/s
cp	Heat capacity	J/mol K
D	Grain outer diameter	m
d	Grain inner diameter	m
E	Electrode potential	J/mol
F	Force	N
f	Specific Helmholtz energy	J/mol
G	Gibbs function	J/mol
g	Specific Gibbs energy	J/kg
H	Enthalpy	J/mol
h	Partial enthalpy	J/mol
I	Impulse	N.s
K	Equilibrium Reaction Constant	Depends on reaction
L	Grain length	m
M	Number of elements	
M	Molecular weight	kg/kmol
Ma	Mach number	
MW	Molecular weight	kg/kmol
N	Number of species	
n	Number of moles	mol
NG	Number of gaseous species	
NS	Number of species	
P	Pressure	Pa
p	Partial pressure	Pa
R	Universal gas constant, 8.314	J/mol K
r	Propellant Burn Rate	$m s^{-1}$
S	Entropy	J/mol K

T	Temperature	K
t_b	Burn time	s
U	Internal energy	J/mol
u'	Specific internal energy	J/kg
V	Volume	m^3
V_p	Grain volume	m^3
V_a	Camber volume	m^3
v	Partial molar volume	$m^3 / kmol$
W_f	Web Fraction	
x	Mole fraction	
z	Number of electrons	

Greek

Symbol	Definition	Units
∂	First derivative	
Δ	Change	
γ	Ratio of heat capacity	
λ	Lagrange multiplier	
μ	Chemical potential	
π	3.14	
ρ	Density	kg/m^3
ξ	Set of real parameters	

Subscript

Symbol	Definition
ad	Adiabatic
c	Chamber
ex	Exit
e	Equilibrium
frz	Frozen condition, equation 2.9
f	Fuel
i	Species i
j	Species j
k	Species k
o	Oxidizer
P	Pressure
r	Reaction

s	At constant entropy
t	Throat
T	Temperature
V	Volume
x	At point x

Superscript

Symbol	Definition
0	At zero K
298	At 298 K
o	Standard
–	Partial molal property
.	Rate
*	Critical condition

Abbreviation

Abbreviation	Definition
AP	Ammonium Perchlorate
Comp.	Composite Fuel
DB	Double Base Fuel
HTPB	Hydroxy Terminated Polybutadine
min	Minimum value
NC	Nitrocellulose
NG	Nitroglycerin

Chapter One

Introduction and Literature Review

1. Introduction and Literature Review

1.1. Complex Chemical Equilibrium

Thermodynamic relationships determine the equilibrium composition of product mixtures resulting from chemical reactions. The nature of the product species, their proportions, their temperature, and their pressure depend upon three major controlling factors: Stoichiometry, the first law, and the second law. For one thing, the composition of the product reaction is affected by material balance considerations. This requires that the total mass of each chemical element in the product mixture be the same as that in the reactants. Second, the resultant temperature and pressure of product mixtures depend upon the first law of thermodynamics. This dictates that the total energy be conserved, just as the total mass is. Third, equilibrium composition is determined by relationships arise indirectly from the second law of thermodynamics. The second law dictates that the equilibrium composition of products depends on temperature and pressure, whereas the first law indicates that the temperature and pressure of the products depend on their composition. Clearly, then, complex interactions are involved⁽⁶⁶⁾.

The calculation of the composition of a system at chemical equilibrium is easily carried out when there is only a single reaction to be considered. In this case, the concentrations of each constituent can be related to a single variable, “the degree of reaction”, and the solution of the mass action equation is straight forward. Difficulties are encountered if this method is extended to a consideration of two simultaneous equilibria, and when the number of such simultaneous equilibria becomes large, the ordinary methods become very laborious⁽¹⁰⁾. As people began to study chemical process at more extreme temperature and pressure conditions, it soon became apparent that they could

no longer consider a small number of simultaneous equilibria. As the number of reactions increased, so did the mathematical difficulties. No longer could the simultaneous equilibrium constant relations be solved in closed form, even approximately. It became necessary to use either a trial and error, or an iterative approach to obtain solutions of the system of simultaneous equations⁽⁸⁴⁾. A new term had been appear, “complex chemical equilibrium”. By “Complex” it is meant that systems consisting of many species (up to about 100) and elements (up to about 10)⁽⁶⁹⁾.

As more complicated chemical reactions are brought under consideration, it becomes desirable to develop simpler and more general methods for the calculation of chemical equilibrium⁽⁸¹⁾. In spite of the problem’s importance, it is surprising that most chemistry and chemical engineering thermodynamics textbooks (except Daubert⁽¹⁷⁾) discuss only relatively simple systems for which calculations are readily performed by hand⁽⁶⁹⁾.

The determination of chemical equilibrium of a closed system at a given temperature, pressure and feed composition is one of the most important calculation problems in applied chemical thermodynamics. The calculation methods are usually based on the solution of a set of equilibrium conditions (each condition corresponds to one considered independent chemical reaction) for the set of points satisfying stoichiometric mass balance equations or on the minimization of the Gibbs energy for the set of points satisfying non- stoichiometric mass balance equations⁽⁷⁹⁾.

1.2 Background of Previous Studies

1.2-1 Previous Studies on Complex Chemical Equilibrium

1.2-1-1 Brinkley, S.R. [1947]:

Prior to 1947, solution methods were oriented toward hand or graphical techniques⁽⁶⁹⁾. The first general-purpose algorithm was devised in 1947 by Brinkley⁽¹⁰⁾. Brinkley algorithm considers systems consisting of only a single ideal solution phase. He stated that the number of components of a system containing s constituents is equal to the rank c of the mixture of the subscripts to the symbols of the elements in the formula of the substances comprising the system.

1.2-1-2 White, W.B., *et al* [1958]:

In 1958⁽⁸¹⁾, White, Johnson and Dantzig, described a new method for the determination of equilibrium composition of complex mixtures. They gave two computation procedures to simplify the difficulties arise from using the minimization of free energy technique. One of their procedures is by using a steepest descent technique applied to a quadratic fit, the other made use of linear programming numerical technique. Their procedures are not recommended by many authors^(84, 78).

1.2-1-3 Zeleznik & Gordon [1968]:

Zeleznik and Gordon⁽⁸⁴⁾ reviewed the development in algorithms in 1968. Their review began by separately examining the applicable thermodynamic principles and the algorithms for solving systems of non linear equations, numerical techniques, effects of non-ideality of the system on the calculations, followed by a historical review of some of the most significant developments.

1.2-1-4 Van Zeggern & Storey [1970]:

In 1970, Van Zeggern and Storey⁽⁷⁸⁾ published a book entitled “The Computation of Chemical Equilibria”, which reviews the literature prior to 1970. They explained the pervious methods in a detailed way with solved examples comparing between methods.

1.2-1-5 Smith, W.R., [1978, 1980, 1982, 1998]:

In 1978, Smith, W.R.⁽⁶⁸⁾, started in this field with a short paper in which he gave some valuable remarks on the calculation of complex chemical equilibrium.

In 1980, Smith, W.R.⁽⁶⁹⁾, Published a review in the computation of chemical equilibrium in complex system. In this review he gave four mathematical formulations to attain equilibrium, an approach to get unique solution, and algorithms for both ideal systems and real systems. He also studied the effect of changing parameters in the problem, and recommended numerical solutions in chemical equilibrium computation.

In 1982 Smith and Missen⁽⁷⁰⁾ published their well-known work in chemical equilibrium. In this book they stated, in details, all the available methods for the calculation of chemical equilibrium, supported with worked examples, and stated algorithms for each case. There work is a very good reference to those who are interesting in the calculation of complex chemical equilibrium.

In 1998 Smith and Missen⁽⁷¹⁾ stated a modified general stoichiometric algorithm for chemical equilibrium analysis, they include non-ideal multiphase equilibrium for both chemical and phase equilibria.

1.2-2 Previous computer program for calculation of Complex Chemical Equilibrium

1.2-2-1 NASA Computer Program

The first computer program for calculation of complex chemical equilibria developed at the NASA Lewis Research center was a 1961-62 code by Gordon and Zeleznik for the IBM 704 or 7090 computer⁽³⁰⁾. The program calculated equilibrium compositions by minimization of Gibbs or Helmholtz free energy. This code was the first to have the ability to draw on the JANAF⁽⁷³⁾ thermochemical database to select all possible species in the database which are possible products for a given list of reactants. Since then, the program has undergone several modifications for a variety of applications.

Gordon and Zeleznik⁽²⁹⁾ produced a revision of the code, the NASA Lewis program for Chemical Equilibrium Calculations, 1971 or CEC71, which included the ability to calculate rocket performance, incident and reflected shocks, and Chapman-Jouguet detonations. In 1976, McBride joined Gordon to make code revisions which included the option of calculating transport properties of complex mixtures, called the NASA Lewis Chemical Equilibrium Code, 1976, or CEC76⁽²⁸⁾.

CEC76 has undergone several revisions and name changes, with the most recent designation being the Chemical Equilibrium with Transport Properties code. It is available in a version for mainframe use, called CET93, and for personal computers as CETPC⁽⁵¹⁾. CETPC uses smaller arrays than CET93 and has smaller storage requirements.

1.2-2-2 STANJAN

Another readily available chemical equilibrium program is STANJAN, developed at the Stanford University Department of Mechanical Engineering⁽⁶³⁾. STANJAN requires the product species to be selected by the

user. In some cases, where required data files are not available, the user must create such files using thermodynamic data for particular species. STANJAN does have a limited user interface.

1.2-2-3 CHEPP

Documentation for the Chemical Equilibrium Program Package (CHEPP)⁽²¹⁾. A program package has been developed that calculates chemical equilibrium and thermodynamic properties of reactants and products of a combustion reaction between fuel and air. The package consists of a program for calculating chemical equilibrium, and a database that contains thermochemical information about the molecules.

1.2-2-4 VTEC

The Virginia Tech Equilibrium Chemistry (VTEC) code is a keyboard interactive chemical equilibrium solver for use on a personal computer. The code is particularly suitable for a teaching/learning environment. For a set of reactants at a defined thermodynamic state given by a user, the program will select all species in the JANAF thermochemical database which can exist in the products. The program will then calculate equilibrium composition, flame temperature, and other thermodynamic properties for many common cases⁽⁵⁴⁾.

1.2-2-5 SCORES

Space Craft Object-oriented Rocket Engine Simulation (SCORES)⁽⁸⁰⁾. It is a complete rocket engine analysis package, which analyzes liquid fuel rocket performance. It uses STANJAN code to solve equilibrium composition, so it is not a chemical equilibrium solver.

1.2-2-6 PHATCAT

Power Head And Thrust Chamber Analysis Tool (PHATCAT)⁽¹⁵⁾. This program also uses STANJAN code to solve equilibrium composition, so it is not a chemical equilibrium solver.

1.3. Importance and Application of Chemical Equilibrium

The importance of chemical reaction equilibrium analysis derives from the circumstances in which equilibrium state is a useful model for describing the state of an actual system. The following circumstances include the usual ones for which the equilibrium model may be useful:

1. When rates of change (reaction and mass transfer) are relatively rapid. This tends to be the case when temperature is relatively high, as in rocket engine, or when catalytic activity is relatively high, as in the case of sulfur dioxide converter. The inferences of analytical chemistry involving ionic species are also normally based on this model⁽⁸²⁾.
2. As a reference state to which rate considerations are applied, as in the cases of maximum conversion in a chemical reactor, electromotive force (emf) of a chemical cell, and stagewise operations in separation processes⁽¹⁾.
3. In a negative sense, such as in predicting too low a conversion or yield or in avoiding equilibrium with respect to certain undesired species⁽⁷⁰⁾.
4. As a guide in choosing process conditions, including the evaluation of a catalyst, particularly in conjunction with the effects of changing conditions^(70, 23).

The usefulness of the equilibrium model will normally diminish in favor of a kinetic model whenever rates of change are relatively slow. We may thus be led lost by a particular equilibrium model, if this is the case in the actual system.

The following illustrate situations in which consideration of complex equilibrium is an important part of the overall analysis.

1- Rocket Propellants In rocket propulsion, equilibrium analysis, together with thermochemical analysis, play a role in evaluating the performance of the propellant system. Chemically powered rockets utilize the heat liberated in the combustion of chemical propellants as a source of energy. Because performance considerations are of prime importance in designing rockets, it is desirable to consider merits of rocket propellant combinations by evaluating their specific impulses, their characteristics exhaust velocities, and other performance parameters. This can be obtained from accurate calculation of chemical rocket propellant performance quantities for any given propellant combination, chamber pressure, nozzle area ratio⁽⁷⁴⁾.

2- Chemical Kinetics The equilibrium concept imposes a restriction on the form of a rate law, whenever we consider a net rate of reaction to be the difference between forward and reverse reaction rates. In reaction mechanisms, equilibrium is frequently postulated for a relatively rapid reaction step and its reverse, to eliminate the unknown concentration of a transient intermediate species whose concentration is not involved in the observed rate law. This is the steady-state hypothesis. In the transition-state theory of reaction rates, equilibrium between the activated complex and reactants is also an important postulate⁽⁷⁰⁾.

- 3- Inorganic chemistry** The formation of a complex ion in a solvent usually involves the association of a central cation with anions or neutral molecules as ligands. A measure of the stability of such a complex is given by a formation (equilibrium) constant. One such constant is associated with each stepwise addition of a ligand to the central cation, up to the maximum coordination number. A knowledge of the stepwise constants allows calculation of the distribution of the various species at equilibrium.
- 4- Organic chemistry** The existence of isomers of organic substances in general has implications for yield and conversion at equilibrium⁽⁷⁰⁾.
- 5- Analytical chemistry** Equilibrium analysis plays a large role in quantitative chemical analysis, because the reactions involved are usually sufficiently rapid for a state of equilibrium to be attained. If the concentration of a solution is sufficiently high, nonideality must be taken into account⁽⁷⁰⁾.
- 6- Chemical Processes** Classical examples of the importance of equilibrium analysis in chemical processes include ammonia synthesis and the conversion of SO_2 to SO_3 in a sulfuric acid plant. In such cases the analysis provides information about maximum possible conversions, as functions of the problem parameters, and, in conjunction with kinetic and thermochemical data, information for development of reactor design criteria⁽⁴⁾.
- 7- Energy conversion** An electrochemical cell may be regarded as a chemical reactor or as an energy-conversion device. A fuel cell is an example of the latter. The overall reaction in a fuel cell (e.g., a hydrogen-oxygen fuel cell) is equivalent to a combustion reaction. The advantage of using a fuel cell, compared with combustion in a heat engine in the normal sense, is that the efficiency of energy conversion is not limited by the Carnot relation. This

is essentially because the former involves conversion of chemical free energy directly into electrical energy rather than through chemical enthalpic energy. Another aspect of equilibrium analysis in this case is that the emf of the cell is determined in terms of electrode potentials associated with electrode processes in the usual way through the Nernst equation⁽⁷⁰⁾.

8- Solutions of Nonelectrolytes Interpretation of the behavior of equilibrium properties of nonideal solutions of nonelectrolytes ranges between the extremes of chemical interactions (characterized by equilibrium constants) and physical interactions (characterized by intermolecular potential energy functions). This is reflected in various theories of solutions and their predictions concerning deviation from ideality in terms of excess functions. Chemical effects in solution may be classed as association (involving one species) or solvation (involving more than one species). Hydrogen bonding is a chemical interaction that can be involved in either class. The ideal continuous-association model for solutions of an alcohol such as methanol with a relatively inert, non-polar substance such as carbon tetrachloride pictures self-association of alcohol molecules through hydrogen bonding in polymer like fashion, together with equilibrium among the monomers, dimers, trimers, and so on of alcohol, and ideal-solution behavior of these species and the second component. Thus all the deviations from ideality of the actual solution are attributed to chemical equilibrium effects⁽⁷⁰⁾.

1.4. The Aim of This Work

- 1- studying the existing methods for calculating chemical equilibrium in a complex system, the stoichiometric mass balance equations (based on equilibrium constant) and non-stoichiometric mass

balance equations (based on the minimization of the Gibbs free energy or the Helmholtz free energy),

- 2- Selection of the suitable method for analysis of complex chemical equilibrium for gaseous product. As the method had been selected, a mathematical model (algorithm) was established for such method.
- 3- Modifying the algorithm to be applicable to a special energy device, such as solid fuel rocket motor, as a case study.
- 4- Designing an experimental device, and executing a set of experiments and comparing the results with those obtained from the model.



Chapter Two

*Theoretical Analysis of Chemical
Equilibrium in Complex Systems*

2. Theoretical Analysis of Chemical Equilibrium in Complex System

2.1. Thermodynamic Potential Functions and Criteria for Equilibrium:

The second law of thermodynamics provides several potential functions governing the direction of natural spontaneous processes. The particular potential function appropriate to a given situation is governed by the choice of thermodynamic variables, which are regarded as independent variables. Specification of the values of these variables defines the state of the system. Thus these functions are referred to as state functions, which imply that any change in the function between two states is independent of the path of the change⁽⁶⁶⁾.

Among the most important potential functions are the entropy function, the Helmholtz function, and the Gibbs function. For each such function there is a statement of the second law of thermodynamics that includes both the criterion for a natural process to occur and for its ultimate equilibrium state; the statement must also incorporate any relevant constraints⁽⁷⁰⁾.

Thus, for the entropy S , the statement is

$$dS_{ad} \geq 0, \quad (2.1-1)$$

where subscript ad refers to an adiabatic system; for the Helmholtz function A ,

$$dA_{T,V} \leq 0, \quad (2.1-2)$$

and for the Gibbs function G ,

$$dG_{T,P} \leq 0, \quad (2.1-3)$$

In each case the symbol d refers to an infinitesimal change, and the inequality refers to a spontaneous process and the equality to equilibrium; for

relation 2.1-2, there is no work interaction of any kind between the system and its environment, and for relation 2.1-3, there is no work involved other than that related to volume change (PV work). At equilibrium, depending on the appropriate constraint(s), entropy is at a maximum, the Helmholtz function is at a minimum, and the Gibbs function is at a minimum. Of the three potential functions, the most important, because of the constraints, temperature and pressure, is the Gibbs function. The Helmholtz function and the Gibbs function are both sometimes referred to as free-energy functions. The Helmholtz function is also sometimes referred to as the work function and the Gibbs function as the free-enthalpy function⁽²⁶⁾.

2.2 The Element-Abundance Equations

A closed system has a fixed mass; that is, it does not exchange matter with its surroundings, although it may exchange energy. It may consist of one or more than one phase and may undergo reaction and mass transfer internally. Its importance in equilibrium computations is that the equilibrium conditions of thermodynamics apply primarily to such a system⁽⁶⁷⁾.

Operationally, any description of a closed system is an expression of the law of conservation of mass. A closed system can be defined by a set of element-abundance equations expressing the conservation of the chemical elements making up the species of the system. There is one equation for each element, as follows⁽⁷⁰⁾:

$$\sum_{i=1}^N a_{ki} n_i = b_k; \quad k = 1, 2, \dots, M, \quad (2.2-1)$$

where a_{ki} = the subscript to the k th element in the molecular formula of species i ,

n_i = the number of moles of i ;

b_k = the fixed number of moles of the k th element in the system;

M = the number of elements; and

N = the number of species.

Alternatively, equation (2.2-1) may be written so as to express the change from one compositional state to another:

$$\sum_{i=1}^N a_{ki} \delta n_i = 0; \quad k = 1, 2, \dots, M, \quad (2.2-2)$$

where δn_i = the change in the number of moles of the i th species between two compositional states system.

In vector matrix form, the element-abundance equations 2.2-1 and 2.2-2 are respectively,

$$\mathbf{A}\mathbf{n} = \mathbf{b}, \quad (2.2-3)$$

and

$$\mathbf{A} \delta \mathbf{n} = \mathbf{0}, \quad (2.2-4)$$

where \mathbf{A} = the formula matrix,

\mathbf{n} = the species-abundance vector, and

\mathbf{b} = the element-abundance vector.

Any one of equations 2.2-1 to 2.2-4 expresses the closed-system constraint.

2.2-1 Equation of State

All gases are assumed to be ideal and that interactions among phases may be neglected (discussed in chapter three). Using the well known ideal gas equation of state for the mixture⁽⁴⁶⁾:

$$PV = nRT \quad (2.2-5)$$

where P = pressure (in Newton per square meter),

V = specific volume (in cubic meters per kilogram),

n = moles per unit mass of mixture (in kilograms-mole per kilogram),

and T = temperature (in Kelvin).

For a reacting chemical system the number of moles n is generally not constant.

Equation (2.2-5) is assumed to be correct even when small amounts of condensed species (up to several percent by weight) are present. In this event the condensed species are assumed to occupy a negligible volume relative to the gaseous species. In the variables V , and n the volume and mole number refer to gases only, but the mass is for the entire mixture including condensed species. The word “mixture” is used here to refer to mixtures of reaction products as distinguished from mixtures of reactants, which are referred to as “total reactants.”

On the basis of this definition, n can be written as

$$n = \sum_{j=1}^{NG} n_j \quad (2.2-6)$$

where n_j is the number of kilogram-moles of species j per kilogram of mixture and the index NG refers to the number of gases in the mixture. The molecular weight of the mixture M is defined as

$$M = \frac{1}{n} \quad (2.2-7a)$$

or equivalently as

$$M = \frac{\sum_{j=1}^{NS} n_j M_j}{\sum_{j=1}^{NG} n_j} \quad (2.2-7b)$$

where M_j is the molecular weight of species j and the index NS refers to the number of species in the mixture.

More conventionally, molecular weight is defined as

$$MW = \frac{\sum_{j=1}^{NS} n_j M_j}{\sum_{j=1}^{NS} n_j} \quad (2.2-8a)$$

Molecular weight is given the symbol MW in equation (2.2-8a) to differentiate it from M . The two different definitions of molecular weight, M and MW , give different results only in mixtures of products containing condensed as well as gaseous species. Only M is given in the output, but MW may be obtained from M by means of

$$MW = M \left(1 - \sum_{j=NG+1}^{NS} x_j \right) \quad (2.2-8b)$$

where x_j is the mole fraction of species j relative to all species in the mixture.

2.3. Thermodynamic Description of a Chemical System⁽⁷⁰⁾:

A homogeneous (single-phase) chemical system, open or closed, is defined thermodynamically by one of the following natural sets of state function and independent variables:

$$U = U(S, V, n_1, n_2, \dots), \quad (2.3-1)$$

$$H = H(S, P, n_1, n_2, \dots), \quad (2.3-2)$$

$$A = A(T, V, n_1, n_2, \dots), \quad (2.3-3)$$

or
$$G = G(T, P, n_1, n_2, \dots), \quad (2.3-4)$$

where U is internal energy and H is enthalpy of the system. Equation 2.3-4, for example, states that G is a (single-valued) function of T , P and the (N) mole numbers \mathbf{n} . Each of these equations gives rise to a corresponding equation for the complete differential of the function involved:

$$dU = TdS - PdV + \sum_{i=1}^N \mu_i dn_i, \quad (2.3-5)$$

$$dH = TdS + VdP + \sum_{i=1}^N \mu_i dn_i, \quad (2.3-6)$$

$$dA = -SdT - PdV + \sum_{i=1}^N \mu_i dn_i, \quad (2.3-7)$$

$$\text{and} \quad dG = -SdT + VdP + \sum_{i=1}^N \mu_i dn_i, \quad (2.3-8)$$

where the chemical potential for the species i , μ_i , is defined by any of

$$\mu_i = \left(\frac{\partial U}{\partial n_i} \right)_{S,V,n_{j \neq i}} = \left(\frac{\partial H}{\partial n_i} \right)_{S,P,n_{j \neq i}} = \left(\frac{\partial A}{\partial n_i} \right)_{T,V,n_{j \neq i}} = \left(\frac{\partial G}{\partial n_i} \right)_{T,P,n_{j \neq i}} \quad (2.3-9)$$

where the subscript j refers to any species except i .

Because of the homogeneity property of these functions, μ_i depends only on the intensive state of the system, such as defined by T , P , and the composition.

Since the most important of these four functions is the Gibbs function G , the use of this function will continuously be exclusively used, with the understanding that corresponding descriptions can be written in terms of U , H , or A as required.

From equation 2.3-8 and the definition of G , the temperature and pressure derivatives for G and μ_i , in their most useful forms, are as follows:

$$\left[\frac{\partial(G/T)}{\partial T} \right]_{P,n} = \frac{-H}{T^2}, \quad (2.3-10)$$

$$\left(\frac{\partial G}{\partial P} \right)_{T,n} = V, \quad (2.3-11)$$

$$\left[\frac{\partial(\mu_i/T)}{\partial T} \right]_{P,n} = \frac{-\bar{h}_i}{T^2}, \quad (2.3-12)$$

$$\text{and} \quad \left(\frac{\partial \mu_i}{\partial P} \right)_{T,n} = \bar{v}_i, \quad (2.3-13)$$

where the subscript n means that all mole numbers are constant and \bar{h}_i and \bar{v}_i are the partial molar enthalpy and partial molar volume, respectively, of species i in the system:

$$\bar{h}_i = \left(\frac{\partial H}{\partial n_i} \right)_{T, P, n_{j \neq i}}, \quad (2.3-14)$$

$$\bar{v}_i = \left(\frac{\partial V}{\partial n_i} \right)_{T, P, n_{j \neq i}}, \quad (2.3-15)$$

The additivity equation for the total Gibbs function of the system is obtained by integration of equation 2.3-8 at fixed T, P, and composition:

$$G(T, P, n) = \sum_{i=1}^N n_i \mu_i, \quad (2.3-16)$$

Differentiation of this equation and comparison of the result with equation 2.2-8 leads to Gibbs-Duhem equation for the homogeneous system:

$$SdT - VdP + \sum_{i=1}^N \mu_i dn_i = 0, \quad (2.3-17)$$

2.4. Formulations of the Equilibrium Conditions⁽⁷⁰⁾:

For either a single phase or multiphase system to be at equilibrium, G is at a minimum value, subject to the closed system constraint and the non-negativity constraint at the given thermodynamic conditions (fixed T and P). This is essentially the statement of equation 2.4-1 below:

$$dG_{T, P=0}, \quad (2.4-1)$$

Two formulations of the minimization problem are thus:

1. The stoichiometric formulation, in which the closed system constraint is treated by means of stoichiometric equations so as to result in an essentially unconstrained minimization problem.
2. The non- stoichiometric formulation, in which stoichiometric equations are not used but, instead, the closed system constraint is treated by means of Lagrange multipliers.

2.4-1 The Stoichiometric Formulation^(70, 42):

The general solution of equations 2.2-1 or 2.2-3, a set of M linear equations in N unknowns, is

$$\mathbf{n} = \mathbf{n}^0 + \sum_{j=1}^R \nu_j \xi_j, \quad (2.4-2)$$

where \mathbf{n}^0 is any particular solution (e.g., an initial composition), $\nu_1, \nu_2, \dots, \nu_R$ is any set of R linearly independent solutions of the homogeneous equation corresponding to equation 2.2-3, and the quantities ξ_j are a set of real parameters.

Hence equation 2.3-4 may be written as

$$G = G(T, P, \xi), \quad (2.4-3)$$

and the problem is one of minimizing G , for fixed T and P , in terms of R ξ_j 's. Since these last ones are independent quantities, the first-order necessary conditions for a minimum in G are

$$\left(\frac{\partial G}{\partial \xi} \right)_{T,P} = \mathbf{0}, \quad (2.4-4)$$

or

$$\left(\frac{\partial G}{\partial \xi_j} \right)_{T,P,\xi_{k \neq j}} = 0; \quad j = 1, 2, \dots, R. \quad (2.4-5)$$

An alternative way of regarding the parameters $\{\xi_j\}$ and the quantities $\{\nu_{ij}\}$ may be obtained from further examination of equation 2.4-2, which may be written as

$$n_i = n_i^0 + \sum_{j=1}^R \nu_{ij} \xi_j; \quad i = 1, 2, \dots, N. \quad (2.4-6)$$

For fixed \mathbf{n}^0 ,

$$\left(\frac{\partial n_i}{\partial \xi_j} \right)_{\xi_{k \neq j}} = \nu_{ij}; \quad i = 1, 2, \dots, N; \quad j = 1, 2, \dots, R, \quad (2.4-7)$$

There are $R = N - C$ equations in the set 2.4-5. Since

$$\left(\frac{\partial G}{\partial \xi_j} \right)_{T, P, \xi_{k \neq j}} = \sum_{i=1}^N \left(\frac{\partial G}{\partial n_i} \right)_{T, P, n_{k \neq i}} \left(\frac{\partial n_i}{\partial \xi_j} \right)_{\xi_{k \neq j}} ; j = 1, 2, \dots, R, \quad (2.4-8)$$

$$\left(\frac{\partial G}{\partial n_i} \right)_{T, P, n_{k \neq i}} = \mu_i, \quad (2.3-9)$$

then, on combining equations 2.4-5, 2.3-9, and 2.4-7, we have

$$\sum_{i=1}^N \nu_{ij} \mu_i = 0 ; \quad j = 1, 2, \dots, R, \quad (2.4-9)$$

Equations 2.4-9 are R conditions for equilibrium in the system and are readily recognized as the “classical” forms of the equilibrium conditions. When appropriate expressions for the μ_i are introduced into the equations in terms of free-energy data and the mole numbers, the solution of these equations provides the composition of the system at equilibrium.

2.4-2 The Non-Stoichiometric Formulation^(70, 14):

The problem is formulated as one of minimizing G , for fixed T and P , in terms of the N mole numbers, subject to the M element-abundance constraints. That is, from equation (2.3-16),

$$\min G(\mathbf{n}) = \sum_{i=1}^N n_i \mu_i, \quad (2.4-10)$$

subject to
$$\sum_{i=1}^N a_{ki} n_i = b_k ; \quad k = 1, 2, \dots, M, \quad (2.2-1)$$

It is assumed, for convenience, that $M = \text{rank}(A) = C$

This is a simple form of constrained optimization problem. One approach is to use the method of Lagrange multipliers to remove the constraints. For this, the Lagrangian ℓ is written as:

$$\ell(\mathbf{n}, \boldsymbol{\lambda}) = \sum_{i=1}^N n_i \mu_i + \sum_{k=1}^M \lambda_k \left(b_k - \sum_{i=1}^N a_{ki} n_i \right), \quad (2.4-11)$$

where $\boldsymbol{\lambda}$ is a vector of M unknown Lagrange multipliers, $\boldsymbol{\lambda} = (\lambda_1, \lambda_1, \dots, \lambda_M)^T$. Then the necessary conditions provide the following set of $(N+M)$ equations in the $(N+M)$ unknowns $(n_1, n_2, \dots, n_N, \lambda_1, \lambda_1, \dots, \lambda_M)$:

$$\left(\frac{\partial \ell}{\partial n_i} \right)_{n_{j \neq i}, \boldsymbol{\lambda}} = \mu_i - \sum_{k=1}^M a_{ki} \lambda_k = 0, \quad (n_i > 0) \quad (2.4-12)$$

$$\left(\frac{\partial \ell}{\partial \lambda_k} \right)_{n, \lambda_{j \neq k}} = b_k - \sum_{i=1}^N a_{ki} n_i = 0, \quad (2.4-13)$$

As in the stoichiometric formulation, the solution of these equations involves the introduction of an appropriate expression for μ .

2.5. The Chemical Potential:

The structure of chemical thermodynamics is general and independent of the functional form of the chemical potential μ_i . Although the structure contains derivatives that show how μ_i depends on temperature and pressure (equations 2.3-12 and 2.3-13), thermodynamics itself provides no comparable expressions for the dependence of μ_i on composition. One must then superimpose on the thermodynamic structure, particularly in equations 2.4-9 and 2.4-12, the equilibrium conditions, specific expressions for μ_i to introduce composition explicitly into these equilibrium conditions. A guideline for this is that the expression for μ_i must satisfy the Gibbs-Duhem equation⁽⁶⁷⁾.

One considers expressions for the chemical potential of a pure species first before turning attention to species in solution, in which latter case, composition must be taken into account in addition to T and P .

2.5-1 Pure Species⁽⁶⁷⁾:

From equation 2.3-13 written for a pure species, the following is obtained

$$\left(\frac{\partial\mu}{\partial P}\right)_T = v, \quad (2.5-1)$$

where v is molar volume. Integration of this at fixed T from a reference pressure P° to P results in

$$\mu(T, P) - \mu(T, P^\circ) = \int_{P^\circ}^P v dP, \quad (2.5-2)$$

Applying this to ideal gas equation, introduction of the equation of state into equation 2.5-2

$$Pv = RT \quad (2.5-3)$$

and a reference or standard state pressure (P°) of unity results in

$$\mu(T, P) = \mu^\circ(T) + RT \ln P, \quad (2.5-4)$$

where P must be in the same unit of pressure as P° . Thus if P° is chosen to be 1 atm, P must be expressed in atmospheres. $\mu^\circ(T)$ is called the standard chemical potential that is function of T only.

2.5-2 Species in Solution^(67, 70):

The form of equation 2.5-4 for the chemical potential of a pure, ideal gas suggests the form for a species in an ideal-gas solution (i.e., a solution of ideal gases):

$$\mu_i(T, P, x_i) = \mu_i^\circ(T) + RT \ln p_i, \quad (2.5-5)$$

in which pressure P is replaced by the partial pressure p_i , where by definition,

$$p_i = \left(\frac{n_i}{n_t}\right)P \equiv x_i P, \quad (2.5-6)$$

x_i is the mole fraction of species i , and n_i is the total number of moles in the solution. A justification for this form is that application of equation 2.3-13 to equation 2.5-5 leads to the equation of state for an ideal-gas solution:

$$\left(\frac{\partial \mu_i}{\partial P} \right)_{T,n} = \frac{RT}{P} = \bar{v}_i, \quad (2.5-7a)$$

Hence

$$V = \sum n_i \bar{v}_i = \frac{RT}{P} \sum n_i = n_t \frac{RT}{P}, \quad (2.5-7b)$$

This can be most easily seen if equation 2.5-5 is written as

$$\mu_i(T, P, x_i) = \mu_i^\circ(T) + RT \ln P + RT \ln x_i, \quad (2.5-5a)$$

2.6. Methods for Obtaining Standard Free-Energy⁽⁶²⁾:

Regardless of which method is used to determine the composition of a system at equilibrium, it is necessary to assign a numerical value to the standard chemical potential μ_i° or its equivalent. There are four main ways in which free-energy information is available for this purpose:

- 1- As standard free energies of formation from the constituent elements (ΔG_f°).
- 2- As values of the free-energy function, $(G^\circ - H_0^\circ)/T$ or $(G^\circ - H_{298}^\circ)/T$.
- 3- As conventional absolute entropies (S°) together with enthalpies of formation (ΔH_f°).
- 4- As standard electrode potentials (E°).

The use of each of these methods will be reviewed in the following.

2.6-1 Use of Free Energy of Formation⁽⁶²⁾:

Since the standard free energy change of a reaction (represented by ΔG°) is related to the μ_i° 's, on the one hand, and to the standard free energies of formation ΔG_{fi}° 's, on the other hand, by

$$\Delta G^\circ = \sum v_i \mu_i^\circ = \sum v_i \Delta G_{fi}^\circ, \quad (2.6-1)$$

The use of ΔG_{fi}° is equivalent to identifying it with μ_i° ; that is

$$\mu_i^\circ \equiv \Delta G_{fi}^\circ, \quad (2.6-2)$$

A variation of this occurs when the equilibrium constant of a reaction is given and ΔG_{fi}° is not all available. Then ΔG° is calculated from the reaction isotherm in the general form

$$\Delta G^\circ = -RT \ln K, \quad (2.6-3)$$

2.6-2 Use of the Free-Energy Function⁽¹⁷⁾:

The free-energy function for a species is defined as $(G^\circ - H_0^\circ)/T$, where G° is the molar standard free energy of the species at T (equivalent to μ° , since the species is normally a pure species), and H_0° is the standard enthalpy of the species at 0 K (298 K may also be used). The standard free-energy change of a reaction is calculated from this function by

$$\Delta G^\circ = \Delta H_0^\circ + T \sum_i v_i \left(\frac{G^\circ - H_0^\circ}{T} \right)_i, \quad (2.6-4)$$

or by

$$\Delta G^\circ = \Delta H_{298}^\circ + T \sum_i v_i \left(\frac{G^\circ - H_{298}^\circ}{T} \right)_i, \quad (2.6-4a)$$

where ΔH_0° and ΔH_{298}° are the standard enthalpy changes at 0 K and 298 K, respectively, and are evaluated according to the way in which enthalpy

data are given. Thus, if standard enthalpies of formation ΔH_{fi}^o are provided, together with the enthalpy function $H_T^o - H_0^o$ or $H_T^o - H_{298}^o$, then

$$\Delta H_0^o = \sum v_i \Delta H_{fi,298}^o - \sum v_i (H_{298}^o - H_0^o), \quad (2.6-5)$$

and
$$\Delta H_{298}^o = \sum v_i \Delta H_{fi,298}^o, \quad (2.6-5a)$$

From equations 2.6-1, 2.6-4, and 2.6-5, it follows that

$$\begin{aligned} \mu_i^o &\equiv \Delta H_{fi,298}^o - (H_{298}^o - H_0^o)_i + T \left(\frac{G^o - H_0^o}{T} \right)_i \\ &\equiv \Delta H_{fi,0}^o + T \left(\frac{G^o - H_0^o}{T} \right)_i, \end{aligned} \quad (2.6-6)$$

and from equations 2.6-1, 2.6-4a, and 2.6-5a, that

$$\mu_i^o \equiv \Delta H_{fi,298}^o + T \left(\frac{G^o - H_{298}^o}{T} \right)_i, \quad (2.6-6a)$$

2.6-3 Use of Conventional Absolute Entropies⁽¹⁷⁾:

The value of ΔG^o may be determined from entropy and enthalpy data by

$$\Delta G^o = \Delta H^o - T \Delta S^o, \quad (2.6-7)$$

where
$$\Delta S^o = \sum v_i S_i^o, \quad (2.6-8)$$

and S_i^o is the conventional absolute entropy of species i .

From equations 2.6-1, 2.6-7, and 2.6-8 and $\Delta H^o = \sum v_i \Delta H_{fi}^o$ it follows that

$$\mu_i^o \equiv \Delta H_{fi}^o - T S_i^o. \quad (2.6-9)$$

2.6-4 Use of Standard Electrode Potentials⁽¹⁾:

ΔG° for a reaction may be obtained from the standard emf E° of a chemical cell in which the given reaction takes place. In turn, E° is obtained from the standard electrode potentials for the two electrode processes (oxidation at the anode and reduction at the cathode) that constitute the overall cell reaction. The electrode potentials are conventionally given for the electrode processes written as reduction processes. E° is related to the standard free-energy change ΔG° for the cell reaction by

$$\Delta G^\circ = -zFE^\circ. \quad (2.6-10)$$

where z is the number of moles of electrons associated with the cell process, and F is the Faraday constant [96,487 coulombs (mole electrons)⁻¹].

2.7 Minimization of Gibbs Energy⁽²⁶⁾

For a mixture of NS species the Gibbs energy per kilogram of mixture g is given by

$$g = \sum_{j=1}^{NS} \mu_j n_j \quad (2.7-1)$$

where the chemical potential per kilogram-mole of species j is defined to be

$$\mu_j = \left(\frac{\partial g}{\partial n_j} \right)_{T, P, n_{i \neq j}} \quad (2.7-2)$$

The condition for chemical equilibrium is the minimization of free energy. This minimization is usually subject to certain constraints, such as the following mass-balance constraints:

$$\sum_{j=1}^{NS} a_{ij} n_j - b_i^\circ = 0 \quad (i = 1, \dots, \ell) \quad (2.7-3a)$$

or
$$b_i - b_i^\circ = 0 \quad (i = 1, \dots, \ell) \quad (2.7-3b)$$

where the stoichiometric coefficients a_{ij} are the number of kilogram-atoms of element i per kilogram-mole of species j , the index is the number of chemical elements (if ions are considered, the number of chemical elements plus one), b_i^o is the assigned number of kilogram-atoms of element i per kilogram of total reactants, and

$$b_i = \sum_{j=1}^{NS} a_{ij} n_j \quad (i = 1, \dots, \ell) \quad (2.7-3c)$$

is the number of kilogram-atoms of element i per kilogram of mixture.

Defining a term G to be

$$G = g + \sum_{i=1}^{\ell} \lambda_i (b_i - b_i^o) \quad (2.7-4)$$

where λ_i are Lagrangian multipliers, the condition for equilibrium becomes

$$\delta G = \sum_{j=1}^{NS} \left(\mu_j + \sum_{i=1}^{\ell} \lambda_i a_{ij} \right) \delta n_j + \sum_{i=1}^{\ell} (b_i - b_i^o) \delta \lambda_i = 0 \quad (2.7-5)$$

Treating the variations δn_j and $\delta \lambda_j$ as independent gives

$$\mu_j + \sum_{i=1}^{\ell} \lambda_i a_{ij} = 0 \quad (j = 1, \dots, NS) \quad (2.7-6)$$

and also gives the mass-balance equation (2.7-3b).

From the assumptions in section 2.2-1, the chemical potential can be written as

$$\mu_j = \begin{cases} \mu_j^o + RT \ln \frac{n_j}{n} + RT \ln P & (j = 1, \dots, NG) \\ \mu_j^o & (j = NG + 1, \dots, NS) \end{cases} \quad (2.7-7)$$

where μ_j^o for gases ($j = 1$ to NG) and for condensed phases (NG) is the chemical potential in the standard state. For a gas the standard state is the hypothetical ideal gas at the standard-state pressure. For a pure solid or liquid the standard state is the substance in the condensed phase at the standard-state

pressure. Historically, the defined standard-state pressure has been one atmosphere (101 325 Pa)⁽⁵⁵⁾. Most early tabulations of thermodynamic data were based on this pressure. However, in 1982 the International Union of Pure and Applied Chemistry recommended that the standard-state pressure should be defined as 1 bar (10⁵ Pa)⁽²³⁾. Most recent compilations have used 1 bar as the standard pressure. The unit of pressure in equation (2.7-7) should be consistent with the unit of pressure in the thermodynamic data being used.

Equations (2.7-3a) and (2.7-6) permit the determination of equilibrium compositions for thermodynamic states specified by an assigned temperature T and pressure P . That is, in addition to equations (2.7-3a) and (2.7-6), there is the pair of trivial equations

$$T = T_0 \quad (2.7-8a)$$

$$P = P_0 \quad (2.7-8b)$$

However, the thermodynamic state can be specified by assigning any two state functions. For example, the thermodynamic state corresponding to a constant- pressure combustion is specified, instead of by equations (5.3-8), by

$$h = h_0 \quad (2.7-9a)$$

$$P = P_0 \quad (2.7-9b)$$

where h is the specific enthalpy of the mixture and h_0 a constant equals to the specific enthalpy of the reactants. The expression for h is

$$h = \sum_{j=1}^{NS} n_j H_j^o \quad (2.7-10)$$

where H_j^o is the standard-state molar enthalpy for species j at temperature T .

For assigned entropy and pressure (such as for an isentropic compression or expansion to a specified pressure), the thermodynamic state is specified by

$$s = s_0 \quad (2.7-11a)$$

$$P = P_0 \quad (2.7-11b)$$

where s is the specific entropy of the mixture and s_0 the assigned specific entropy, or the specific entropy of the total reactant. The expression for s is

$$s = \sum_{j=1}^{NS} n_j S_j^o \quad (2.7-12)$$

where

$$S_j = \begin{cases} S_j^o + R \ln \frac{n_j}{n} + R \ln P & (j=1, \dots, NG) \\ S_j^o & (j=NG+1, \dots, NS) \end{cases} \quad (2.7-13)$$

and S_j^o is the standard-state molar entropy for species j . Equation (2.7-13) is similar to equation (2.7-7), and the same discussion concerning standard-state pressure that applied to equation (2.7-7) also applies to equation (2.7-13).

2.8 Minimization of Helmholtz Energy⁽⁴⁰⁾

The equations presented in this section are similar to those in section 2.7. Whatever differences appear are due to the different forms of the chemical potential μ_j ($j = 1, \dots, NG$). In section 2.7, pressure was one of the assigned thermodynamic states, and consequently Gibbs energy was minimized. In this section volume (or density) is one of the assigned thermodynamic states, and consequently Helmholtz energy is minimized.

The two energies (Gibbs and Helmholtz) have the following thermodynamic relationship:

$$f = g - PV \quad (2.8-1)$$

where f is the Helmholtz energy per kilogram of mixture. Substituting Gibbs energy g as given by equation (2.7-1), into equation (2.8-1) gives

$$f = \sum_{j=1}^{NS} \mu_j n_j - PV \quad (2.8-2)$$

The chemical potential can be expressed as a thermodynamic derivative in several ways. One way is given by equation (2.7-2). Another expression is

$$\mu_j = \left(\frac{\partial f}{\partial n_j} \right)_{T, P, n_{i \neq j}} \quad (2.8-3)$$

If
$$F = f + \sum_{i=1}^{\ell} \lambda_i (b_i - b_i^o) \quad (2.8-4)$$

the condition for equilibrium based on the minimization of Helmholtz energy subject to mass-balance constraints is

$$\delta F = \sum_{j=1}^{NS} \left(\mu_j + \sum_{i=1}^{\ell} \lambda_i a_{ij} \right) \delta n_j + \sum_{i=1}^{\ell} (b_i - b_i^o) \delta \lambda_i = 0 \quad (2.8-5)$$

Treating δn_j and $\delta \lambda_j$ as independent again gives, as in section 2.7, equations (2.7-3) and (2.7-6). Now, however, instead of equation (2.7-7),

$$\mu_j = \begin{cases} \mu_j^o + RT \ln \frac{n_j RT}{V} & (j=1, \dots, NG) \\ \mu_j^o & (j=NG+1, \dots, NS) \end{cases} \quad (2.8-6)$$

Equations (2.7-3) and (2.7-6), with μ_j given by equation (2.8-6), permit the determination of equilibrium compositions for thermodynamic states specified by an assigned temperature T_0 and volume V_0 ; that is, in addition to equations (2.7-3) and (2.7-6), there is the pair of trivial equations

$$T = T_0 \quad (2.8-7a)$$

$$V = V_0 \quad (2.8-7b)$$

Analogous to equation (2.7-9) for a constant pressure combustion process, one can set down the following conditions for constant-volume combustion:

$$u' = u'_0 \quad (2.8-8a)$$

$$V = V_0 \quad (2.8-8b)$$

where u' is the specific internal energy of the mixture and u'_0 a constant equals to the specific internal energy of the reactants. The expression for u' is

$$u' = \sum_{j=1}^{NS} n_j U_j^o \quad (2.8-9)$$

where U_j^o is the standard-state molar internal energy for species j .

Analogous to equation (2.7-11), for assigned entropy and volume (such as for an isentropic compression or expansion to a specified volume), the thermodynamic state is specified by

$$s = s_0 \quad (2.8-10a)$$

$$V = V_0 \quad (2.8-10b)$$

2.9 Thermodynamic Derivatives From Matrix Solution

All thermodynamic first derivatives can be expressed in terms of any three independent first derivatives. The Bridgman tables⁽⁴⁶⁾, express first derivatives in terms of $(\partial V / \partial T)_P$, $(\partial V / \partial P)_T$, and $(\partial H / \partial T)_P \equiv c_p$. The logarithmic form of the volume derivatives is used because it gives an indication of the extent of chemical reaction occurring among the reaction species. These derivatives may have more than one value depending on what is assumed occurring to composition in a thermodynamic process from one condition to another. If, for example, composition is assumed to reach its

equilibrium value instantaneously, the derivatives are referred to as “equilibrium” derivatives. If, on the other hand, reaction times are assumed to be infinitely slow, composition remains fixed (frozen) and derivatives are referred to as “frozen”. Special subscripts are used to differentiate these different conditions only for c_p . The equilibrium value of c_p may be expressed as the sum of a “frozen” contribution and a “reaction” contribution as follows:

$$c_{p,e} = c_{p,f} + c_{p,r} \quad (2.9-1a)$$

where

$$c_{p,f} = \sum_{j=1}^{NS} n_j C_{p,j}^o \quad (2.9-1b)$$

and

$$c_{p,r} = \sum_{j=1}^{NG} n_j \frac{H_j^o}{T} \left(\frac{\partial \ln n_j}{\partial \ln T} \right)_P + \sum_{j=NG+1}^{NS} \frac{H_j^o}{T} \left(\frac{\partial n_j}{\partial \ln T} \right)_P \quad (2.9-1c)$$

the expressions in equations (2.9-1b) and (2.9-1c) were obtained by differentiating equation (2.7-10).

From equation (2.2-5)

$$\left(\frac{\partial \ln V}{\partial \ln T} \right)_P = 1 + \left(\frac{\partial \ln n}{\partial \ln T} \right)_P \quad (2.9-2)$$

$$\left(\frac{\partial \ln V}{\partial \ln P} \right)_T = -1 + \left(\frac{\partial \ln n}{\partial \ln P} \right)_T \quad (2.9-3)$$

2.9-1 Derivatives With Respect to Temperature⁽⁴⁸⁾

The derivatives of n_j and n with respect to temperature are needed to evaluate equations (2.9-1c) and (2.9-2). These may be obtained by differentiating equations (2.7-6), (2.7-3), and (2.2-7), which gives the following:

$$\left(\frac{\partial \ln n_j}{\partial \ln T} \right)_P - \sum_{i=1}^{\ell} \left(\frac{\partial \pi_i}{\partial \ln T} \right)_P - \left(\frac{\partial \ln n}{\partial \ln T} \right)_P = \frac{H_j^o}{RT} \quad (j=1, \dots, NG) \quad (2.9-4)$$

$$-\sum_{i=1}^{\ell} \left(\frac{\partial \pi_i}{\partial \ln T} \right)_P = \frac{H_j^O}{RT} \quad (j = \text{NG} + 1, \dots, \text{NS}) \quad (2.9-5)$$

$$\sum_{j=1}^{\text{NG}} a_{kj} n_j \left(\frac{\partial \ln n_j}{\partial \ln T} \right)_P + \sum_{j=\text{NG}+1}^{\text{NS}} a_{kj} \left(\frac{\partial n_j}{\partial \ln T} \right)_P = 0 \quad (k = 1, \dots, \ell) \quad (2.9-6)$$

$$\sum_{j=1}^{\text{NG}} n_j \left(\frac{\partial \ln n_j}{\partial \ln T} \right)_P - n \left(\frac{\partial n}{\partial \ln T} \right)_P = 0 \quad (2.9-7)$$

As in the case of the iteration correction equations previously discussed, the derivative equations can be reduced to a much smaller number of simultaneous equations by eliminating $(\partial \ln n_j / \partial T)_P$, obtained from equation (2.9-4), from equations (2.9-6) and (2.9-7). When equation (2.9-5) written with the sign reversed is included, the resulting reduced number of temperature derivative equations is

$$\begin{aligned} \sum_{i=1}^{\ell} \sum_{j=1}^{\text{NG}} a_{kj} a_{ij} n_j \left(\frac{\partial \pi_i}{\partial \ln T} \right)_P + \sum_{j=\text{NG}+1}^{\text{NS}} a_{kj} \left(\frac{\partial n_j}{\partial \ln T} \right)_P + \sum_{j=1}^{\text{NG}} a_{kj} n_j \left(\frac{\partial \ln n}{\partial \ln T} \right)_P \\ = - \sum_{j=1}^{\text{NG}} \frac{a_{kj} n_j H_j^O}{RT} \quad (k = 1, \dots, \ell) \end{aligned} \quad (2.9-8)$$

$$\sum_{i=1}^{\ell} a_{ij} \left(\frac{\partial \pi_i}{\partial \ln T} \right)_P = - \frac{H_j^O}{RT} \quad (j = \text{NG} + 1, \dots, \text{NS}) \quad (2.9-9)$$

$$\sum_{i=1}^{\ell} \sum_{j=1}^{\text{NG}} a_{ij} n_j \left(\frac{\partial \pi_i}{\partial \ln T} \right)_P = - \sum_{j=1}^{\text{NG}} \frac{n_j H_j^O}{RT} \quad (2.9-10)$$

The values of the derivatives obtained from equations (2.9-8) to (2.9-10) can be used in equation (2.9-4) to obtain derivatives for gaseous species $(\partial \ln n_j / \partial T)_P$ ($j = 1, \dots, \text{NG}$) and all the temperature derivatives can then be used to evaluate c_p from equations (2.9-1). However, there is an alternative and much simpler procedure for obtaining c_p . Substituting $(\partial \ln n_j / \partial T)_P$

obtained from equation (2.9-4) into equations (2.9-1) and dividing by R yields:

$$\begin{aligned} \frac{c_{p,e}}{R} = & \sum_{i=1}^{\ell} \left(\sum_{j=1}^{NG} \frac{a_{ij} n_j H_j^O}{RT} \right) \left(\frac{\partial \pi_i}{\partial \ln T} \right)_P + \sum_{j=NG+1}^{NS} \frac{H_j^O}{RT} \left(\frac{\partial n_j}{\partial \ln T} \right)_P \\ & + \left(\sum_{j=1}^{NG} \frac{n_j H_j^O}{RT} \right) \left(\frac{\partial \ln n}{\partial \ln T} \right)_P + \sum_{j=1}^{NS} \frac{n_j C_{p,j}^O}{R} + \sum_{j=1}^{NG} \frac{n_j (H_j^O)^2}{R^2 T^2} \end{aligned} \quad (2.9-11)$$

In equation (2.9-11) only the temperature derivatives obtained directly from solution of equations (2.9-8) to (2.9-10) are required. Furthermore, all the coefficients appearing in equation (2.9-11) are exactly the coefficients in the reduced-enthalpy equation (2.7-23). The second-last term in equation (2.9-11) is the frozen contribution to specific heat (equation (2.9-1b)); the remainder of the terms are the reaction contribution (equation (2.9-1c)).

2.9-2 Derivatives With Respect to Pressure⁽⁴⁸⁾

The derivative $(\partial \ln n / \partial P)_T$ can be obtained in a manner similar to that described for obtaining derivatives with respect to the temperature. Differentiating equations (2.7-6), (2.7-3), and (2.2-7) gives

$$\left(\frac{\partial \ln n_j}{\partial \ln P} \right)_T - \sum_{i=1}^{\ell} \left(\frac{\partial \pi_i}{\partial \ln P} \right)_T - \left(\frac{\partial \ln n}{\partial \ln P} \right)_T = -1 \quad (j=1, \dots, NG) \quad (2.9-12)$$

$$- \sum_{i=1}^{\ell} \left(\frac{\partial \pi_i}{\partial \ln P} \right)_T = 0 \quad (j=NG+1, \dots, NS) \quad (2.9-13)$$

$$\sum_{j=1}^{NG} a_{kj} n_j \left(\frac{\partial \ln n_j}{\partial \ln P} \right)_T + \sum_{j=NG+1}^{NS} a_{kj} \left(\frac{\partial n_j}{\partial \ln P} \right)_T = 0 \quad (k=1, \dots, \ell) \quad (2.9-14)$$

$$\sum_{j=1}^{NG} n_j \left(\frac{\partial \ln n_j}{\partial \ln P} \right)_T - n \left(\frac{\partial \ln n}{\partial \ln P} \right)_T = 0 \quad (2.9-15)$$

Equations (2.9-12) to (2.9-15) can be reduced to a smaller set by eliminating $(\partial \ln n_j / \partial P)_T$, obtained from equation (2.9-12), from equations (2.9-14) and (2.9-15). When equation (2.9-13) written with the sign reversed is included, the results are

$$\begin{aligned} \sum_{i=1}^{\ell} \sum_{j=1}^{NG} a_{kj} a_{ij} n_j \left(\frac{\partial \pi_i}{\partial \ln P} \right)_T + \sum_{j=NG+1}^{NS} a_{kj} \left(\frac{\partial n_j}{\partial \ln P} \right)_T \\ + \sum_{j=1}^{NG} a_{kj} n_j \left(\frac{\partial \ln n}{\partial \ln P} \right)_T = \sum_{j=1}^{NG} a_{kj} n_j \quad (k = 1, \dots, \ell) \end{aligned} \quad (2.9-16)$$

$$\sum_{i=1}^{\ell} a_{ij} \left(\frac{\partial \pi_i}{\partial \ln P} \right)_T = 0 \quad (j = NG + 1, \dots, NS) \quad (2.9-17)$$

$$\sum_{i=1}^{\ell} \sum_{j=1}^{NG} a_{ij} n_j \left(\frac{\partial \pi_i}{\partial \ln P} \right)_T = - \sum_{j=i}^{NG} n_j \quad (2.9-18)$$

2.9-3 Other Thermodynamic Derivatives^(48, 83)

As stated previously, all thermodynamic first derivatives can be expressed in terms of the previous sections, namely, c_p , $(\partial \ln V / \partial T)_P$, $(\partial \ln V / \partial P)_T$. Velocity of sound a , a frequently used parameter, is defined by (see Bridgman tables in "Thermodynamics" Lewis and Randal, 1961)

$$a^2 = \left(\frac{\partial P}{\partial \rho} \right)_S = \frac{P}{\rho} \left(\frac{\partial \ln P}{\partial \ln \rho} \right)_S = - \frac{P}{\rho} \left(\frac{\partial \ln P}{\partial \ln V} \right)_S \quad (2.9-19)$$

From Bridgman tables

$$\left(\frac{\partial \ln P}{\partial \ln V} \right)_S = \frac{c_P}{c_P \left(\frac{\partial \ln V}{\partial \ln P} \right)_T + \frac{PV}{T} \left(\frac{\partial \ln V}{\partial \ln T} \right)_P} \quad (2.9-20)$$

This may be written as

$$\left(\frac{\partial \ln P}{\partial \ln V}\right)_S = \frac{c_P}{c_V \left(\frac{\partial \ln V}{\partial \ln P}\right)_T} \quad (2.9-21)$$

where

$$c_V \equiv \left(\frac{\partial u'}{\partial T}\right)_V = c_P + \frac{PV \left(\frac{\partial \ln V}{\partial \ln T}\right)_P^2}{\left(\frac{\partial \ln V}{\partial \ln P}\right)_T} \quad (2.9-22)$$

Using the symbols

$$\gamma_S = \left(\frac{\partial \ln P}{\partial \ln \rho}\right)_S \quad (2.9-23)$$

and

$$\gamma = \frac{c_P}{c_V} \quad (2.9-24)$$

equation (2.9-21) may be written as

$$\gamma_S = -\frac{\gamma}{\left(\frac{\partial \ln V}{\partial \ln P}\right)_T} \quad (2.9-25)$$

Using the equation of state given in equation (2.2-5), from equation (2.9-19) the familiar expression for velocity of sound is found as

$$a = \sqrt{nRT\gamma_S} \quad (2.9-26)$$

Noting that the γ_S defined by equation (2.9-23) is required in equation (2.9-26) and not the specific heat ratio γ defined in equation (2.9-24)

Gordon⁽⁴⁴⁾ gives first derivative relations that are of interest in rocket performance calculations. One of these derivatives is:

$$\left(\frac{\partial \ln P}{\partial \ln T}\right)_S = \frac{c_P}{nR \left(\frac{\partial \ln V}{\partial \ln T}\right)_P} \quad (2.9-27)$$

Chapter Three

Theoretical Analysis of Solid Rocket Motor

3. Theoretical Analysis of Solid Rocket Motor

3.1. Introduction:

A rocket motor is a jet propulsion device that produces thrust by ejecting stored matter, called the propellant⁽⁹⁾. A rocket motor provides the means whereby chemical matter is burned to release the energy stored in it and the energy expanded by ejection at high velocity of the products of combustion. The ejection imparts motion to the vehicle in a direction opposite to that of the ejected matter. Rocket engines can be classified according to the type of energy source used (chemical, nuclear, solar), the type of vehicle (aircraft motor, missile motor, assisted take-off motor, space vehicle motor), size, type of propellant, type of construction, or number of motors used at a given vehicle⁽⁴⁷⁾.

The primary goal of the “Theoretical Analysis of a Solid Rocket Motor” chapter is to present the theoretical basis for the functioning of a solid propellant rocket motor. The secondary goal is to present the fundamental tools that may be used in the design of rocket motors.

3.2. Chemical Rocket motor:

The energy from a high-pressure combustion reaction of propellant chemicals, usually a fuel and an oxidizing chemical, permits the heating of reaction product gases to very high temperatures (2500 to 4000 °C). These gases subsequently are expanded in a nozzle and accelerated to high velocities (2000 to 4000 m/s). According to the physical state of the propellant, there are several different types of chemical rocket engines⁽⁸⁵⁾.

Liquid propellant rockets use liquid propellants that are fed under pressure from tanks into the thrust chamber. (The term *thrust chamber* is used

for the assembly of the injector, nozzle, and chamber). The liquid propellants usually consist of liquid oxidizer (e.g., liquid oxygen) and a liquid fuel (e.g., gasoline). In the thrust chamber the propellants react to form hot gases, which in turn are accelerated and ejected at a high (supersonic) velocity through a convergent-divergent nozzle, thereby imparting momentum to the system. A liquid rocket unit usually permits repetitive operation and can be started and shut off at will. If the thrust chamber is provided with adequate cooling capacity, it is possible to run liquid rockets for periods exceeding one hour, dependent only on the propellant supply. A liquid rocket propulsion system is, however, relatively complicated; it requires several precision valves and a complex feed mechanism which often includes propellant pumps, turbines, or a propellant pressurizing device, and a relatively complex combustion or thrust chamber.

In solid propellant rockets⁽⁷⁷⁾ the propellant to be burned is contained within the combustion chamber or case. The propellant charge is called the *grain* and it contains all the chemical elements for complete burning. Once ignited, it usually burns smoothly at a nearly constant rate on the exposed surface of the charge. Because there are no feed systems or valves, such as there are in liquid units, solid propellant rockets are usually relatively simpler in construction.

Gaseous propellant engines⁽⁷⁴⁾, also commonly referred to as *cold gas jets*, use stored high-pressure gas as their working fluid or propellant. The stored gas requires relatively heavy tanks.

Hybrid propellant rocket engines⁽⁷⁴⁾ use both a liquid and a solid propellant. For example, if a liquid oxidizing agent is injected into a combustion chamber filled with solid carbonaceous fuel grain, the chemical reaction produces hot combustion gases.

3.3. Basic Assumptions⁽⁷⁴⁾:

The various physical and chemical processes that occur in an actual rocket motor during operation are highly complex. These processes include the complex chemical reactions that occur during combustion; the manner in which consumption of the propellant grain occurs during burning; the behavior of the flow of exhaust gases as they form at the burning surface, travel through the chamber, and exit through the nozzle; the interaction between the exhaust gases and condensed particles (smoke). The theoretical analysis of a solid rocket motor necessitates certain simplifications, that is, the assumption is of an *ideal rocket motor*. An ideal rocket motor assumes the following:

- ⊗ The propellant combustion is complete and does not vary from that assumed by the combustion equation.
- ⊗ The combustion products obey the *perfect gas law*.
- ⊗ There is no friction impeding the flow of exhaust products.
- ⊗ The combustion and flow in the motor and nozzle is *adiabatic*, that is, no heat loss occurs to the surroundings.
- ⊗ Unless noted otherwise, *steady-state* conditions exist during operation of the motor. This means that the conditions or processes that occur do not change with time (for a given geometric conditions) during burning.
- ⊗ Flow through the nozzle is one-dimensional and non-rotational.
- ⊗ The flow velocity, pressure, and density is uniform across any cross-section normal to the nozzle axis.
- ⊗ Chemical equilibrium is established in the combustion chamber and does not shift during flow through the nozzle. This is known as “frozen equilibrium” conditions.

- ⊗ Burning of the propellant grain always progresses normal (perpendicular) to the burning surface, and occurs in a uniform manner over the entire surface area exposed to combustion.

Any further assumptions that may be required are stated as necessary in the following analyses. Although it seems like a lot of simplifying assumptions must be made, in fact, these are all reasonable and can be expected to reflect the actual behavior of the rocket motor fairly closely.

3.4 Propellants

Despite demonstrated rocket propulsion by methods including nuclear thermal rockets, and hall effect thrusters, chemical rocket engines remain the most commonly used type. Chemical reactants are second only to nuclear fuels in terms of energy density, which for kerosene is on the order of 3.5×10^7 J/lit. Chemical propellants have also been widely researched and used reliably in applications ranging from booster rockets for the space shuttle to hobby rockets. Due to proven reliability and wide availability, only chemical propellants were considered for this research⁽⁷⁷⁾.

The characteristics of different types of chemical rocket propellants were investigated to choose the most appropriate fuel for a rocket. Chemical propellants are usually either solid or liquid (Figure 3.4-1). Solid propellants are easy to use without special operating and handling equipment and the fuel and oxidizer can be stored mixed at room temperature. Liquid propellants are composed of liquid fuels and oxidizers that are stored separately and mixed at the time of combustion. They require systems for storage and usage, including pumps, valves and sometimes cryogenic tanks. For some applications, however, the complexity of handling liquid propellants is warranted because they often have higher specific impulses than solid propellants, and combustion can be readily throttled or stopped altogether⁽⁷⁴⁾.

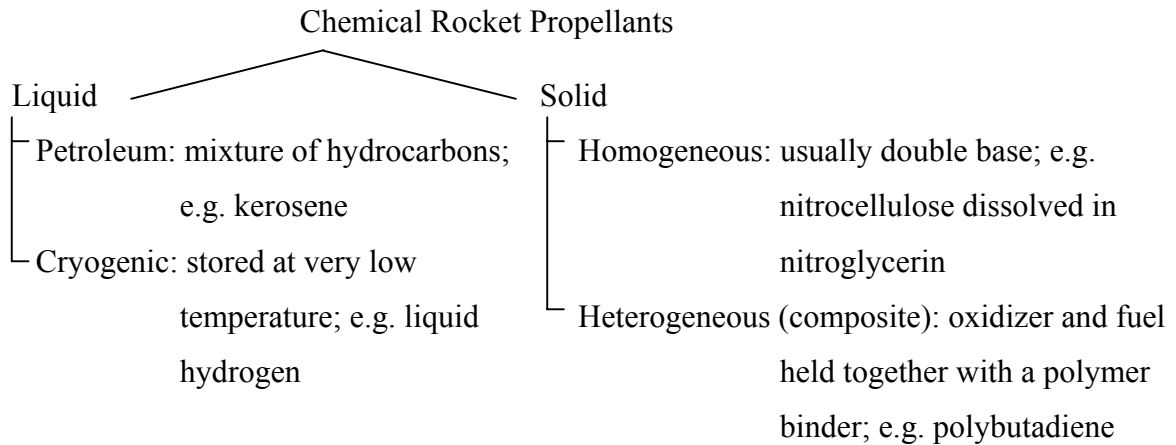


Figure 3.4-1: Types of chemical rocket propellants⁽⁷⁷⁾

3.4-1 Liquid Propellants⁽⁹⁾

Liquid propellant rockets usually use two or more propellant components. In some cases a liquid monopropellant may be used. Liquid bipropellant rocket engines commonly are used in large missile systems. A liquid fuel and a liquid oxidizer are carried in separate propellant tanks. They are pressurized, injected into the combustion chamber, and ignited to produce high-pressure gases that provide the reaction force through an exhaust nozzle.

A liquid monopropellant contains the oxidizing agent and the fuel in a single substance. It may be a mixture of compounds such as hydrogen peroxide and alcohol or it may be a homogeneous chemical agent such as nitromethane. Monopropellant must be stable at ordinary environmental conditions and decomposes when heated in the presence of a catalyst under pressurized conditions to yield the combustion gases.

3.4-2 Solid Propellants⁽³⁾

A solid propellant is a chemical or mixture of chemicals in a plastic or rubber form, which produces high-pressure gases when it burns. These high-pressure gases when exhausted from a combustion chamber provide a reactive force for rocket propulsion. A typical solid propellant may include two or

more of the following functional ingredients: oxidizer, fuel, additives, and inhibitors. Solid propellant are formulated to include all the materials necessary for reaction. The solid block of propellant is called the grain and is formed in or inserted into the combustion chamber.

For military applications solid propellant rockets are usually preferred over liquid propellant systems, especially for applications in aerodynamically stabilized free rockets. One of the main capabilities of the liquid system (control of thrust during flight) is seldom required in aerodynamically stabilized free rockets. The advantages of the solid propellant rocket are its simplicity, mobility, reliability, ease of storage, and ease of launching. The solid propulsion system has no moving parts such as valves, pressurization system, and controls. It is simple and easy to use and requires little servicing.

Three general types of processed solid propellant are double-base, composite, and composite double-base propellant. The composite propellant is a heterogeneous mixture of oxidizing crystals in an organic rubber or plastic-like fuel binder. The double-base propellant, sometimes called homogeneous propellant, is a propellant in which the fuel and oxidant are contained in the same molecule. The composite double-base propellant consists of a combination of the chemical compounds of the other two types of propellants. Each type of propellant is discussed further in the paragraphs that follows.

3.4-2-1 Double-Base Propellants⁽⁷⁾

Double-base propellant, of which there are several kinds, in general are colloidal monopropellant mixtures comprising three principal ingredients: a polymer, an oxidizer-plasticizer, and a fuel plasticizer. The polymer is the binder, which acts as a suspension medium for the fuel and oxidizer in the

double-base propellant. The oxidizer and fuel are chemically linked in the same molecule, and energy is released when the mixture burns.

The most widely used double-base polymer is nitrocellulose or cellulose hexanitrate (NC)⁽⁴⁾. It is an amorphous material, which ignites at about 160° to 170°C. Since it is under oxidized, it can also be regarded as a fuel.

The oxidizer-plasticizer must be physically compatible with the polymer. A widely used double-base oxidizer-plasticizer is nitroglycerin or glycerol trinitrate (NG), a high-energy explosive in the form of an oily liquid that explodes at 260°C. Another double-base propellant was developed that replaces NG with diethylene glycol dinitrate. This material is safer to handle than NG and is a better gelatinizing agent for NC. The optimum stoichiometric mixture from energy considerations of these two compounds should contain about 8.6 parts of NG to 1 part of NC. However, to obtain reasonable physical and storage characteristics of the solid colloid, the amount of NG must be limited to approximately 25%⁽³⁾. This under oxidation results in the tactical double-base propellants attaining energy levels far less than the optimum available.

The fuel-plasticizer must be physically compatible with the polymer. The fuel-type plasticizers are frequently some form of plastic. Some propellants tend to deteriorate or thermally degrade in storage at high temperature, and stabilizer additives are added to suppress the thermal degradation process⁽⁴⁵⁾.

Small quantities of other additives are usually included to promote smooth burning, improve mechanical properties, and tailor performance characteristics⁽⁴⁵⁾.

3.4-2-2 Composite Propellants⁽⁵⁾

Modern composite propellants have three principals ingredients: a fuel, which is an organic polymer, called the binder; a finely powered inorganic oxidizer (generally ammonium perchlorate (AP)); and additives⁽⁶⁾. The additives are for the purpose of catalyzing the combustion process, increasing density, increasing specific impulse, improving physical properties, and increasing storage life. The fuel-binder acts as a suspension medium for the oxidizer and a metallic fuel additive if an additive is used. The fuel-binder can be any combustible material with reasonable strength and adhesion to the oxidizer particles. Various rubbers and plastics have been used over the years as the fuel-binder. The present preferred binder for tactical solid motors is a hydroxy terminated polybutadiene (HTPB) rubber. Binders used in composite propellants are primarily the elastomeric monomers. Binder receiving the most development effort and application are listed in table 3.4-1.

Table 3.4-1

Binders For Composite Propellants

Polysulfides
Polyurethane
Butadiene Acrylic Acid Copolymers (PBAA)
Polyvinyl Chloride
Carboxy Terminated Polybutadiene (CTPB)
Hydroxy Terminated Polybutadiene (HTPB)

The oxidizers used in composite propellants are the chlorates, and inorganic nitrates. Table 3.4-2 lists some of the inorganic oxidizers which might be considered for use in solid propellants. Variables that must be considered in selecting an oxidizer are the amount of available oxygen, heat of formation of the oxidizer, molecular weight of the exhaust gases, oxidizer density, and toxicity and corrosive properties of the exhaust products. The

total amount of oxygen in the oxidizer cannot be made available to support the combustion of the fuel; some of this oxygen reacts chemically with other elements and is exhausted as by-products of the combustion.

Table 3.4-2

Inorganic Oxidizers For Composite Propellants

Oxidizer	Chemical Symbol
Ammonium Nitrate	NH_4NO_3
Ammonium Perchlorate	NH_4ClO_4
Sodium Nitrate	NaNO_3
Potassium Perchlorate	KClO_4
Sodium Perchlorate	NaClO_4
Potassium Nitrate	KNO_3
Lithium Perchlorate	LiClO_4
Lithium Nitrate	LiNO_3
Nitronium Perchlorate	NO_2ClO_4

Most solid propellants have ingredients that are hydroscopic; consequently, it is necessary to consider the effects of moisture on these materials. Ammonium perchlorate (AP) and potassium perchlorate (KP) are useful in situations in which the propellant is exposed to moisture since these perchlorates are only slightly soluble in water.

Transition metal oxides (TMO) catalysts such as Fe_2O_3 , CuO , MnO_2 , and CuCr_2O_4 , form a very popular group of catalysts for burning rate modification of composite solid propellants⁽⁴⁵⁾. It is known that these oxides affect the decomposition characteristics of polymers and oxidizers such as AP and KP. These burning rate modifiers give composite propellants a wide range of burning rates and must be considered in the propellant selection.

The energy content of a solid propellant can be increased by including certain light metals such as finely powdered aluminum in the propellant formulation. The addition of aluminum increases the combustion temperature and thereby the specific impulse.

3.4-2-3 Composite Double-Base Propellants⁽⁴⁵⁾

Composite modified double-base propellants contain both homogeneous (double-base) propellants and heterogeneous mixture (composite propellant). In these propellants, solid oxidizers such as ammonium salts or nitramines are held together in a matrix of nitrocellulose-nitroglycerin. Since nitrocellulose and nitroglycerin are both explosive, processing and handling of double-base and composite double-base propellants involves hazards; consequently, special precautionary measures are required.

3.4-3 Propellant Grain⁽⁶⁵⁾

Experimental composite propellants may have a composition that is complex, and may contain oxidizer of various mesh sizes, polymer binder, and even metals such as aluminum or magnesium. Curing agents, phase stabilizers, and solvents may be other additives included in small percentages. For any propellant, additives may control the burn rate, either to accelerate or to slow the rate. Regardless of the composition, however, all propellants are processed into a similar basic geometric form, referred to as a propellant grain. As a rule, propellant grains are cylindrical in shape to fit neatly into a rocket motor in order to maximize volumetric efficiency. The grain may consist of a single cylindrical segment (Figure 3.4-2), or may contain many segments. Usually, a central *core* that extends the full length of the grain is

introduced, in order to increase the propellant surface area initially exposed to combustion.

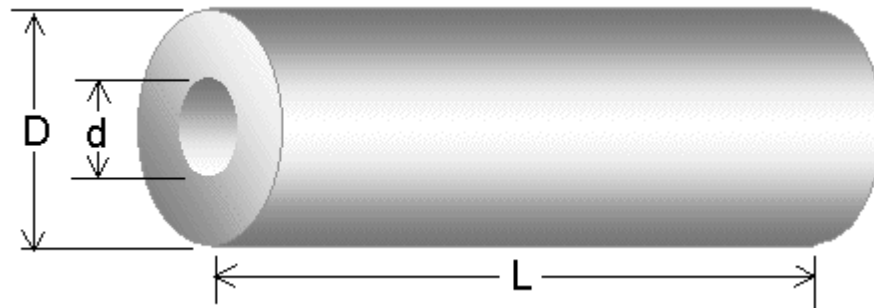


Figure 3.4-2: Hollow cylindrical grain

The core may have a wide variety of cross-sections such as circular, star, cross, dog-bone, wagon-wheel, etc., however, for amateur motors, the most common shape is circular. The core shape has a profound influence on the shape of the thrust-time profile, as shown in Figure 3.4-3.

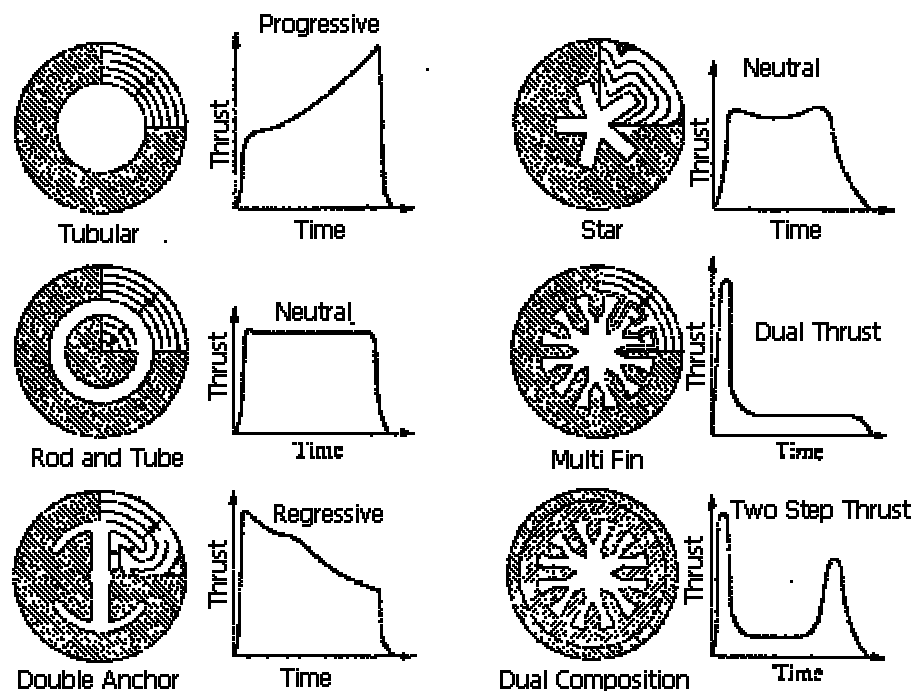


Figure 3.4-3: Core shapes and influence on thrust curve⁽⁷⁴⁾

The thrust (and chamber pressure) that a rocket motor generates is proportional to the burning area at any particular instant in time. This is referred to as the instantaneous burning area. The burning surface at any point recedes in the direction normal (perpendicular) to the surface at that point, the result being a relationship between burning surface and web distance burned that depends almost entirely on the grain initial shape and restricted (inhibited) boundaries. This important concept is illustrated in Figure 3.4-4, where the contour lines represent the core shape at successive moments in time during the burn. Notice that the shape of the thrust-time curve changes with the vertical lines corresponding to the same successive moments during the burn. As can be seen, the star grain provides an approximately neutral burn, as the surface area remains constant throughout the burn duration. A neutral burn is usually desirable because it provides for greater efficiency in delivery of total impulse, as a nozzle operates most efficiently at a constant chamber pressure.

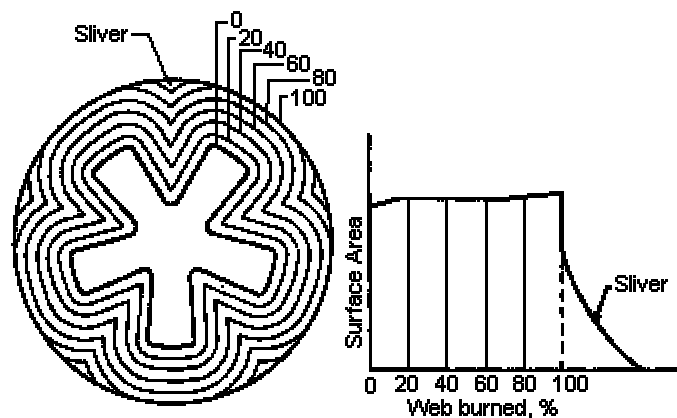


Figure 3.4-4: Grain regression

It is important to recognize that the burning area of a propellant grain is a key parameter in determining the performance of a rocket motor. The primary function of a propellant grain is to produce combustion products at a prescribed flowrate defined by⁽⁷⁴⁾:

$$\dot{m}_g = A_b \rho_p r \quad (3.4-1)$$

where ρ_p = the propellant mass density,

A_b = the burning area, and

r = the propellant burn rate.

A complete discussion on burn rate is shown in appendix A. The total burning area consists of all propellant surfaces that are exposed to combustion (and thus not inhibited from burning by some means). The grain burning area is dependant upon:

- Grain geometry, as described above
- Use of inhibitors⁽⁴⁵⁾

An inhibitor is a material or coating that is sufficiently heat resistant such that any propellant surfaces protected by the inhibitor do not combust during the entire operating duration of the motor.

An important physical property of the propellant grain is the Mass Density, which is used in performance calculations. If a propellant is comprised of two constituents, and oxidizer and a fuel, the *ideal density* is given by

$$\rho_p = \frac{1}{\frac{f_o}{\rho_o} + \frac{f_f}{\rho_f}} \quad (3.4-2)$$

where ρ_p = the propellant mass density,

f = the mass fraction, and

subscripts “o” and “f” refer to oxidizer and fuel , respectively.

If a propellant is comprised of more than two constituents, then the ideal density is given by (where a, b, c... denote the individual constituents):

$$\rho_p = \frac{1}{\frac{f_a}{\rho_a} + \frac{f_b}{\rho_b} + \frac{f_c}{\rho_c} + \dots} \quad (3.4-3)$$

The actual density can be obtained by accurately weighing a grain to determine its mass, and by measuring its volume, with the density expressed as

$$\rho_p = \frac{m_{\text{grain}}}{V_{\text{grain}}} \quad (3.4-4)$$

$$V_{\text{grain}} = \frac{\pi}{4} (D^2 - d^2) L \quad (3.4-5)$$

For a hollow cylindrical grain, where D = outer diameter,

d = inner (core) diameter

L = length of grain

The actual density will usually be some percentage less than the ideal density (typically 94%-97%), owing to tiny voids in the grain, and is dependant upon manufacturing technique. Volume is best obtained by the Archimedes principle, which involves immersion of the grain in an appropriate liquid, and measuring the displaced volume.

The Volumetric Loading Fraction is defined as the fraction of grain volume to available chamber volume, and relates the volumetric efficiency of the motor, as well as a measure of performance efficiency:

$$V_l = \frac{V_p}{V_a} = \frac{I_t}{I_{sp} \rho_p V_a} \quad (3.4-6)$$

where V_p = the grain volume,

V_a = the available chamber volume,

I_t = the total impulse (deliverable), and

I_{sp} = the propellant specific impulse.

The Web Fraction is the ratio of propellant web thickness to grain outer radius, and is given by:

$$W_f = \frac{D-d}{D} = \frac{2r t_b}{D} \quad (3.4-7)$$

where t_b = the motor burn time.

Clearly, to maximize burn duration, it is necessary to maximize the web fraction (i.e. thickness). The disadvantage of maximizing web thickness is the reduction of the grain core diameter. This must be carefully considered, as explained below.

The Port-to-Throat area ratio is given by the flow channel cross-sectional area to the nozzle throat cross-sectional area:

$$\frac{A_p}{A_t} = \frac{\pi D^2 (1 - V_l)}{4 A_t} \quad (3.4-8)$$

where A_p = the flow (channel) area of the grain and

A_t = the throat cross-sectional area.

Gas velocity along the length of the flow channel is influenced significantly by the magnitude of the port-to-throat area ratio. Choked flow occurs when the ratio is 1.0, with flow velocity through the port being equal to the flow velocity through the nozzle throat (sonic). Severe erosive burning (core stripping) may occur under such a condition, and is generally avoided in design. The criticality of the port-to-throat ratio, however, depends upon the mass flowrate at a given location. In fact, a ratio of 1.0 (or less) may be used at the forward end of the grain where mass flowrate is minimum. The port-to-

throat area ratio is often used as an index from which erosive burning tendencies are established. For those propellants where this has not been established, a ratio of 2.0 to 3.0 (dependant upon grain L/D ratio) is suggested.

Length-to-Diameter ratio is the grain overall length in relation to the grain outer diameter. This parameter is very significant in motor design, as larger L/D values tend to result in greater erosive burning effects (including negative erosive burning). High L/D values tend to generate high mass flow rate differentials along the grain length, and may be best served with a tapered core or stepped core diameters (largest nearer the nozzle)⁽⁵³⁾.

3.4-4 Propellant Combustion⁽⁷²⁾

A rocket motor operates on the basic principle of converting heat energy, from chemical reactions, to kinetic energy. In other words, the heat liberated by the combustion of propellant supplies the heat energy; the high velocity exhaust products exiting the motor have gained kinetic energy. This is why the exhaust experiences a significant drop in temperature as it flows through the nozzle, a requirement of the thermodynamics law of “conservation of energy”.

Combustion is an exothermic chemical reaction. To start the combustion, an external heat source is required (igniter) to supply the necessary energy to a threshold level. The combustion is represented by a chemical equation.

Derivation of the complete combustion equation is potentially the most complex step in the analysis of a rocket motor. The propellant is burned, at (assumed) constant pressure, and forms a set of molecular products that are in thermal and chemical equilibrium with each other. The first step is to assume what the products of combustion might be. For propellants containing only

carbon, oxygen, hydrogen, and nitrogen (C, H, O & N) there are (at least) twelve possible products (carbon, carbon dioxide, carbon monoxide, hydrogen, steam, oxygen, nitrogen, nitric oxide as well as the dissociation products H, O, N and OH). If the propellant contains metallic elements such as potassium (K), sodium (Na), or aluminum (Al), or contains Chlorine (Cl), this will result in condensed (liquid or solid) products of combustion, such as potassium carbonate, (or sodium equivalents), aluminum oxide or potassium chloride.

Once a set of possible products has been arrived at, the next step is to determine the mole numbers (or fractions) that will result. The mole numbers are the coefficients in the chemical equation.

Determining the mole numbers is accomplished by simultaneously solving a set of equations relating the reactants and products with respect to the conditions of:

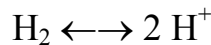
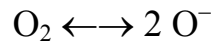
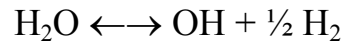
- Mass balance
- Chemical equilibrium conditions
- Energy balance

Mass balance is straightforward, and refers to the principle of conservation of mass. The number of moles of any given element (e.g. C, H, O, N) before a chemical reaction must be equal to that after a chemical reaction.

Many reactants, when mixed in definite quantities, react to form products only, in a so-called irreversible reaction. An example is the burning of a propellant. In a reversible reaction, however, the process goes both ways. Reactants form into products at the same rate that products form into the original reactants. This is the type of reaction with which chemical equilibrium conditions of hot combustion products are concerned. For example, the reaction $(2 \text{ H}_2 + \text{ O}_2 \longleftrightarrow 2 \text{ H}_2\text{O})$ is a reversible reaction. But

what determines the relative concentration of these constituents (i.e. whether the reaction will proceed more to the left or to the right in this equation)? For each equation like this, there is an equilibrium constant (K_p) associated with it that determines this. This constant is a function of the temperature at which the reaction is occurring, and is essentially independent of other physical conditions, such as pressure. Values for various K_p can be found in thermochemical tables, such as the JANAF tables^(73, 11).

It should be noted that the equilibrium of the combustion gases is very sensitive to temperature. Products existing at a high combustion temperature are very different from those existing at a lower combustion temperature. At high temperatures (above 3000 K), dissociation of the products occurs, as thermal energy causes the products to break up into simpler and monatomic constituents, such as



At lower combustion temperatures, negligible quantities of these constituents form. Dissociation consumes energy that would otherwise be available for conversion to kinetic energy of the exhaust, and tends to limit the combustion temperature.

The above describes a complete set of information that is necessary in order to determine the complete combustion processes and the solution of this problem was already discussed in chapter two.

3.5 Nozzle Theory

A nozzle is a device that causes the interchange of internal and kinetic energy of a fluid as a result of changing cross-sectional area available for

flow⁽⁶⁷⁾. The primary function of the nozzle in the rocket engine is to expand the hot propellant gases from the high pressure combustion chamber to or near the external ambient pressure, thereby converting thermal energy into directed kinetic energy or thrust. The theoretical thermodynamic relations provide methods for calculations of rocket motor performance and design parameters. The flow of combustion gases as they are expanded through the nozzle is assumed to be isentropic flow (adiabatic and reversible) based on an average nozzle specific heat ratio or from a knowledge of the chemical equilibrium composition of the reactant products⁽¹⁸⁾.

The maximum thrust from an engine is obtained when the combustion gases are expanded to the ambient atmospheric pressure. Since rockets usually operate at varying altitudes and the atmospheric pressure varies with altitude, the selected design expansion ratio of the nozzle is usually a compromise between the thrust and the nozzle expansion ratio, length, and weight⁽⁶⁵⁾.

The primary function of a nozzle (as stated before) is to channel and accelerate the combustion products produced by the burning propellant in such a way as to maximize the velocity of the exhaust at the exit, to supersonic velocity. The familiar rocket nozzle, also known as a convergent-divergent, or deLaval nozzle, accomplishes this remarkable achievement by simple geometry. In other words, it does this by varying the cross-sectional area (or diameter) in an exacting form. The analysis of a rocket nozzle involves the concept of “steady, one-dimensional compressible fluid flow of an ideal gas”. Briefly, this means that⁽³⁹⁾:

- The flow of the fluid (exhaust gases + condensed particles) is constant and does not change over time during the burn

- One-dimensional flow means that the direction of the flow is along a straight line. For a nozzle, the flow is assumed to be along the axis of symmetry

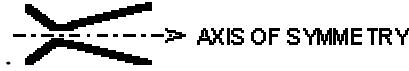


Figure 3.5-1: Nozzle symmetry

- The flow is compressible. The concept of compressible fluid flow is usually employed for gases moving at high (usually supersonic) velocity, unlike the concept of incompressible flow, which is used for liquids and gases moving at speeds well below sonic velocity. A compressible fluid exhibits significant changes in density, an incompressible fluid does not.
- The concept of an ideal gas is a simplifying assumption, one that allows use of a direct relationship between pressure, density and temperature, which are properties that are particularly important in analyzing flow through a nozzle.

Fluid properties, such as velocity, density, pressure and temperature, in compressible fluid flow, are affected by

1. Cross-sectional area change
2. Friction
3. Heat loss to the surroundings

The goal of rocket nozzle design is to accelerate the combustion products to as high an exit velocity as possible⁽⁵⁶⁾. This is achieved by designing the necessary nozzle geometric profile with the condition that isentropic flow is to be aimed for. Isentropic flow is considered to be flow that is dependant only upon cross-sectional area -- which necessitates frictionless and adiabatic (no heat loss) flow. Therefore, in the actual nozzle, it is necessary to minimize frictional effects, flow disturbances and conditions that can lead to shock losses. In addition, heat transfer losses are to be

minimized. In this way, the properties of the flow are near isentropic, and are simply affected only by the changing cross-sectional area as the fluid moves through the nozzle.

Typical nozzle cross-sectional areas of particular interest are shown in the figure below⁽⁵⁷⁾

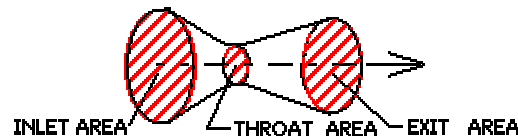


Figure 3.5-2: A typical nozzle

The analysis of compressible fluid flow involves four equations of particular interest:

1. Energy
2. Continuity
3. Momentum
4. The equation of state

The energy equation is a statement of the principle of conservation of energy. For adiabatic flow between any two points, x_1 and x_2 , it is given by

$$h_1 - h_2 = \frac{1}{2}(v_2^2 - v_1^2) = c_p (T_1 - T_2) \quad (3.5-1)$$



where h represents enthalpy of the fluid (which can be considered the energy available for heat transfer),

v = the flow velocity in the x-direction,

c_p = the effective heat capacity of the fluid, and

T = the fluid temperature.

This equation provides valuable insight into how a rocket nozzle works. Looking at the first two terms shows that the change (decrease) in enthalpy is

equal to the change (increase) in kinetic energy. In other words, heat of the fluid is being used to accelerate the flow to a greater velocity. The third term represents the resulting change (decrease) in temperature of the flow. The heat capacity may be approximated to be constant, and is a property determined by the composition of the combustion products⁽⁶⁶⁾.

It is apparent, then, that the properties of a fluid (e.g. temperature) are a function of the flow velocity. In describing the state of a fluid at any point along its flow, it is convenient to consider the stagnation state as a reference state. The stagnation properties may be considered as the properties that would result if the fluid are (isentropically) decelerated to zero velocity (i.e. stagnant flow).

The stagnation temperature, T_0 , is found from the energy equation (by setting $v_2 = 0$) to be

$$T_0 = T + \frac{v^2}{2c_p} \quad (3.5-2)$$

For an isentropic flow process, the following important relationship between stagnation properties for temperature, pressure, and fluid density hold

$$\frac{T_0}{T} = \left(\frac{P_0}{P}\right)^{\frac{\gamma-1}{\gamma}} = \left(\frac{\rho_0}{\rho}\right)^{\gamma-1} \quad (3.5-3)$$

where γ = the ratio of specific heats, also referred to as the isentropic exponent, defined as

$$\gamma = \frac{c_p}{c_v} = \frac{c_p}{c_p - R'} \quad (3.5-4)$$

Both c_p and R' (specific gas constant) are properties determined by the composition of the combustion products, where $R' = R / M$, where R is the universal gas constant, and M is the effective molecular weight of the

combustion products. If the combustion products contain an appreciable percentage of condensed phase particles (smoke), the value of the effective molecular weight, M , must account for this. As well, the proper γ must be used which takes into account two-phase flow⁽⁷⁵⁾.

The local sonic velocity, a , and the Mach number, Ma , (defined as the ratio of the flow velocity to the local sonic velocity), is given by

$$a_s = \sqrt{\gamma_s RT} \quad (3.5-5)$$

$$Ma = \frac{v}{a_s} \quad (3.5-6)$$

From equations (3.5-2), (3.5-3) & (3.5-6), the relationship between the stagnation temperature (also referred to as total temperature) and Mach number may be written as

$$\frac{T_o}{T} = 1 + \frac{\gamma - 1}{2} Ma^2 \quad (3.5-7)$$

It can be shown from the first and second laws of thermodynamics, for any isentropic process, that

$$\frac{P}{\rho} = \text{constant} \quad (3.5-8)$$

From equations (3.5-7) & (3.5-8), and from the equation of state for an ideal gas, $P = \rho RT$, the relationship between stagnation pressure; density and Mach number may be expressed as given in the following two equations

$$\frac{P_o}{P} = \left(1 + \frac{\gamma - 1}{2} Ma^2\right)^{\frac{\gamma}{\gamma - 1}} \quad (3.5-9)$$

$$\frac{\rho_o}{\rho} = \left(1 + \frac{\gamma - 1}{2} Ma^2\right)^{\frac{1}{\gamma - 1}} \quad (3.5-10)$$

Equations (3.5-3), (3.5-9) & (3.5-10) are particularly useful, as these allow each property to be determined in a flow if the Mach number and the stagnation properties are known. The stagnation (or total) properties T_o , P_o , and ρ_o are simply the properties that are present in the combustion chamber of the rocket, since the flow velocity is (considered to be) zero at this location. In other words, T_o is the combustion temperature of the propellant, P_o is the chamber pressure, and ρ_o is the density of the combustion products under chamber conditions⁽⁷⁵⁾.

Another important stagnation property is the stagnation enthalpy. This is obtained from the energy equation (by setting $v_2=0$)

$$h_0 = h + \frac{v^2}{2} \quad (3.5-11)$$

Physically, the stagnation enthalpy is the enthalpy that would be reached if the flow (at some point) were somehow decelerated to zero velocity. It is useful to note that the stagnation enthalpy is constant throughout the flow in the nozzle. This is also true of the other stagnation properties (temperature, pressure, and density).

The second of the four equations of interest regarding compressible fluid flow, as discussed earlier, is the continuity (or conservation of mass) equation, which is given by

$$\rho A v = \text{constant} = \rho^* A^* v^* \quad (3.5-12)$$

where A = the nozzle cross-sectional area,

v = the velocity of the flow.

This equation simply states that the mass flowing through the nozzle must be constant. The star (*) signifies a so-called critical condition, where Mach number is unity, $Ma=1$ (flow velocity is equal to the speed of sound). The importance of the critical condition will soon be made clear.

Taking equations (3.5-6), (3.5-7), (3.5-10) & (3.-12), it is possible to express the area ratio, A/A^* , in terms of the Mach number of the flow. The area ratio is simply the cross-sectional area at any point (x) in the nozzle, to the cross-sectional area where the critical condition exists ($Ma=1$)

$$\frac{A}{A^*} = \frac{1}{Ma} \left(\frac{1 + \frac{\gamma - 1}{2} Ma^2}{1 + \frac{\gamma - 1}{2}} \right)^{\frac{\gamma + 1}{2(\gamma - 1)}} \quad (3.5-13)$$

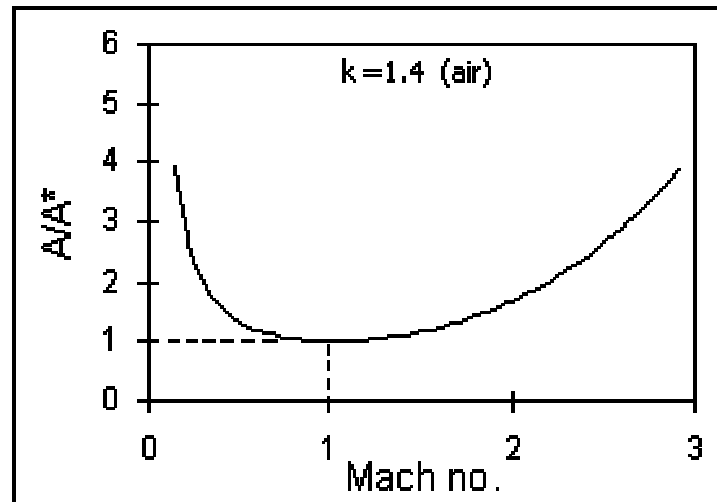


Figure 3.5-1: A/A^* versus Mach number⁽⁷⁵⁾

When a plot is made of A/A^* versus Mach number, using equation (3.5-13), a very interesting result is obtained. It clearly shows that a converging-diverging passage with a section of minimum area is required to accelerate the flow from subsonic to supersonic speed. The critical point where the flow is at sonic velocity ($Ma=1$ at $A/A^*=1$) is seen to exist at the throat of the nozzle. This shows the importance of the nozzle having a diverging section, without it, the flow could never be greater than sonic velocity⁽⁷⁵⁾.

From equations (3.5-11) & (3.5-12), the flow velocity at the nozzle exit can be expressed as

$$v_e = \sqrt{2(h_x - h_e) + v_x^2} \quad (3.5-14)$$

where subscripts e and x signify exit and any point x along the nozzle axis, respectively. This equation can then be put into the far more useful form with the aid of the energy equation and the definition of γ , as well as equation (3.5-3)⁽⁷⁴⁾.

$$v_e = \sqrt{2T_o \left(\frac{R}{M} \right) \left(\frac{\gamma}{\gamma - 1} \right) \left[1 - \left(\frac{P_e}{P_o} \right)^{\frac{\gamma-1}{\gamma}} \right]} \quad (3.5-15)$$

Equation (3.5-15) is one of the most useful equation, as it allows the nozzle exit velocity to be calculated. In summarizing, it is necessary to know

- γ , effective ratio of specific heats of the exhaust products, obtained from the combustion analysis.
- R is the universal gas constant ($R = 8.3143 \text{ J/mol-K}$)
- M is the effective molecular weight of the exhaust products, obtained from the combustion analysis, and must take into account the presence of all condensed-phase species.
- T_o is the combustion temperature of the propellant, also obtained from the combustion analysis
- P_e and P_o are the nozzle exit pressure and the chamber pressure, respectively. For most rockets, P_e can be taken as ambient atmospheric pressure: $P_e = P_a = 1 \text{ atmosphere}$. P_o may be the measured chamber pressure, design chamber pressure, or the calculated chamber pressure.

The ratio between the throat area, A^* , and any downstream area in the nozzle, A_x , at which pressure P_x exists can be conveniently expressed as a

function of the pressure ratio, P_x/P_o , and γ . By noting that at the throat Ma is unity, and using equations (3.5-3), (3.5-6), 3.5-7), (3.5-10) & (3.5-15), leads to

$$\frac{A^*}{A_x} = \left(\frac{\gamma + 1}{2}\right)^{\frac{1}{\gamma-1}} \left(\frac{P_x}{P_o}\right)^{\frac{1}{\gamma}} \sqrt{\left(\frac{\gamma + 1}{\gamma - 1}\right) \left[1 - \left(\frac{P_x}{P_o}\right)^{\frac{\gamma-1}{\gamma}}\right]} \quad (3.5-16)$$

This is another important and useful equation. It allows the exit area, A_e , to be calculated such that the exit pressure, P_e , is equal to the ambient pressure, P_a (typically 1 atm.), by simply substituting P_a for P_x .

$$\frac{A^*}{A_e} = \left(\frac{\gamma + 1}{2}\right)^{\frac{1}{\gamma-1}} \left(\frac{P_e}{P_o}\right)^{\frac{1}{\gamma}} \sqrt{\left(\frac{\gamma + 1}{\gamma - 1}\right) \left[1 - \left(\frac{P_e}{P_o}\right)^{\frac{\gamma-1}{\gamma}}\right]} \quad (3.5-16)$$

This is known as the nozzle design condition where it will later be shown that for such a condition maximum thrust is achieved. For this design, the area ratio A_e/A^* is known as the Optimum Expansion Ratio.

3.6 Rocket Motor Thrust and the Thrust Coefficient^(56, 57, 74)

The thrust that a rocket motor generates is the most fundamental measure of performance. Without a doubt, this parameter is primary in the mind of any rocket motor designer. Thrust, being the force that a motor exerts, is what propels a rocket. Thrust is generated by the expelling of mass (the exhaust) flowing through the nozzle at high velocity. The expression for thrust is given by

$$F = \int P dA = \dot{m} v_e + (P_e - P_a) A_e \quad (3.6-1)$$

where the left hand term in equation (3.6-1) represents the integral of the pressure forces (resultant) acting on the chamber and nozzle, projected on a plane normal to the nozzle axis of symmetry, as shown in the figure 3.6-1.

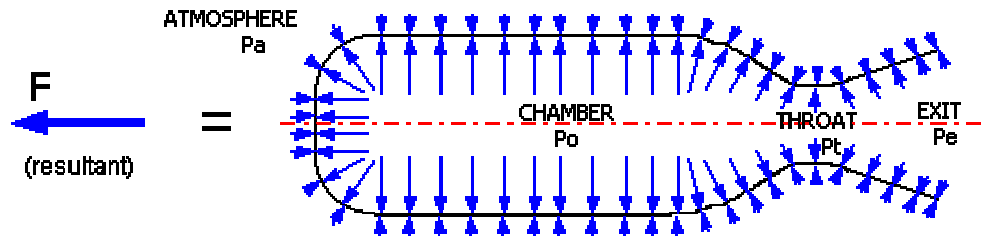


Figure 3.6-1: the thrust

The internal pressure is highest inside the chamber and decreases steadily in the nozzle toward the exit. External (atmospheric) pressure is uniform over the outside surfaces.

In the first term on the right-hand side of the equation, \dot{m} is the mass flowrate of the exhaust products and v_e is the exhaust velocity. The second term on the right-hand side is the so-called pressure thrust, which is equal to zero for a nozzle with an optimum expansion ratio ($P_e = P_a$); A_e is the nozzle exit area.

Considering continuity (conservation of mass) at the nozzle throat, equation (3.6-1) may be rewritten as

$$F = \rho^* A^* v^* v_e + (P_e - P_a) A_e \quad (3.6-2)$$

This expression can now be modified using some equations that were presented in the nozzle theory section, that is, the expressions for

- Fluid density ratio (noting that at the throat $Ma=1$), $\frac{\rho_o}{\rho}$, equation (3.5-10)
 - Critical (throat) flow velocity, v^* (equation (3.5-6), noting that $v^*=a$)
 - Nozzle exit velocity, v_e (equation 3.5-15)
 - and the equation of state for an ideal gas, $P = \rho R T$
- gives

$$F = A^* P_o \sqrt{\frac{2\gamma^2}{\gamma-1} \left(\frac{2}{\gamma-1}\right)^{\frac{\gamma+1}{\gamma-1}} \left[1 - \left(\frac{P_e}{P_o}\right)^{\frac{\gamma-1}{\gamma}}\right]} \quad (3.6-3)$$

Equation (3.6-3) shows that, if the pressure thrust term is zero, thrust is directly proportional to throat area, A^* , and is nearly directly proportional to chamber pressure, P_o .

This means that if the throat size is doubled, the thrust will be doubled (if the chamber pressure is maintained). The same holds for the chamber pressure, if it is doubled, thrust is approximately doubled. In reality, things are not so simple, as throat size and chamber pressure are tied together, as will be explained in the chamber pressure section. This means that doubling a throat size would likely involve significant design changes, such as an increase in grain burning area. Likewise, if pressure is to be increased, the casing would have to be made stronger. Thrust is also seems to be proportional to

- Pressure thrust (additive term, may be positive or negative)
- Ratio of specific heats, γ . The sensitivity to γ is quite low.
- Pressure ratio across the nozzle, P_e/P_o , as shown in figure 3.6-2.

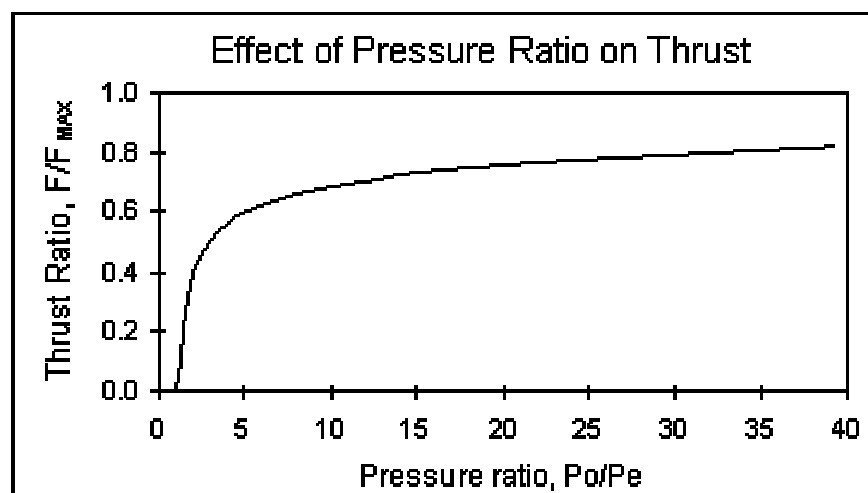


Figure 3.6-2

Figure (3.6-2) plots the thrust ratio, F/F_{\max} , to the pressure (or expansion) ratio, where F_{\max} is the thrust that could be obtained with an infinite expansion ratio (i.e. expanding into a vacuum, with $P_e=0$). In the figure, the indicated thrust, F , excludes the pressure thrust term. The total thrust produced is given by $F_{\text{total}} = F + (P_e - P_a) A_e$.

The pressure ratio of the nozzle is determined solely by the area ratio, A^*/A_e , as given by equation (3.5-17). From figure(3.6-2), it can be seen that:

- If the pressure ratio (and thus expansion ratio) is 1, then $F = 0$. The only thrust produced by such a nozzle is the pressure thrust, or $F_{\text{total}} = (P_e - P_a) A_e$. Such a nozzle, of course, would have no divergent portion, since $A^*/A_e=1$, and would be a badly designed rocket nozzle.
- The slope of the curve is very steep initially, then begins to flatten out beyond $P_o/P_e = 5$. This is significant, as it indicates that even a nozzle provided with a minimal expansion will be of significant benefit. With such a pressure ratio of 5, the resulting thrust is about 60% of maximum theoretical.

The degree to which the thrust is amplified by the nozzle is quantified by the thrust coefficient, C_f , and is defined in terms of the chamber pressure and throat area:

$$F = C_f A^* P_o \quad (3.6-4)$$

The thrust coefficient determines the amplification of thrust due to gas expansion in the nozzle as compared to the thrust that would be exerted if the chamber pressure acted over the throat area only. Equation (3.6-4) is useful, as it allows for the experimental value of C_f to be obtained from measured values of chamber pressure, throat diameter, and thrust. The ideal value of C_f is calculated from equations (3.6-3) & (3.6-4), as shown:

$$C_f = \sqrt{\frac{2\gamma^2}{\gamma-1} \left(\frac{2}{\gamma-1}\right)^{\frac{\gamma+1}{\gamma-1}} \left[1 - \left(\frac{P_e}{P_o}\right)^{\frac{\gamma-1}{\gamma}}\right]} + \frac{(P_e - P_a)A_e}{P_o A^*} \quad (3.6-5)$$

3.7 Total Impulse^(65, 74)

Although thrust is an important measure for characterizing the lift capability of a rocket motor, it provides no indication of how high the rocket will be propelled. For this, one needs a measure of the total output in terms of propulsion capability. The essential measure for this is the Total Impulse of the rocket motor, which incorporates the essential element of time, or thrust duration.

Total Impulse is defined as the time integral of the thrust over the operating duration of the motor, and is represented by the area under the thrust-time curve as shown in figure (3.7-1).

$$I_t = \int_0^{t_b} F dt \quad (3.7-1)$$

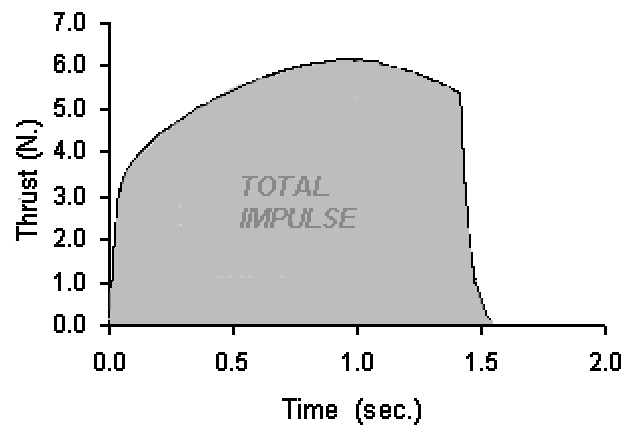


Figure (3.7-1): Thrust - time curve for a typical motor

Units are those of force multiplied by time, typically pound-seconds (lb-s) or Newton-seconds (N-s). It is important to note that the total impulse only tells part of the story regarding a motor's capacity to propel a rocket

skyward. For example, a motor that delivers a Total Impulse of 200 lb-s may provide an average thrust of 100 lb. for 2 seconds ($100 \text{ lb.} \times 2 \text{ s} = 200 \text{ lb-s}$), or may deliver a thrust of 25 lb. for 8 seconds ($25 \text{ lb} \times 8 \text{ s} = 200 \text{ lb-s}$), as shown in figure (3.2-7). Both deliver the same Total Impulse, which is usually abbreviated It.

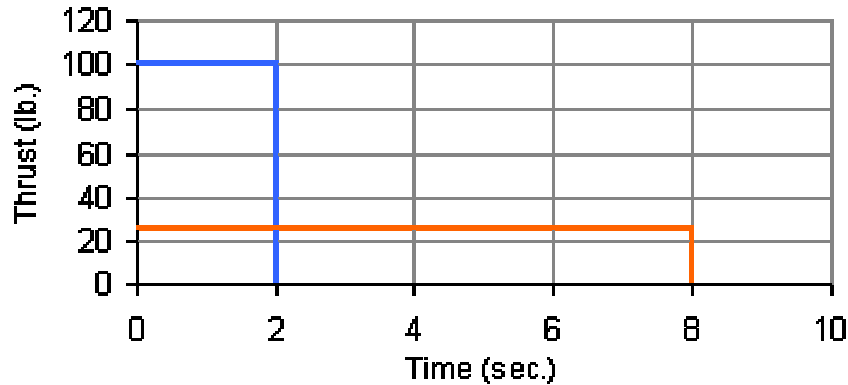


Figure (3.2-7): Two thrust-times curves with identical total impulse

The altitude achieved will differ to some extent, with this effect being more significant as the thrust/mass ratio drops. The more pronounced difference will be with the rocket's acceleration, since initial acceleration is given by:

$$a = \frac{F}{m} - g \quad (3.7-2)$$

where F = thrust,

m = rocket liftoff mass, and

g = acceleration of gravity.

With lower acceleration, the longer it takes for the rocket to achieve a velocity at which the fins provide effective stability. And in the extreme case, if the thrust is less than the liftoff weight, the rocket will not even leave the launch pad, regardless of the motor's Total Impulse.

3.8 Characteristic Velocity⁽⁷⁴⁾

The characteristic velocity, also called c-star (c^*), is a figure of thermochemical value for a particular propellant and may be considered to be indicative of the combustion efficiency. The expression for ideal c^* is given in equation (3.8-1), and is seen to be solely a function of the products of combustion (γ , M , T_o).

$$c^* = \sqrt{\frac{\frac{R'}{M} T_o}{\gamma \left(\frac{2}{\gamma - 1} \right)^{\frac{\gamma + 1}{\gamma - 1}}} \quad (3.8-1)$$

The value used for γ should be that for the mixture of gases and condensed phase.

The delivered specific impulse is related to c^* as follows:

$$I_{sp} = \frac{c^* C_f}{g} \quad (3.8-2)$$

where c^* accounts for the influence of the combustion and C_f (thrust coefficient) accounts for the influence of the nozzle. As such, c^* may be considered to be analagous to the specific impulse with a $C_f=1$.

The delivered c^* may be obtained from a rocket motor's pressure-time trace, being given by time integral of chamber pressure over the burn, multiplied by the ratio of throat area to propellant mass, as shown:

$$c^* = \frac{A_t}{m_p} \int_0^{t_b} P(t) dt \quad (3.8-3)$$

3.9 Specific Impulse⁽⁷⁴⁾

The specific impulse that a propellant is capable of producing (either theoretical or delivered) is the key measure of performance potential. In its

basic form, specific impulse can be considered to relate the thrust produced by a unit mass (e.g. 1 lb or kg) of propellant over a burning time of one second. As such, the units of specific impulse would be lb-s/lb or N-s/kg. In the former set of units, the "lb" can be considered to cancel, giving the more conventional units of seconds. For the latter set of units, division of specific impulse in N-s/kg by the acceleration of gravity, g (9.806 metre/s) results in the more conventional "seconds".

Delivered specific impulse produced by a motor, for example from static test measurements, is obtained from the expression:

$$I_{sp} = \frac{I_t}{w_p} \quad (3.9-1)$$

where w_p = the propellant weight (lb or kg \times g).

Delivered specific impulse has a dependency upon:

- Mass flowrate, and thus on motor size
- Available combustion energy of the propellant
- Nozzle efficiency
- Ambient pressure conditions
- Heat loss to the motor hardware
- Two-phase flow losses
- Combustion efficiency

These factors are discussed in detail the Corrections for "Actual" Rocket Motors section

The ideal specific impulse of a rocket propellant is calculated using equation (3.5-15), which expresses exhaust velocity, v_e , in terms of the flow properties and the pressure ratio. Since $v_e = c^* C_f$, ideal I_{sp} can be determined from equation (3.8-2):

$$I_{sp} = \frac{1}{g} \sqrt{2T_o \left(\frac{R}{M} \right) \left(\frac{\gamma}{\gamma - 1} \right) \left[1 - \left(\frac{P_e}{P_o} \right)^{\frac{\gamma-1}{\gamma}} \right]} \quad (3.9-2)$$

3.10 Chamber Pressure⁽⁷⁴⁾

The chamber pressure that a rocket motor develops is of crucial importance with regard to the successful operation of a rocket motor. Not only does Chamber Pressure strongly influence propellant burn rate, thermodynamic efficiency and thrust, the Chamber Pressure structurally loads the rocket motor casing and closures to a critical extent. Understanding the nature of chamber pressure generation, and accurate prediction of such, is one of the keys to successful rocket motor design.

Intuitively, the pressure buildup is a result of the combustion of the propellant grain, whereby the gases produced hasten to escape through the nozzle throat. If the throat is sufficiently small, the gases cannot escape quickly enough and the accumulation of gases in the chamber results in pressurization.

In actuality, the intuitive explanation is essentially correct. However, an important factor that determines the magnitude of chamber pressure is not at all intuitive, the concept of choked flow. This concept provides for a convenient means to calculate chamber pressure, and is valid for both transient and steady state modes of motor operation, as discussed below.

By looking at a plot of chamber pressure over the operating duration of a rocket motor (Figure 3.10-1), one sees that there are three distinct and important phases of operation:

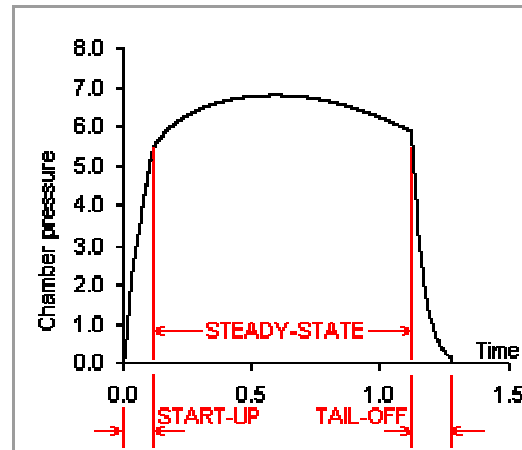


Figure 3.10-1: Motor chamber pressure

The pressure curve of the rocket motor exhibits transient and steady state behavior. The transient phases are when the pressure varies substantially with time, during the ignition and start-up phase, and following complete (or nearly complete) grain consumption, when the pressure falls down to ambient level during the tail-off phase. The variation of chamber pressure during the steady-state burning phase is due mainly to variation of grain geometry (burning surface area) with associated burn rate variation. Other factors may play a role, however, such as nozzle throat erosion and erosive burn rate augmentation.

First of all, the start-up and steady-state pressure phases will be considered. The start-up phase is hypothetically very brief, although in reality, ignition of the complete grain does not occur instantaneously. The actual duration of the start-up phase is strongly dependant upon the effectiveness of the igniter system employed. The steady-state phase clearly dominates the overall performance of the motor, and as such, constitutes the design condition. In determining the start-up pressure growth, and the steady-state pressure level, it is first noted that the rate of combustion product generation is equal to the rate of consumption of the propellant grain, given by:

$$\dot{m}_g = A_b \rho_p r \quad (3.10-1)$$

where ρ_p = the propellant density,

A_b = the grain burning area, and

r = the propellant burn rate (surface regression rate).

It is important to note that the combustion products may consist of both gaseous and condensed-phase mass. The condensed-phase, which manifests itself as smoke, may be either solid or liquid particles. Only the gaseous products contribute to pressure development. The condensed-phase certainly does, however, contribute to the thrust (overall performance) of the rocket motor, due to its mass and velocity, as shown in equation (3.6-1).

The rate at which combustion products are increasingly stored within the combustion chamber is given by:

$$\frac{dMs}{dt} = \frac{d}{dt}(\rho_o v_o) = \rho_o \frac{dv_o}{dt} + v_o \frac{d\rho_o}{dt} \quad (3.10-2)$$

where ρ_o = the instantaneous gas density in the chamber, and

v_o = the instantaneous gas volume (which is equal to the free volume within the chamber).

The change in gas volume with respect to time is equal to the change in volume due to propellant consumption, given by $\frac{dv_o}{dt} = A_b r$. This leads to:

$$\frac{dMs}{dt} = \rho_o A_b r + v_o \frac{d\rho_o}{dt} \quad (3.10-3)$$

The rate at which combustion products flow through the nozzle throat is limited by the condition of choked flow. As described in the nozzle theory section, the flow achieves sonic (Mach = 1) velocity at the narrowest portion of the convergent-divergent nozzle (throat). Flow velocity, at this location, can never exceed the local speed of sound, and is said to be in a choked

condition. This allows to determine the rate at which the combustion products flow through the nozzle is given by equation (3.10-4):

$$\dot{m}_a = P_o A^* \sqrt{\frac{\gamma}{RT_o}} \left(\frac{2}{\gamma + 1} \right)^{\frac{\gamma+1}{2(\gamma-1)}} \quad (3.10-4)$$

Mass flow rate through the nozzle seems to be a function of the chamber pressure (which determines the flow density), throat area, and the gas properties (which establish sonic velocity).

The principle of mass conservation requires the balance between mass generation rate and the sum of the rates at which mass storage in the chamber and outflow through the nozzle:

$$\dot{m}_g = \frac{dMs}{dt} + \dot{m}_a \quad (3.10-5)$$

Substituting equations (3.10-1) & (3.10-3) into equation (3.10-5) gives:

$$A_b \rho_p r = A_b \rho_o r + v_o \frac{d\rho_o}{dt} + \dot{m}_a \quad (3.10-6)$$

Propellant burn rate may be expressed in terms of the chamber pressure by the Saint Robert's law (See Appendix A):

$$r = a P_o^n \quad (3.10-7)$$

where a and n are the burn rate coefficient and pressure exponent, respectively. Substituting equations (3.10-7) & (3.10-4) (mass flowrate through nozzle) into equation (3.10-6) leads to the following equation:

$$A_b \rho_p a P_o^n = A_b \rho_o a P_o^n + v_o \frac{d\rho_o}{dt} + P_o A^* \sqrt{\frac{\gamma}{RT_o}} \left(\frac{2}{\gamma + 1} \right)^{\frac{\gamma+1}{2(\gamma-1)}} \quad (3.10-8)$$

From the ideal gas law, the density derivative in the above equation may be expressed as:

$$\frac{d \rho_o}{d t} = \frac{1}{R T_o} \frac{d P_o}{d t} \quad (3.10-9)$$

As well, considering that chamber temperature, T_o , is essentially independent of chamber pressure, equation (3.10-8) may be re-written as:

$$\frac{v_o}{R T_o} \frac{d P_o}{d t} = A_b a P_o^n (\rho_p - \rho_o) - P_o A^* \sqrt{\frac{\gamma}{R T_o}} \left(\frac{2}{\gamma + 1} \right)^{\frac{\gamma + 1}{2(\gamma - 1)}} \quad (3.10-10)$$

This is a particularly useful equation, as it allows us to determine the rate of change of chamber pressure ($d P_o / d t$) during the transient start-up phase of motor operation, where the chamber pressure is rapidly climbing up to the operating steady-state level. Once the steady-state phase is reached, when the outflow of combustion gases is in equilibrium with the production of gases from propellant consumption, $(d P_o / d t) = 0$, and the left-hand side of equation (3.10-10) vanishes. The steady-state chamber pressure may then be expressed as:

$$P_o = \left[\frac{A_b a \rho_p}{A^* \sqrt{\frac{\gamma}{R T_o}} \left(\frac{2}{\gamma + 1} \right)^{\frac{\gamma + 1}{2(\gamma - 1)}}} \right]^{\frac{1}{(1-n)}} \quad (3.10-11)$$

Note that the combustion product density term has been dropped, as it is small in comparison to the propellant density.

Equation (3.10-11) may be greatly simplified by use of equation (3.10-7), letting $K_n = A_b / A^*$ and by noting that the characteristic exhaust velocity (c^*) is given by:

$$c^* = \sqrt{\frac{RT_o}{\gamma \left(\frac{2}{\gamma+1}\right)^{\frac{\gamma+1}{\gamma-1}}}} \quad (3.10-12)$$

This leads to the simplified expression for steady-state chamber pressure:

$$P_o = K_n \rho_p r c^* \quad (3.10-13)$$

where r is the burn rate at the chamber pressure, P_o .

The third and final phase of the pressure curve, the tail-down phase, ideally occurs immediately after the propellant grain has been completely consumed. In actuality, slivers or fragments of propellant grain remain once the bulk of the grain has been consumed. This results in a pressure tail-down that is more gradual than for the ideal case. However, it is impractical to account for this effect, and the tail-down pressure is determined on the assumption that the grain has been fully depleted. After burnout, when $A_b = 0$, equation (3.10-10) becomes

$$\frac{v_o}{RT_o} \frac{dP_o}{dt} = -\frac{P_o A^*}{c^*} \quad (3.10-14)$$

This differential equation may then be solved to express tail-off chamber pressure as a function of bleed down time for choked flow:

$$P_o = P_{bo} \exp\left(-\frac{R T_o A^*}{v_o c^*} t\right) \quad (3.10-15)$$

where P_{bo} = the chamber pressure at burn-out, and

t = the time from burn-out.

The pressure is seen to exhibit exponential decay. In addition to the consequence of sliver burning during tail-off, nozzle slagging will tend to make the pressure decay more gradual than predicted by equation (3.10-14).

Nozzle slagging is the tendency of condensed-phase (in particular liquid matter) to accumulate around the throat, effectively reducing the diameter. Slagging is more significant during tail-off due to the dropping pressure level and lower exhaust velocity.

3.11 Corrections for Actual Rocket Motors^(2, 3, 65)

The preceding sections dealing with solid rocket motor theory considers the analysis of an ideal rocket, which of course, does not exist. The ideal rocket represents the maximum performance condition that could be attained if it were not for real-world factors and other approximations that lead to performance reductions in actual solid rocket motors. These are accounted for by using various correction factors in the design or analysis of a rocket motor.

3.11-1 Chamber Conditions

Combustion efficiency and heat losses through the chamber wall both tend to produce a lower chamber pressure than predicted by theory. Solid propellant, however, typically has a high combustion efficiency if well mixed and the oxidizer particle size is very fine. A measure of the combustion efficiency of a propellant can be taken by comparing the measured (delivered) value of characteristic velocity (c^*) to the ideal value:

$$\eta^* = \frac{\bar{c}^*}{c^*} \quad (3.11-1)$$

The delivered value of c^* can be obtained from pressure measurements of static test results:

$$\bar{c}^* = \frac{At}{mp} \int_0^{t_b} P(t) dt \quad (3.11-2)$$

To some degree, the combustion efficiency is a function of the motor size. Motors with longer combustion chambers provide more time for the chemical reactions to occur before dispelling through the nozzle.

Heat loss through (or into) the chamber walls is also dependant upon motor size, as well as casing material and wall thickness. For example, a larger sized motor with a thin-walled steel casing would have much less heat loss than a small motor with relatively thick walled aluminum casing. However, the overall detrimental effect is probably insignificant for both.

As experimental rocket motors typically have short burn times, a significant portion of the total impulse may result from the pressure start-up or tail-off phases of the burn, when the chamber pressure is well below the steady-state operating pressure level. As a result, the total delivered specific impulse suffers. This is one reason why delivered specific impulse can be lower than ideal, which is based on constant steady-state pressure (usually referenced at 70 atm). The extent of loss, designated ζ_p , is highly dependant upon the motor burn time and pressure-time profile, but may be 5% or greater. Thus a typical pressure correction factor would be $\zeta_p = 0.95$.

3.11-2 Nozzle Corrections

The flow through a real nozzle differs from that of an ideal nozzle because of frictional effects, heat transfer (particularly at the throat), imperfect gases and incomplete combustion, non-axial flow, nonuniformity of the fluid, and particle velocity and thermal lag. Conical nozzles are used almost for amateur motors, due to the relative simplicity in manufacturing such a nozzle. In nozzle theory, flow is assumed to be one-dimensional (axial). In a conical nozzle, the flow is two-dimensional, with the extent of the

non-axial velocity dependant upon the divergence cone half-angle, α . The correction factor for non-axial flow is given by:

$$\lambda = \frac{1}{2} (1 + \cos \alpha) \quad (3.11-3)$$

This loss is usually quite small, with typical values being $\lambda = 0.99$ for a 12 degree half-angle and $\lambda = 0.97$ for a 20 degree half-angle.

The discharge correction factor is used to express how well the nozzle design permits the mass flow rate through the throat to approach the theoretical rate, and is given by the ratio of delivered mass flow rate to ideal mass flow rate:

$$\zeta_d = \frac{\overline{\dot{m}}^*}{\dot{m}^*} \quad (3.11-4)$$

The most significant design parameter which determines the discharge factor is the contour at the entrance region of the throat. A well rounded contour tends to maximize the actual flow rate. For propellants that have a significant fraction of particles in the exhaust, good contouring minimizes acceleration of the flow at the entrance, thus minimizing the two-phase flow loss associated with particle velocity lag. Certain factors tend to increase the actual mass flow rate in comparison to the idealized mass flow rate. These factors include

- Heat transfer of the fluid to the nozzle walls, tending to decrease the flow temperature, increasing the density.
- The specific heat ratio and other gas properties change through the nozzle in such a way as to increase the discharge factor.

Consequently, for a rocket motor that has no condensed-phase products in the exhaust, the discharge correction factor may be close to unity. However, for a rocket motor that utilizes a propellant with a large fraction of condensed-phase products, the losses can be quite significant, even with a

well contoured nozzle entrance. The value of the discharge correction factor would typically be $\zeta_d = 0.90$ for this propellant with a well designed nozzle with smooth flow surfaces and minimal heat loss.

3.11-3 Corrections for Specific Impulse

The ideal specific impulse must be corrected to obtain the delivered specific impulse of an actual rocket motor, by applying the correction factors discussed above:

$$\bar{I}_{sp} = \eta * \zeta_p \zeta_d \lambda I_{sp} \quad (3.11-5)$$



Chapter Four

*Analysis and Models for
Computation of Chemical
Equilibrium in Complex Systems*

4. Analysis and Models for Computation of Chemical Equilibrium in Complex Systems

4.1. Introduction

Chemical equilibrium has been calculated theoretically, and a computer program for this purpose has been built. This program has been modified to give results, which satisfy those obtained from the experiments. This chapter shows the main equations used in building the computer program, how the program works, and the source of data used in the program.

4.2. Thermodynamic Analysis

Thermodynamic analysis of the chemical equilibrium system was already shown in chapter two. In chapter two it was stated that this system can be solved using either stoichiometric technique or non-stoichiometric techniques.

The stoichiometric techniques are based on the use of the chemical equilibrium constant for each proposed reaction. This leads to difficulties which arises from the assumption of the reactions occur, and the assumed reaction temperature.

The assumptions of the reactions occur leads either to assume few numbers of reactions (decrease in accuracy), or to assume many numbers of reactions (increase in complicity). The second problem due to the results is rises from the assumed temperature, i.e., the assumed temperature will be used as the final chamber temperature.

The non-stoichiometric techniques are based on the use of the minimization of either Gibbs free energy or Helmholtz free energy. The minimization of Helmholtz free energy is used for constant volume problems,

while the minimization of Gibbs free energy is used to constant pressure problems. As the treated system (rocket motor) is a constant pressure problem, the minimization of Gibbs free energy was used to build the program.

4.3. Input and Output Data

Thermodynamic data are included in the program for reaction products and reactants. The data are selected from a number of sources. These sources are Chase *et al*⁽¹¹⁾, Cohen *et al*⁽¹³⁾, Cox *et al*⁽¹⁶⁾, Garvin *et al*⁽²⁵⁾, Gordon *et al*⁽³²⁾, McBride *et al*^(49, 50, 51, 52), Stull *et al*⁽⁷³⁾, and Zeleznik *et al*⁽⁸³⁾. For each species heats of formation were combined with sensible heats to give assigned enthalpies.

For each reaction species the thermodynamic functions specific heats, enthalpy, and entropy as function of temperature are given in the form of least squares coefficients^(83, 48). The general form of these equations is as follows

$$\frac{C_p^o}{R} = \sum a_i T^{q_i} \quad (4.3-1)$$

$$\frac{H^o}{RT} = \frac{\int C_p^o dt}{RT} \quad (4.3-2)$$

$$\frac{s^o}{R} = \frac{\int C_p^o dt}{RT} \quad (4.3-3)$$

The least square form consists of seven terms for $\frac{C_p^o}{R}$ and corresponding terms for enthalpy and entropy as well as the integration constants a_8 and a_9 as follows:

$$\frac{C_p^o}{R} = \frac{a_1}{T^2} + \frac{a_2}{T} + a_3 + a_4 T + a_5 T^2 + a_6 T^3 + a_7 T^4 \quad (4.3-4)$$

$$\frac{H^{\circ}}{RT} = -\frac{a_1}{T^2} + a_2 \frac{\ln T}{T} + a_3 + a_4 \frac{T}{2} + a_5 \frac{T^2}{3} + a_6 \frac{T^3}{4} + a_7 \frac{T^4}{5} + \frac{a_8}{T} \quad (4.3-5)$$

$$\frac{s^{\circ}}{R} = -\frac{a_1}{2T^2} + \frac{a_2}{T} + a_3 \ln T + a_4 T + a_5 \frac{T^2}{2} + a_6 \frac{T^3}{3} + a_7 \frac{T^4}{4} + a_9 \quad (4.3-6)$$

For gases the temperature intervals are 200 to 1000 K and 1000 to 6000K. For the condensed species, each phase has its own set of coefficients.

The above thermochemical data are set in the program into two database files, the first one is the INPUT data file, and the second is the OUTPUT data file. The INPUT data file contains different types of propellants, both solid and liquid, with their properties such as molecular weight, number of atoms of each element, and data to calculate their chemical potentials.

The OUTPUT data file contains the expected reaction product species, also with their related properties.

As the program starts, it asks the user to select the reactant(s) and its (their) amount in grams. These data must be input in such away that the overall weight of the reactants equals 100 gram. The initial assumed value of reaction temperature and pressure both must be stated in SI unit.

After giving the program the asked data, the program starts to calculate the equilibrium composition. In few seconds, the results will appear, which will be divided into three parts. The first part is of equilibrium composition in the combustion chamber, the chamber temperature and pressure, number of moles of each product, the molecular weight of the mixture, number of moles of gas and of condensed species, enthalpy and entropy.

The second part is the exhaust results, which gives the same properties of the chamber results but at exhaust conditions. The third part are those of the throat, temperature, pressure, characteristic velocity, specific impulse,

specific heat ratio, and expansion ratio. Details of the results are well shown in chapter six.

4.4 Gibbs Iteration Equations

The equations required to obtain composition are not all linear in the composition variables and, therefore, an iteration procedure is generally required. In the iteration procedure to be described it will be convenient to treat n as an independent variable. A Newton-Raphson method is used to solve for corrections to the initial estimates of compositions n_j , Lagrangian multipliers λ_j , moles of gaseous species n , and (when required) temperature T . This method involves a Taylor series expansion of the appropriate equations with all terms truncated which contain derivatives higher than the first. The correction variables used are $\Delta \ln n_j$ ($j = 1, \dots, NG$), Δn_j ($j = NG+1, \dots, NS$), $\Delta \ln n$, $\pi_i = -\lambda_i/RT$, and $\Delta \ln T$. It is no restriction to start each iteration with the estimate for the Lagrangian multipliers equal to zero inasmuch as they appear linearly in equation (2.7-6). After making dimensionless those equations containing thermodynamic functions, the Newton-Raphson equations obtained from equations (2.7-6), (2.7-3), (2.7-9a), and (2.7-11a) are

$$\Delta \ln n_j - \sum_{i=1}^{\ell} a_{ij} \pi_i - \Delta \ln n - \frac{H_j^o}{RT} \Delta \ln T = -\frac{\mu_j}{RT} \quad (j = 1, \dots, NG) \quad (4.4-1)$$

$$-\sum_{i=1}^{\ell} a_{ij} \pi_i - \frac{H_j^o}{RT} \Delta \ln T = -\frac{\mu_j}{RT} \quad (j = NG+1, \dots, NS) \quad (4.4-2)$$

$$\sum_{j=1}^{NG} a_{kj} n_j \Delta \ln n_j + \sum_{j=NG+1}^{NS} a_{kj} \Delta n_j = b_k^o - b_k \quad (k = 1, \dots, \ell) \quad (4.4-3)$$

$$\sum_{j=1}^{NG} n_j \Delta \ln n_j - n \Delta \ln n = n - \sum_{j=1}^{NG} n_j \quad (4.4-5)$$

$$\sum_{j=1}^{NG} \frac{n_j H_j^o}{RT} \Delta \ln n_j + \sum_{j=NG+1}^{NS} \frac{H_j^o}{RT} \Delta n_j + \left(\sum_{j=1}^{NS} \frac{n_j C_{p,j}^o}{R} \right) \Delta \ln T = \frac{h_0 - h}{RT} \quad (4.4-6)$$

$$\sum_{j=1}^{NG} \frac{n_j S_j^o}{R} \Delta \ln n_j + \sum_{j=NG+1}^{NS} \frac{S_j^o}{R} \Delta n_j + \left(\sum_{j=1}^{NS} \frac{n_j C_{p,j}^o}{R} \right) \Delta \ln T = \frac{s_0 - s}{R} + n - \sum_{j=1}^{NG} n_j \quad (4.4-7)$$

where $C_{p,j}^o$ is the standard-state specific heat at constant pressure for species j at temperature T .

4.4-1 Reduced Gibbs Iteration Equations

For problems with assigned thermodynamic states tp , hp , or sp , various combinations of equations (4.4-1) to (4.4-7) can be used to obtain corrections to estimates. However, for chemical systems containing many species, it would be necessary to solve a large number of simultaneous equations. This large number of equations can be reduced quite simply to a much smaller number by algebraic substitution. The expression for $\Delta \ln n_j$ obtained from equation (4.4-1) is substituted into equations (4.4-3) to (4.4-7). When equation (4.4-2) written with signs reversed is included, the resulting reduced equations become

$$\sum_{i=1}^{\ell} \sum_{j=1}^{NG} a_{kj} a_{ij} n_j \pi_i + \sum_{j=NG+1}^{NS} a_{kj} \Delta n_j + \left(\sum_{j=1}^{NG} a_{kj} n_j \right) \Delta \ln n + \left(\sum_{j=1}^{NG} \frac{a_{kj} n_j H_j^o}{RT} \right) \Delta \ln T = b_k^o - b_k + \sum_{j=1}^{NG} \frac{a_{kj} n_j \mu_j}{RT} \quad (k = 1, \dots, \ell) \quad (4.4-8)$$

$$\sum_{i=1}^{\ell} a_{ij} \pi_i + \frac{H_j^o}{RT} \Delta \ln T = \frac{\mu_j}{RT} \quad (j = NG + 1, \dots, NS) \quad (4.4-9)$$

$$\begin{aligned} \sum_{i=1}^{\ell} \sum_{j=1}^{NG} a_{ij} n_j \pi_i + \left(\sum_{j=1}^{NG} n_j - n \right) \Delta \ln n + \left(\sum_{j=1}^{NG} \frac{n_j H_j^o}{RT} \right) \Delta \ln T \\ = n - \sum_{j=1}^{NG} n_j + \sum_{j=1}^{NG} \frac{n_j \mu_j}{RT} \end{aligned} \quad (4.4-10)$$

$$\begin{aligned} \sum_{i=1}^{\ell} \left(\sum_{j=1}^{NG} \frac{a_{ij} n_j H_j^o}{RT} \right) \pi_i + \sum_{j=NG+1}^{NS} \frac{H_j^o}{RT} \Delta n_j + \left(\sum_{j=1}^{NG} \frac{n_j H_j^o}{RT} \right) \Delta \ln n \\ + \left[\sum_{j=1}^{NG} \frac{n_j C_{p,j}^o}{R} + \sum_{j=1}^{NG} \frac{n_j (H_j^o)^2}{R^2 T^2} \right] \Delta \ln T = \frac{h_0 - h}{RT} + \sum_{j=1}^{NG} \frac{n_j H_j^o \mu_j}{R^2 T^2} \end{aligned} \quad (4.4-11)$$

$$\begin{aligned} \sum_{i=1}^{\ell} \left(\sum_{j=1}^{NG} \frac{a_{ij} n_j S_j}{R} \right) \pi_i + \sum_{j=NG+1}^{NS} \frac{S_j}{R} \Delta n_j + \left(\sum_{j=1}^{NG} \frac{n_j S_j}{R} \right) \Delta \ln n \\ + \left[\sum_{j=1}^{NG} \frac{n_j C_{p,j}^o}{R} + \sum_{j=1}^{NG} \frac{n_j H_j^o S_j}{R^2 T} \right] \Delta \ln T = \frac{s_0 - s}{R} + n \\ - \sum_{j=1}^{NG} n_j + \sum_{j=1}^{NG} \frac{n_j S_j \mu_j}{R^2 T} \end{aligned} \quad (4.4-12)$$

4.5 Procedure for Obtaining Equilibrium Compositions

In principle, obtaining equilibrium compositions by means of the Newton-Raphson iteration procedure discussed in sections 4.4, and 4.4-1 should offer no difficulties. However, a number of practical items require detailed attention in order to avoid numerical difficulties: initial estimates, tests for condensed phases, convergence, accidental singularities, special handling of ions, and consideration of trace species.

4.5-1 Initial Estimates

An extremely simple procedure is used in this work to assign estimates for composition. For the first iteration of the first point in a schedule of points, n is assigned to be $n = 0.1$, which is equivalent to an estimate of 10 for molecular weight. Then the number of kilogram- moles of each gaseous species per kilogram of mixture is set equal to $0.1/NG$, where NG is the number of gaseous species being considered. The number of moles of each condensed species is set equal to zero.

Admittedly, this simple procedure will often give poor initial estimates. However, this technique was found to be preferable to the alternative of devising numerous special routines for obtaining good estimates for numerous possible chemical systems⁽²⁹⁾. Furthermore, the estimating technique is used only for the first point in any schedule of points. For all points after the first the results of a preceding point serve as initial estimates.

Because no attempt is made to obtain good initial estimates, the question arises whether convergence can be guaranteed. This question is discussed in section 4.5-3.

4.5-2 Magnitude of Species Used During Iteration

Both the linear and logarithmic composition variables are used for gaseous species during the composition iteration process. Only the linear variable is used for condensed species. Corrections to compositions for gases are in the form of logarithmic variables $\Delta \ln n_j$, and therefore the logarithmic values of gaseous compositions $\ln n_j$ are continuously updated from iteration to iteration. The linear values of the compositions n_j are obtained by taking the antilogarithm of $\ln n_j$. However, to save computer time during iteration, n_j are calculated only for those species whose mole fractions are greater than a certain specified size.

This specified size has only one value, namely $n_j/n = 10^{-7}$ (or $\ln n_j = -16.1180957$). A program variable was defined as SPSZ = 16.1180957. Thus, antilogarithms of $\ln n_j$ were obtained only for gases meeting the following condition: $\ln n_j/n \geq -\text{SPSZ}$ ($n_j/n > 10^{-07}$). For gaseous species not passing this test were set equal to zero. In addition, the maximum number of iterations permitted is 50. Two variables relating to the mole fraction size for which antilogarithms are obtained are NSPSZ for non-ionized species and ISPSZ for ionized species. NSPSZ may be modified for any of the following reasons: inclusion of species in the calculation with mole fractions smaller than 10^{-7} (by means of an input parameter TRACE); a singular matrix; or the chemical system under consideration containing a chemical element that differs in magnitude from the largest of the other elements by more than 10^{-5} . The purpose of changing NSPSZ in the last case is to ensure that not all species containing the trace element will be eliminated during iteration. To aid in testing for trace elements, a parameter RATIO is defined to be the ratio of the elements with the lowest to highest kilogram-atoms per kilogram of mixture. The following, then, are the conditions under which several parameters relating to species size are set to various values.

- (1) NSPSZ = SPSZ until convergence or a singular matrix occurs
- (2) NSPSZ = XSPSZ if TRACE $\neq 0$ after first convergence, or if a singular matrix or new components occur.
- (3) ITN = maximum number of iterations.

Default⁽²⁸⁾:

- (1) SPSZ = $-\ln 10^{-07} = 16.1180957$
- (2) XSPSZ = $-\ln 10^{-11} = 25.328436$
- (3) ISPSZ = $-\ln 10^{-14} = 32.236191$
- (4) ITN = 50
- (5) TRACE = 0

Nondefault:

- (1) If $\underline{\text{TRACE}} \neq 0$, $\underline{\text{ITN}} = 50 + \text{NS}/2$
- (2) If $\underline{\text{TRACE}} < 10^{-07}$, $\underline{\text{XSPSZ}} = -\ln \underline{\text{TRACE}}$ and

$$\underline{\text{ISPSZ}} = -\ln (\underline{\text{TRACE}} \times 10^{-03}) = \underline{\text{XSPSZ}} + 6.9077553$$
- (3) If $\underline{\text{RATIO}} < 10^{-05}$, $\underline{\text{SPSZ}} = \ln 1000/\underline{\text{RATIO}}$
 and $\underline{\text{XSPSZ}} = \underline{\text{SPSZ}} + \ln 1000 (6.9077553)$
- (4) If singular matrix, $\underline{\text{XSPSZ}} = \underline{\text{NSPSZ}} = 80$.

The use of $\underline{\text{ISPSZ}}$ to control the size of ionized species permitted to be present during iteration is discussed in the section 4.5-5.

4.5-3 Convergence

The problem of convergence is discussed in Zeleznik *et.al*⁽⁸⁴⁾ and Gordon *et.al*⁽²⁸⁾. Zeleznik points out that the iteration equations sometimes give large corrections that, if used directly, could lead to divergence. Two situations can cause large corrections. The first situation occurs in the early stages of the calculation and is due to poor estimates. The second may occur at later stages of the calculation when the iteration process sometimes attempts to make extremely large increases in moles of species that are present in small amounts. In both of these cases a control factor λ is used to restrict the size of the corrections to $\ln n_j$ ($j = 1, \dots, \text{NG}$) and n_j ($j = \text{NG} + 1, \dots, \text{NS}$) as well as to $\ln n$ and $\ln T$ obtained by solving the equations in section 4.4.

The numerical value of λ is determined by empirical rules that experience has shown to be satisfactory⁽²⁸⁾. For T and n , corrections are limited to a factor of $e^{0.4} = 1.4918$. For gas-phase species two different correction controls are calculated that depend on the magnitude of the mole

fractions. The logarithm of each mole fraction is compared with the parameter $\underline{\text{SPSZ}}$. If $\ln(n_j/n) > -\underline{\text{SPSZ}}$, corrections to n_j are limited to a factor of $e^2 = 7.3891^{(29)}$. For these limitations on corrections to T , n , and n_j/n the value of a control factor λ_1 may be calculated as:

$$\lambda_1 = \frac{2}{\max\left(5|\Delta \ln T|, 5|\Delta \ln n|, |\Delta \ln n_j|\right)} \quad (4.5-1)$$

For those gaseous species for which $\ln(n_j/n) \leq -\underline{\text{SPSZ}}$ and $\Delta \ln n_j \geq 0$, a control factor λ_2 is defined as

$$\lambda_2 = \left| \frac{-\ln \frac{n_j}{n} - 9.2103404}{\Delta \ln n_j - \Delta \ln n} \right| \quad (4.5-2)$$

This prevents a gaseous species with a small mole fraction from increasing to a mole fraction greater than 10^{-4} . The control factor λ to be used in equations (4.5-4) is defined in terms of λ_1 and λ_2 as

$$\lambda = \min(1, \lambda_1, \lambda_2) \quad (4.5-3)$$

A value for λ is determined for each iteration. Whenever current estimates of composition and/or temperature are far from their equilibrium values, λ will be less than 1. Whenever they are close to their equilibrium values, λ will equal 1. New estimates for composition and temperature are then obtained from the correction equations

$$\begin{aligned} \ln n_j^{(i+1)} &= \ln n_j^{(i)} + \lambda^{(i)} (\Delta \ln n_j)^{(i)} & (j = 1, \dots, NG) \\ n_j^{(i+1)} &= n_j^{(i)} + \lambda^{(i)} (\Delta n_j)^{(i)} & (j = NG + 1, \dots, NS) \\ \ln n^{(i+1)} &= \ln n^{(i)} + \lambda^{(i)} (\Delta \ln n)^{(i)} \\ \ln T^{(i+1)} &= \ln T^{(i)} + \lambda^{(i)} (\Delta \ln T)^{(i)} \end{aligned} \quad (4.5-4)$$

where the superscript i represents the i^{th} estimate.

The iteration procedure is continued until corrections to composition satisfy the following criteria⁰:

$$\frac{n_j |\Delta \ln n_j|}{\sum_{j=1}^{NS} n_j} \leq 0.5 \times 10^{-5} \quad (j = 1, \dots, NG)$$

$$\frac{|\Delta n_j|}{\sum_{j=1}^{NS} n_j} \leq 0.5 \times 10^{-5} \quad (j = NG + 1, \dots, NS)$$

$$\frac{n |\Delta \ln n|}{\sum_{j=1}^{NS} n_j} \leq 0.5 \times 10^{-5} \quad (4.5-5)$$

For those chemical elements for which $b_o^i > 1.0 \times 10^{-6}$, the convergence test for mass balance is

$$\left| b_o^i - \sum_{j=1}^{NS} a_{ij} n_j \right| \leq (b_o^i)_{\max} \times 1.0 \times 10^{-6} \quad (i = 1, \dots, \ell) \quad (4.5-6a)$$

where the subscript “max” refers to the chemical element i with the largest value of b_o^i . When temperature is a variable, the convergence test for temperature is

$$|\Delta \ln T| \leq 1.0 \times 10^{-4} \quad (4.5-6b)$$

For a constant-entropy problem (rocket), the following convergence test on entropy is also required:

$$\left| \frac{s_0 - s}{R} \right| \leq 0.5 \times 10^{-4} \quad (4.5-6c)$$

When TRACE $\neq 0$, an additional test is used:

$$\left| \frac{\pi_i^{(k)} - \pi_i^{(k+1)}}{\pi_i^{(k+1)}} \right| \leq 0.001 \quad (i = 1, \dots, \ell) \quad (4.5-6d)$$

where the superscript refers to the k th iteration. The convergence tests in equations (4.5-5) and (4.5-6) ensure accuracy to five places in composition when expressed as mole fractions.

4.5-4 Tests for Condensed Phases

For the first point in a schedule of points, the program considers only gaseous species during the iteration to convergence. For each point after the first, the program uses the results of a previous point for its initial estimate. After every convergence the program automatically checks for the inclusion or elimination of condensed species.

The test is based on the minimization of Gibbs energy. At equilibrium, equation (4.5-5) is satisfied (*i.e.*, $\delta G = 0$). The requirement for a condensed species j , is that its inclusion will decrease Gibbs energy; that is, from equation (4.5-5)

$$\frac{\partial G}{\partial n_j} = \left(\frac{\mu_j^o}{RT} \right)_c - \sum_{i=1}^{\ell} \pi_i a_{ij} < 0 \quad (4.5-7)$$

where the subscript c refers to a condensed species.

At most, only one new condensed species is included after each convergence. In the event that several condensed species pass the test required by equation (4.5-7), only that species giving the largest negative change to Gibbs energy is included as a possible species and convergence to a new equilibrium composition is obtained. This process is repeated until all condensed species required by equation (4.5-7) are included.

If, after convergence, the concentration of a condensed species is negative, the species is removed from the list of currently considered species, and convergence to a new equilibrium composition is obtained.

4.5-5 Iteration Procedure and Tests for Ions

For ions to be considered, the charge balance equation

$$\sum_{j=1}^{NG} a_{ej} n_j = 0 \quad (4.5-8)$$

is required, where a_{ej} indicates the excess or deficiency of electrons in the ion relative to the neutral species. For example, in a mole of an ionized species, $a_{ej} = -3$ for Ar^{+++} and $+1$ for O_2^- . To prevent difficulties in matrix solutions, the program automatically removes the charge balance equation when, for each ionized species being considered, $\ln n_j/n < -\text{ISPSZ}$.

There are situations when all the previous convergence tests have been passed but the ion balance is still incorrect. A special iteration procedure was developed to obtain the correct ion balance for these situations⁽⁶¹⁾. It consists of obtaining a value of the Lagrangian multipliers for ions divided by RT , based on the assumption that the magnitude of the ionized species is small relative to the un-ionized species. The initial estimate for π_e is taken to be the value in storage for the current point or from a previous point. The iteration procedure consists of the following steps:

(1) Corrections to π_e are obtained from

$$\Delta\pi_e = \frac{-\sum_{j=1}^{NG} a_{ej} n_j}{\sum_{j=1}^{NG} (a_{ej})^2 n_j} \quad (4.5-9)$$

(2) The test for convergence is

$$|\Delta\pi_e| \leq 0.0001 \quad (4.5-10)$$

(3) If this convergence test is not met, new estimates for the composition of ionized species are obtained from:

$$(\ln n_j)^{i+1} = (\ln n_j)^i + a_{ej} \Delta \pi_e \quad (4.5-11)$$

where the subscript i refers to the i^{th} iteration. The previous sequence of steps is repeated until equation (4.5-10) is satisfied.

4.6 Procedure for Obtaining Equilibrium Rocket Performance

The procedure consists of first determining combustion properties and then determining exhaust properties at the throat and at other assigned stations, if any, in the nozzle exit. Combustion and throat conditions are always obtained first automatically by the program.

4.6-1 Combustion Conditions

The combustion temperature and equilibrium compositions are obtained by the program for an assigned chamber pressure and the reactant enthalpy (from the assigned temperature). From the combustion compositions and temperature the combustion entropy and other combustion properties are determined. The combustion entropy s_c is assumed to be constant during isentropic expansion in the nozzle.

4.6-2 Exit Conditions

Exit conditions include the throat conditions and assigned area ratios A_e/A_t or pressure ratios P_e/P_t . Throat conditions are always determined automatically by the program. Other exit conditions, on the other hand, are optional and, if included, will be calculated after throat calculations are completed.

For an assigned pressure ratio equilibrium compositions and exit temperature are determined for the pressure P corresponding to the assigned pressure ratio and for the combustion entropy s_c . For throat and assigned area ratios iteration procedures are used to determine the correct pressure ratios.

After equilibrium compositions and temperature are obtained for an assigned pressure ratio or area ratio, all the rocket parameters for that point can be determined.

4.6-3 Throat Conditions

Throat conditions can be determined by locating the pressure or pressure ratio for which the area ratio is a minimum or, equivalently, for which the velocity of flow is equal to the velocity of sound⁽³¹⁾. The second procedure is used in this work. Throat pressure is determined by iteration.

The initial estimate for the pressure ratio at the throat is obtained from the approximate formula

$$\frac{P_c}{P_t} = \left(\frac{\gamma_s + 1}{2} \right)^{\gamma_s / (\gamma_s - 1)} \quad (4.6-1)$$

Equation (4.6-1) is found in many references on rocket propulsion⁽⁷⁴⁾, but is exact only when γ_s is constant from combustion point to throat. Because the value of γ_s is not yet known at the throat, the value of γ_s from the combustion point is used by the program in equation (4.6-1). It generally gives an excellent initial estimate.

Equilibrium properties for s_c and for the value of P_t calculated from equation (4.6-1) are obtained as for any exit point. From these properties v_e^2 (using eq. (3.5-14)) and a_e^2 (using eq. (2.9-26)) are calculated and the following test for convergence is made:

$$\left| \frac{v_e^2 - a_e^2}{v_e^2} \right| \leq 0.4 \times 10^{-4} \quad (4.6-2)$$

This criterion is equivalent to ensuring that at the throat the Mach number is within $1 \pm 0.2 \times 10^{-04}$.

If the convergence test is not met, an improved estimate of the throat pressure ratio is obtained from the iteration formula

$$P_{t,k+1} = \left(P \frac{1 + \gamma_s M_a^2}{1 + \gamma_s} \right)_{t,k} \quad (4.6-3)$$

where the subscript k indicates the k^{th} iteration.

4.6-4 Discontinuities at Throat

Gordon⁽⁴³⁾ gives a special procedure for obtaining throat conditions when the velocity of sound is discontinuous at the throat. This type of discontinuity may occur when a transition point, such as a melting point, is being calculated at the throat. The solution of this problem requires the following equation, which permits estimating the throat pressure at the melting point, where the solid phase just begins to appear:

$$\ln P_t = \ln P + \left(\frac{\partial \ln P}{\partial \ln T} \right)_s (\ln T_m - \ln T) \quad (4.6-4)$$

where the derivative is given by equation (2.9-27).

4.6-5 Empirical Formulas for Initial Estimates of P_c/P_e

Initial estimates of pressure ratios corresponding to subsonic area ratios are obtained from the following empirical formulas:

$$\ln \frac{P_c}{P_e} = \frac{\ln \frac{P_c}{P_t}}{\frac{A_e}{A_t} + 10.587 \left(\ln \frac{A_e}{A_t} \right)^3 + 9.454 \ln \frac{A_e}{A_t}} \quad (4.6-5)$$

$$\left(\frac{A_e}{A_t} \geq 1.09 \right)$$

and

$$\ln \frac{P_c}{P_e} = \frac{0.9 \ln \frac{P_c}{P_t}}{\frac{A_e}{A_t} + 10.587 \left(\ln \frac{A_e}{A_t} \right)^3 + 9.454 \ln \frac{A_e}{A_t}} \quad (4.6-6)$$

$$\left(1.0001 < \frac{A_e}{A_t} < 1.09 \right)$$

When an assigned supersonic area ratio requires an initial estimate of pressure ratio to be obtained from an empirical formula, the following formulas are used:

$$\ln \frac{P_c}{P_e} = \ln \frac{P_c}{P_t} + \sqrt{3.294 \left(\ln \frac{A_e}{A_t} \right)^2 + 1.535 \ln \frac{A_e}{A_t}} \quad (4.6-7)$$

$$\left(1.0001 < \frac{A_e}{A_t} < 2 \right)$$

and

$$\ln \frac{P_c}{P_e} = \gamma_s + 1.4 \ln \frac{A_e}{A_t} \quad \left(\frac{A_e}{A_t} \geq 2 \right) \quad (4.6-8)$$

In equation (4.6-8) the value of γ_s is that determined for throat conditions.

4.6-6 Analytic Expressions for Improved Estimates of P_c/P_e

The equilibrium properties obtained for the initial and each subsequently improved estimate of P_c/P_e are used in equations (4.6-9) and

(4.6-10) to obtain the next improved estimates. From table I of Gordon⁽³⁷⁾ the following derivative can be obtained:

$$\left(\frac{\partial \ln \frac{P_c}{P_e}}{\partial \ln \frac{A_e}{A_t}} \right)_s = \frac{1}{\left(\frac{1}{\gamma_s} - \frac{nRT}{u^2} \right)_e} = \left(\frac{\gamma_s u^2}{u^2 - a^2} \right)_e \quad (4.6-9)$$

This derivative is used in the following correction formula to obtain an improved estimate for P_c/P_e :

$$\left(\ln \frac{P_c}{P_e} \right)_{k+1} = \left(\ln \frac{P_c}{P_e} \right)_k + \left[\left(\frac{\partial \ln \frac{P_c}{P_e}}{\partial \ln \frac{A_e}{A_t}} \right)_s \right]_k \times \left[\ln \frac{A_e}{A_t} - \left(\ln \frac{A_e}{A_t} \right)_k \right] \quad (4.6-10)$$

where the subscript k refers to the k^{th} estimate and where the area ratio with no iteration subscript is the assigned value. The iteration procedure is continued until

$$\left| \left(\ln \frac{P_c}{P_e} \right)_{k+1} - \left(\ln \frac{P_c}{P_e} \right)_k \right| \leq 0.00004 \quad (4.6-11)$$

with a maximum of 10 iterations permitted. Generally, convergence is reached within two to four iterations.

4.7 Procedure for Obtaining Frozen Rocket Performance

The procedure for obtaining rocket performance assuming that composition is frozen (infinitely slow reaction rates) during expansion is simpler than that assuming equilibrium composition. The reason is that equilibrium compositions need be determined only for combustion conditions.

After obtaining combustion conditions in the identical way described for equilibrium rocket performance, the remainder of the procedure is as follows.

4.7-1 Exit Conditions

Improved estimates of the exit temperature corresponding to some assigned P are obtained by means of the following iteration formulas:

$$(\ln T_e)_{k+1} = (\ln T_e)_k + (\Delta \ln T_e)_k \quad (4.7-1)$$

where

$$(\Delta \ln T_e)_k = \frac{S_c - S_{e,k}}{C_{p,e,k}} \quad (4.7-2)$$

and where k refers to the k^{th} estimate. The initial estimate of an exit temperature is the value of temperature for the preceding point. The iteration procedure is continued until

$$|\Delta \ln T_e| < 0.5 \times 10^{-4} \quad (4.7-3)$$

The maximum number of iterations permitted by the program is eight, although the convergence criterion of equation (4.7-3) is generally reached in two to four iterations.

Phases are also considered to be frozen. Therefore, the program will calculate frozen rocket performance for assigned schedules of pressure and/or area ratios only until an exit temperature is reached that is 50 K below the transition temperature of any condensed species present at the combustion point. If a calculated exit temperature is more than 50 K below the transition temperature, this point and all subsequent points in the schedule are ignored by the program and do not appear in the output.

After an exit temperature has been determined, all the rocket performance parameters (chapter 3) can be determined.

4.7-2 Throat Conditions

Calculations for frozen throat conditions are similar to those for equilibrium conditions. That is, equation (4.6-1) is used to get initial estimates for P_c/P_t , equation (4.6-3) is used to get improved estimates for P_c/P_t , and equation (4.6-2) is used as the convergence criterion. With composition and phases frozen, there is no possibility of discontinuities at the throat, in contrast to equilibrium compositions.

4.7-3 Thermodynamic Derivatives for Frozen Composition

The thermodynamic derivatives discussed in previous sections were based on the assumption that in any thermodynamic process, from one condition to another, composition reaches its equilibrium values instantaneously. If, on the other hand, reaction times are assumed to be infinitely slow, composition remains fixed (frozen). In this event expressions for derivatives become simpler. An expression for specific heat, based on frozen composition, has already been given in equation (2.9-1b). Some other derivatives based on frozen composition are as follows: From equations (2.9-2) and (2.9-3), respectively.

$$\left(\frac{\partial \ln V}{\partial \ln T}\right)_P = 1 \quad (4.7-4)$$

$$\left(\frac{\partial \ln V}{\partial \ln P}\right)_T = -1 \quad (4.7-5)$$

From equation (2.9-22)

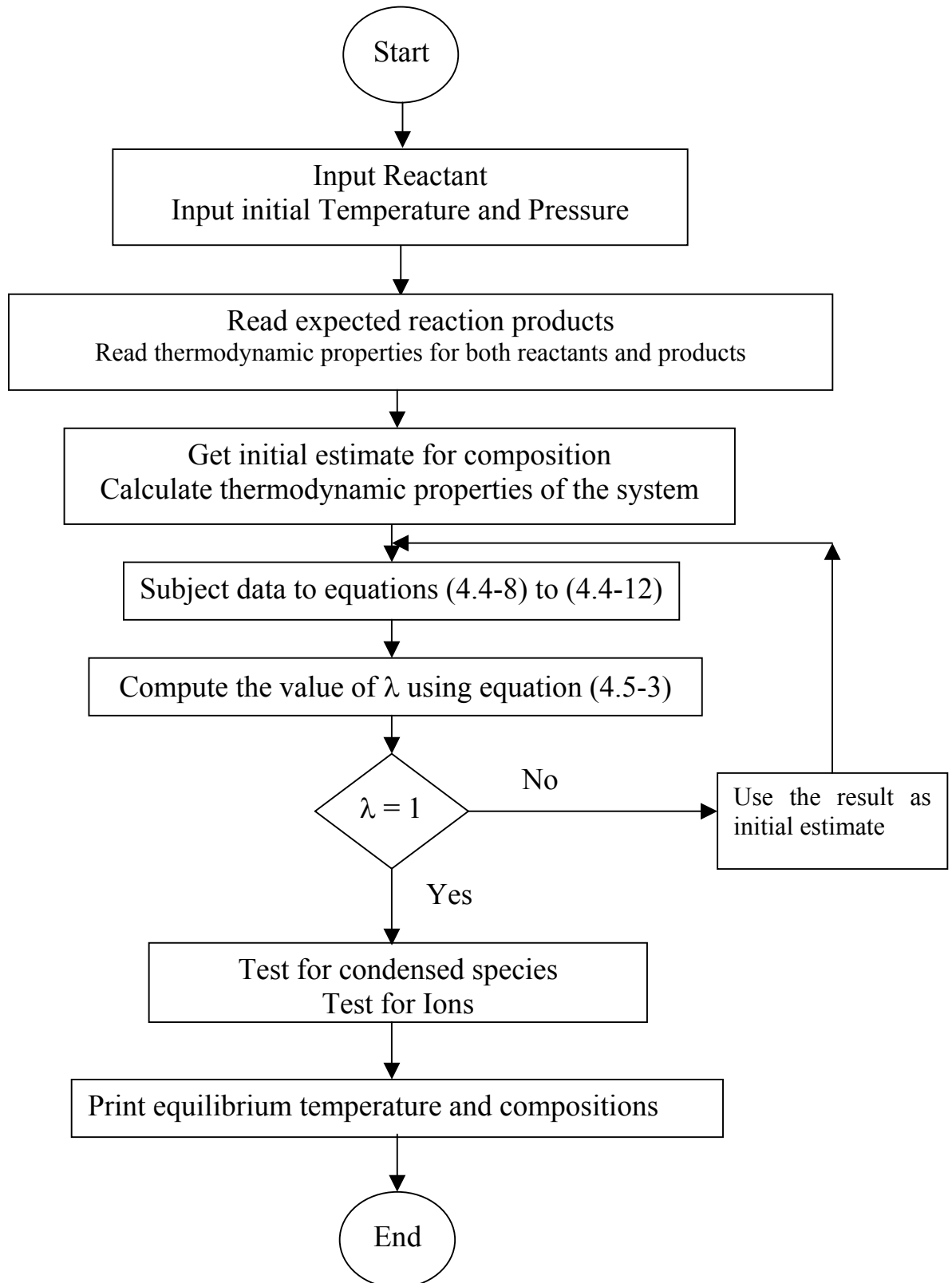
$$c_v = c_{p,f} - nR \quad (4.7-6)$$

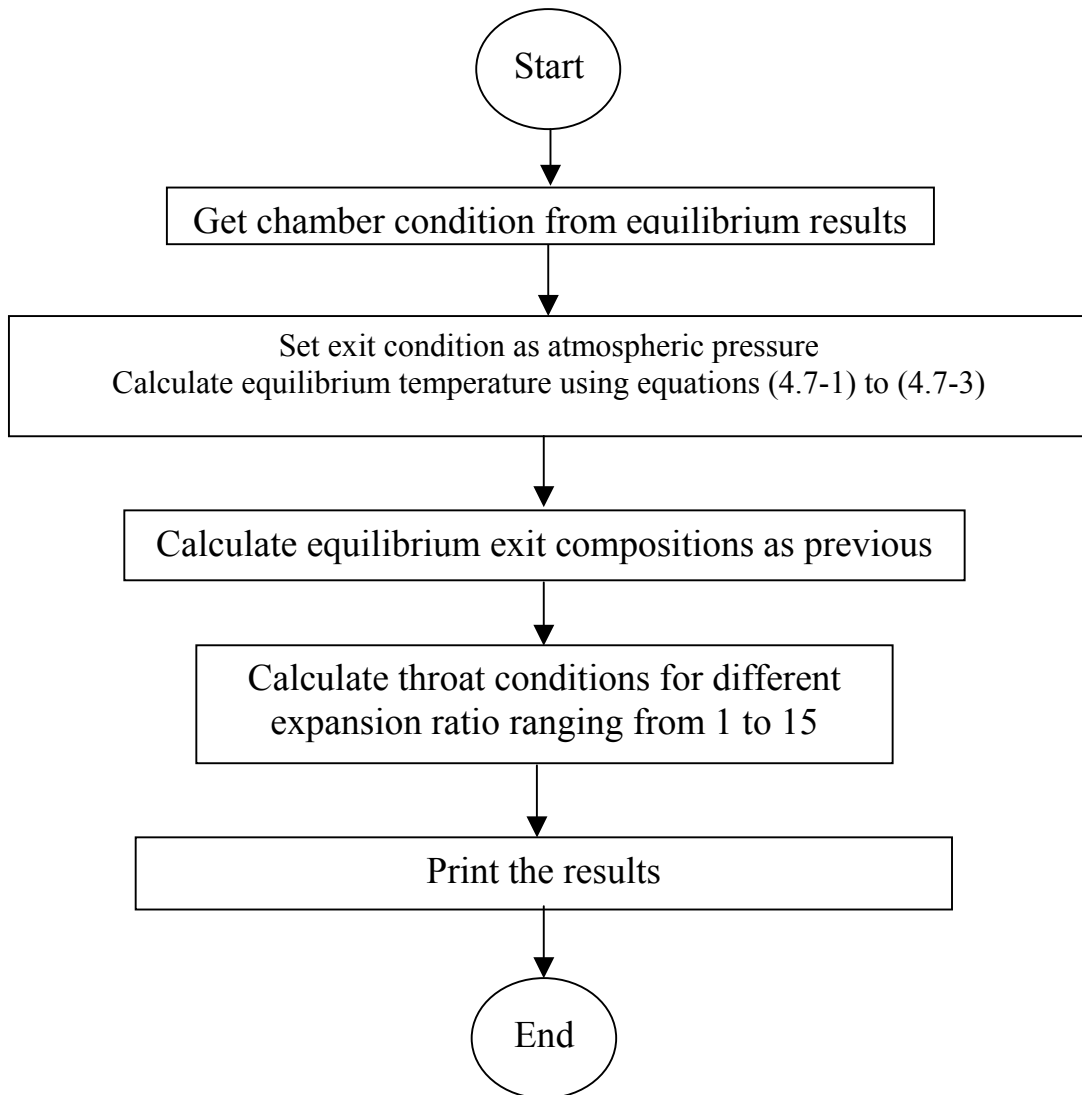
From equations (2.9-25) and (4.9-5), it is clear that for frozen composition

$$\gamma_s = \gamma \quad (4.7-7)$$

4.8 Algorithms

4.8-1 Algorithm for Chemical Equilibrium Calculations



4.8-2 Algorithm for Calculating Rocket Performance

Chapter Five

Experimental Work

5. Experimental Work

Rocket Motor Static Testing

5.1. Introduction

It is a well-known fact that the proof of the reliability of any theoretical model is obtained when its result match with those obtained from the experiments. As shown in chapters two and three; the study of the chemical equilibrium in a rocket engine is the best approach to understand its criteria at high temperature and pressure. Therefore, an experimental rocket engine was designed and experiments with various types of solid propellants were conducted. This chapter shows the detailed steps of these experiments

5.2 Experimental System

The arrangement of the system used for experiments can be well explained according to the diagram shown in figure 5.1.

5.2-1 The Testing Rig

The testing rig includes the rig for fixing the test rocket motor with all connections and sensors to measure pressure and thrust.

5.2-2 The Room of Measuring Apparatus

It includes:

1. Control panel used to trigger the test rocket motor
2. Computer to analyze the pressure-time curve and the thrust-time curve.
3. Printer, TV set, and CD recorder.

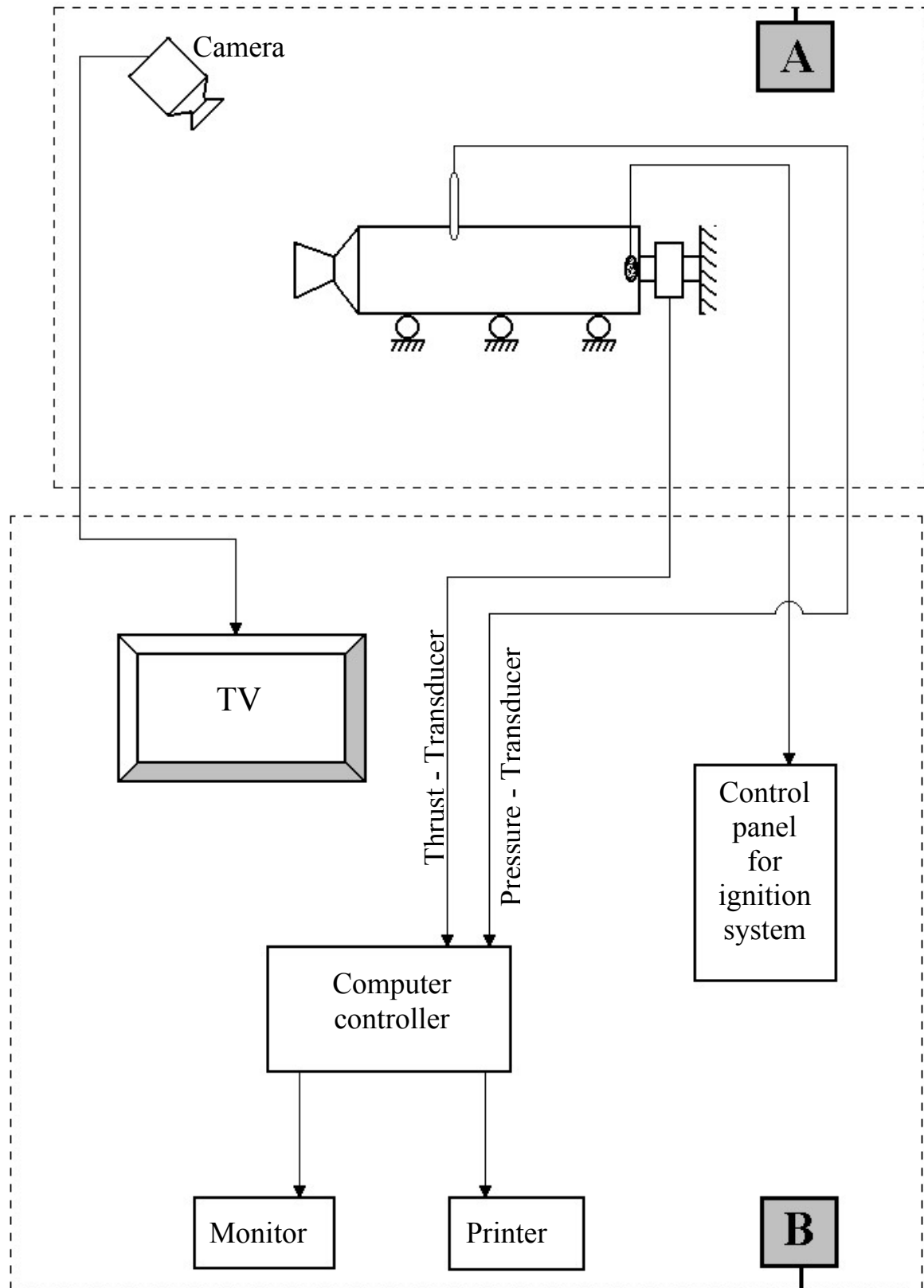


Figure 5.1: Block diagram of the measuring room and testing rig
 (A) Test rig, (B) Measuring room

5.3 Determination of Total and Specific Impulse from Test Data

The thrust sensor, as well as the pressure sensor, takes 500 readings per second, which enables to get very accurate readings from the experiments. By plotting the thrust (or pressure) versus time, one can get the thrust (or pressure) time curve explained in section 3.7 (or section 3.10 for pressure). As stated in section 3.7, the total impulse is the integration of the thrust time curve. Such a large number of readings give a very accurate numerical integration, which can be considered acceptable as an analytical integration. The specific impulse is now found by dividing the total impulse by the propellant weight (section 3.9).

Before executing the experiment, the computer controller asked for the propellant weight. Knowing that the computer is supplied with a program that calculates numerical integrations, the results of the computer at the end of the experiment were, thrust-time curve, pressure-time curve, total and specific impulses, and burning time.

5.4 Cases Studied

5.4-1 The Test Rocket Motor

A testing rocket motor was designed and used for the experiments execution. Figure 5.2 shows the test rocket motor parts.

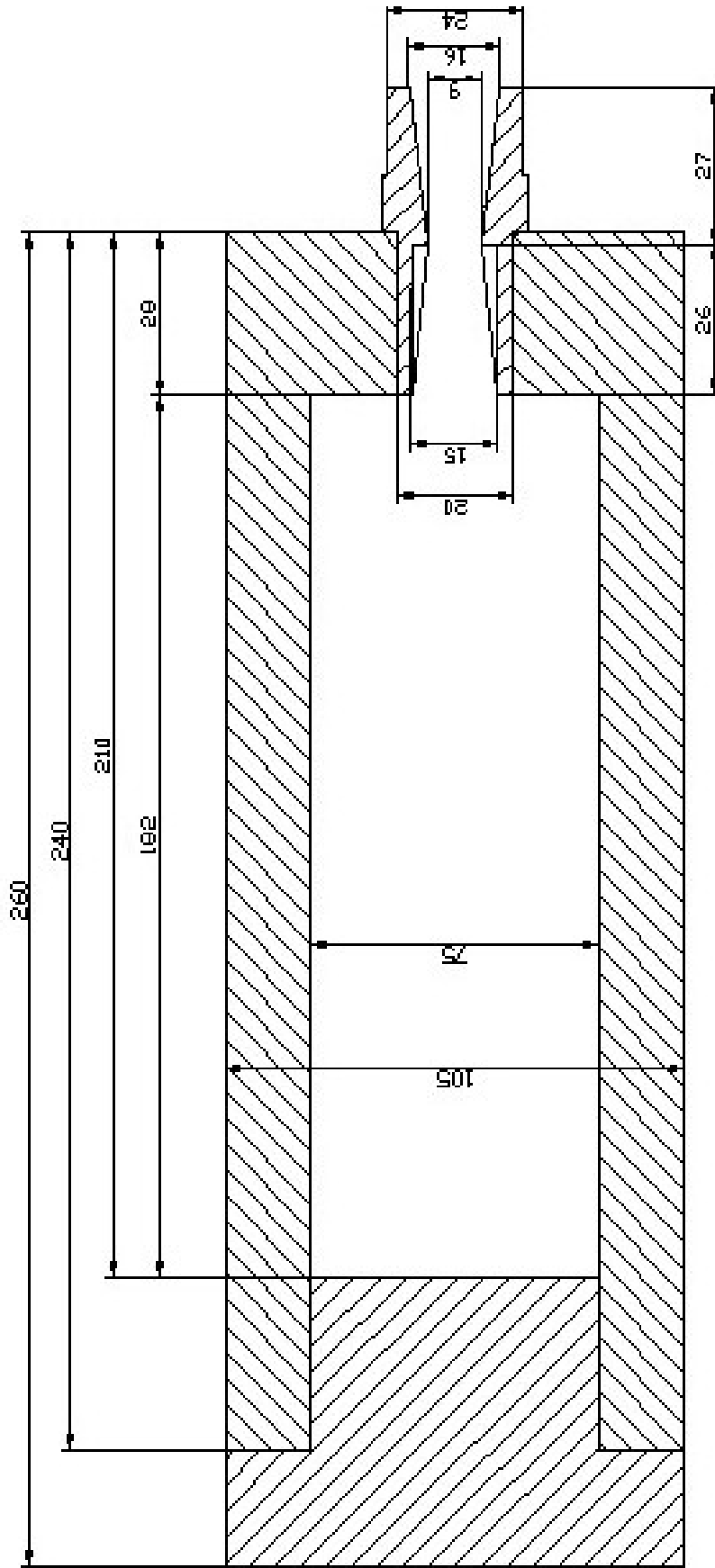


Figure 5.2: Section of Test Rocket Motor
(dimensions in mm)



a- The rig without the motor



b- The rig without the motor



c- The rig with the thrust meter only



d- The rig with the motor



e- The rig with the motor



f- The rig with the motor

Figure 5.3: Different Pictures of the Testing Rig

The rocket motor was designed to withstand a combustion pressure of three times the expected combustion pressure (the expected combustion pressure was 90 bar, and the motor was designed to work at 270 bar). It was constructed of stainless steel with minimum wall thickness of 15-mm and maximum bottom thickness of 50-mm. The nozzle part consists of a convergent diameter of 15-mm, a throat diameter of 9-mm, and a divergent diameter of 16-mm. The motor was designed with an internal diameter of 75-mm and external diameter of 105-mm. Total length of 260-mm and effective length of 182-mm. The dimensions of the rocket motor were chosen to obtain a small (experimental) rocket motor. The design of the motor was based on two reference books^(53, 74), and it was constructed in Al-Qadisya general company.

The nozzle part has screws by which it is attached to the motor body. The insert part of the nozzle (the convergent to the throat) was constructed of graphite carbon, while the remaining body (main body) of the nozzle was constructed of carbon steel similar to the rocket motor body.

5.4-2 The Solid Propellant

Two basic types of solid propellant were used, the double base solid propellant, consists mainly of nitrocellulose and nitroglycerine as fuel and centralite as plasticizer, produced in Al-Qaqua general company, and the composite solid propellant, consists of aluminum powder (Al) as fuel, ammonium perchlorate (AP) as oxidizer, iron oxide (Fe_2O_3) as catalyst, and Hydroxy Terminated Polybutadiene (HTPB) as rubber base binder, produced in Al-Rasheed general company. Tables 5.1 and 5.2 shows the types and compositions of these propellants.

Table 5.1: Composition of Double Base Fuel used in Experiments

Fuel Type	Nitrocellulose	Nitroglycerine	Centralite
DB Fuel No.1	56.0 %	42.0 %	2.0 %
DB Fuel No.2	56.3 %	42.1 %	1.6 %
DB Fuel No.3	58.8 %	39.0 %	2.2 %
DB Fuel No.4	59.7 %	37.3 %	3.0 %
DB Fuel No.5	60.0 %	36.8 %	3.2 %
DB Fuel No.6	60.6 %	37.5 %	1.9 %
DB Fuel No.7	62.0 %	37.6 %	0.4 %
DB Fuel No.8	62.6 %	34.3 %	3.1 %
DB Fuel No.9	98.6 %	00.0 %	1.4 %

Table 5.2: Composition of Composite Fuel used in Experiments

Fuel Type	HTPB	AP	Al	Fe ₂ O ₃
Comp. Fuel No.1	9.9 %	72.2 %	15.9 %	2.0 %
Comp. Fuel No.2	11.9 %	72.1 %	14.9 %	1.1 %
Comp. Fuel No.3	12.4 %	72.2 %	14.4 %	1.0 %
Comp. Fuel No.4	12.4 %	72.5 %	14.5 %	0.6 %

Another type of composite fuel used consists of Mg instead of Al

Fuel Type	HTPB	AP	Mg	Fe ₂ O ₃
Comp. Fuel No.5	18.0 %	74.6 %	5.3 %	2.1 %

5.5 Preparation of the Experiments

First step was to examine the empty motor case using X ray from three different horizontal directions to ensure that it is free of defects and cracks.

The second step was to use X ray to examine the propellant grain, which was already isolated to prevent the combustion from getting in touch with the inner wall of the case. Depending on the propellant mechanical type (either free stand or cast); in free stand propellant (e.g. double base), the grain was tested individually, while the cast propellant grain (e.g. composite) was to be tested together with the motor case.

The third step was the use of thin plates to close the inner side of the nozzles to insure getting the pressure of the propellant's combustion

In step four the igniter was placed with the propellant inside the case and the case was closed and using epoxy resin and was left for twenty-four hours to insure its curing. The system was now ready to execute the experiment.

5.6 Executing the Experiment

The experiment was repeated five times for each type of propellant. The first run was just to burn the propellant without taking any reading to insure that the propellant was burning smoothly and would not cause an explosion. The second run was to take the thrust reading only, which helps taking decisions concerning the continuation of the experiments. Finally if the propellant passed the first two tests, the run was repeated for three times and the readings of thrust and pressure were taken. The motor case was left for at least 24 hours between experiments to prepare it for next run. When opened after 24 hours the nozzle insert was replaced with a new one and prepared as being stated above.

Chapter Six

Results & Discussion

6. Results and Discussion

6.1 Experimental Results

The results of experiments, as obtained from the computer, are shown in figures 6.1 – 6.14. These figures show a sample result for each propellant composition.

In figures 6.1 to 6.9 the results of double base propellants are plotted. Double base oxidizers compositions are decrease, as shown in table 5.1, from DB1, with oxidizer composition of 0.42, to Db9 in which oxidizer composition is zero. From these figures it can be noticed that as oxidizer decrease, the combustion pressure increase, till it reach a maximum (an optimum) value of 241.5 bar for DB4, then it decreases again to almost the same starting pressure. While the specific impulse has its maximum value of 2395.172 N.s/kg for DB5 which means the maximum performance is achieved at this composition. It important to notice that DB5 has the second higher chamber pressure after DB4, in which its chamber pressure is 216.7 bar. From these experimental results one can get an idea of the optimum fuel to oxidizer ratio to get the higher performance of the propellant.

Figures 6.10 to 6.13 shows the results of the first four composite propellants composition. It is important to notice here that the propellant performance (specific impulse) is increases with decreasing the oxidizer, in which the maximum performance of 2332 N.s/kg was achieved for comp.4. The minimum performance, for the composite propellants, was achieved by using comp.5, but this disadvantage was overcome by the fact that comp.5 is the only smokeless composite fuel in comparison with the other four used composite propellants.

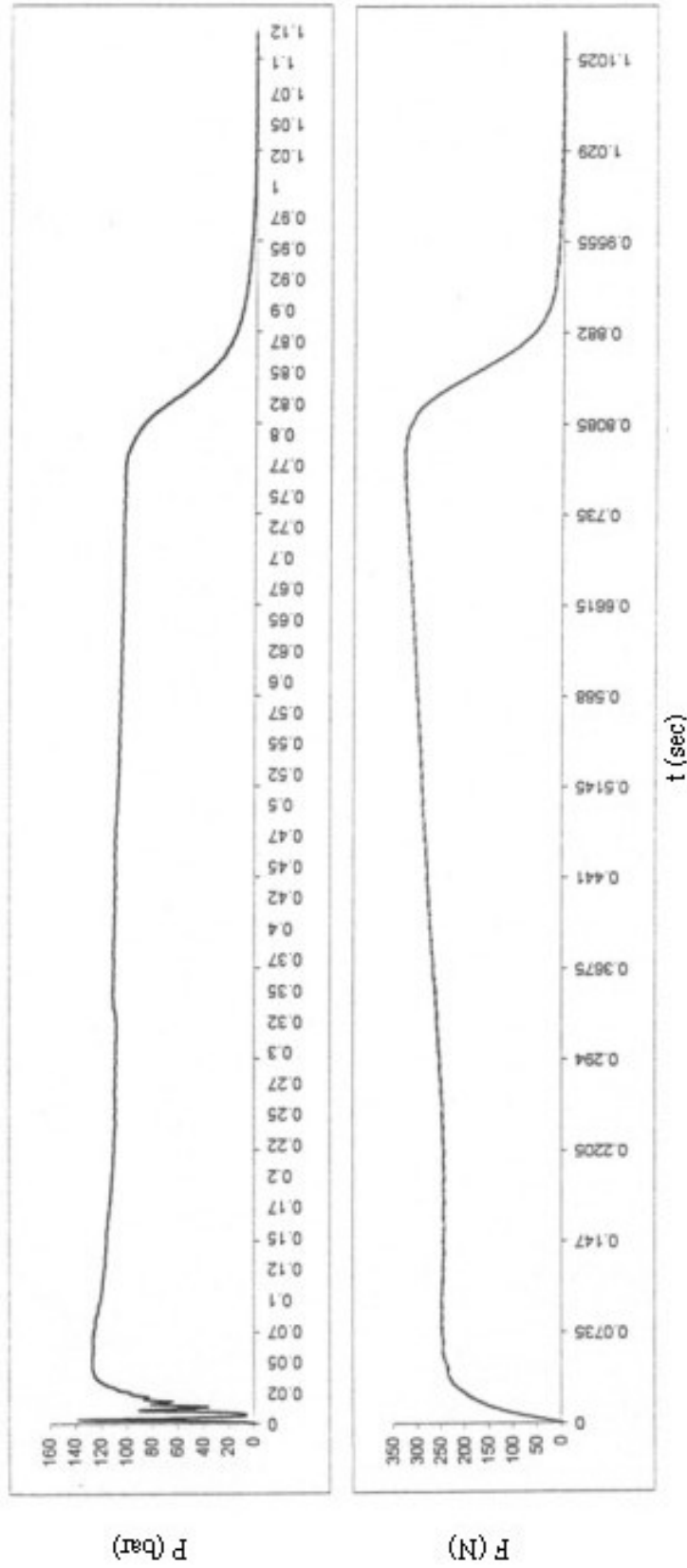


Figure 6.1: Results for DB1, as pressure-time curve and thrust-time curve

Action Time = 0.926 sec

Maximum Pressure = 138.1261 bar

Total Impulse = 2294.134 N.s

Burning time = 0.7745 sec

Average Pressure = 106.1942 bar

Specific Impulse = 1911.778 N.s/kg

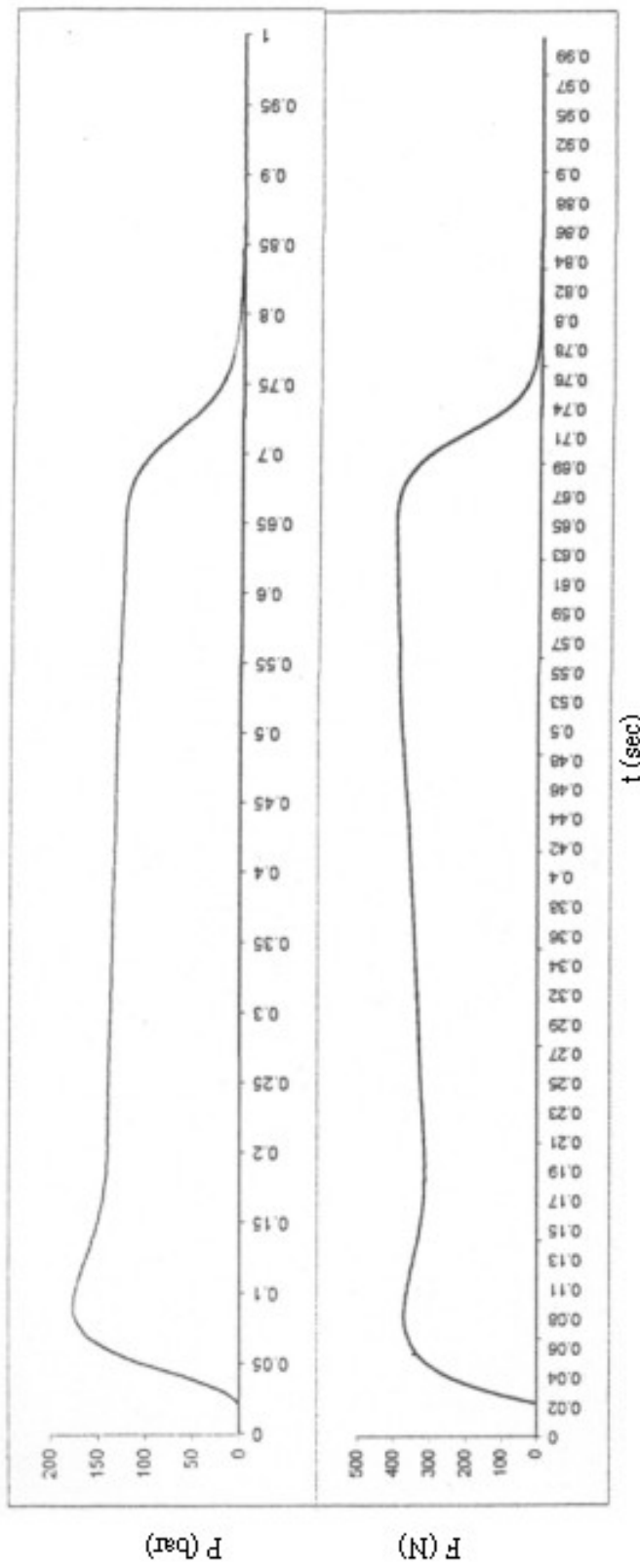


Figure 6.2: Results for DB2, as pressure-time curve and thrust-time curve

Action Time = 0.751 sec

Maximum Pressure = 176.1422 bar

Total Impulse = 2301.198 N.s

Burning time = 0.6395 sec

Average Pressure = 128.6279 bar

Specific Impulse = 1917.665 N.s/kg

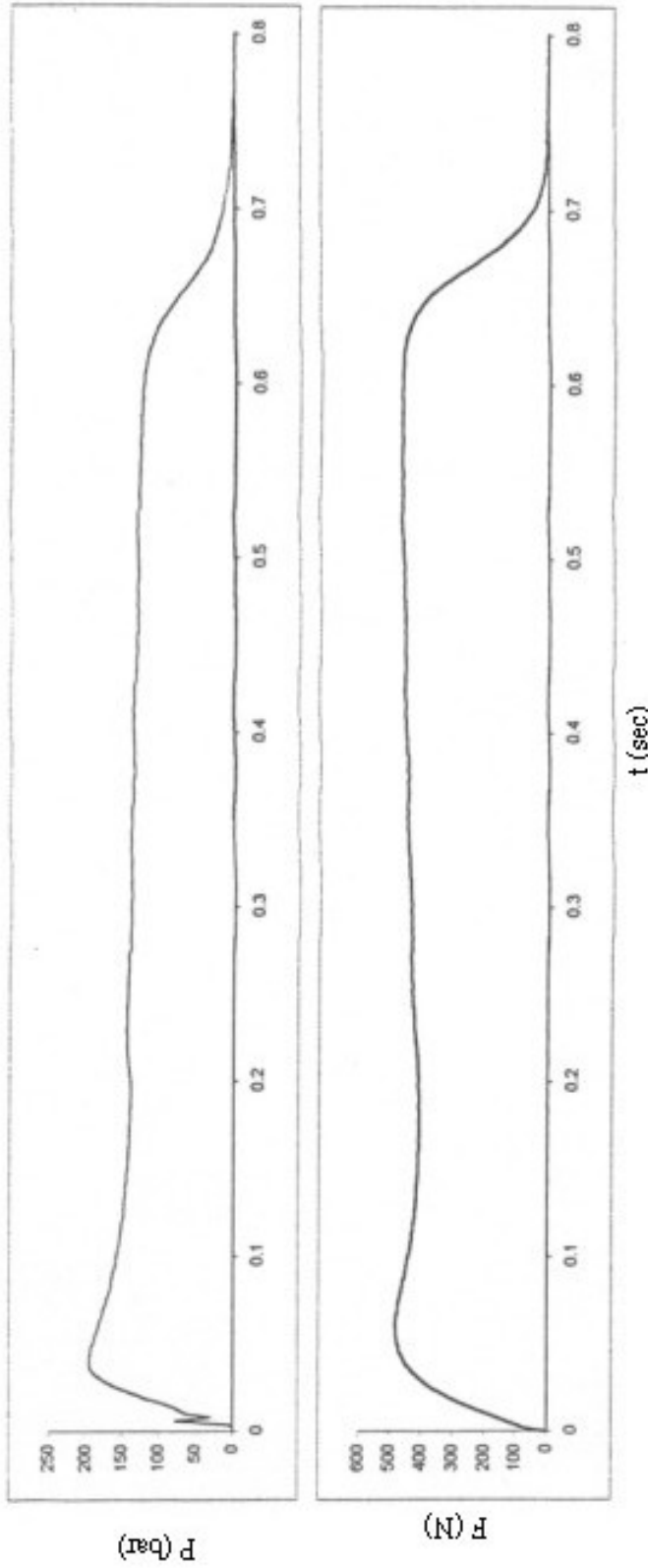


Figure 6.3. Results for DB3, as pressure-time curve and thrust-time curve

Action Time = 0.67 sec

Maximum Pressure = 212.524 bar

Total Impulse = 2488.126 N.s

Burning time = 0.556 sec

Average Pressure = 145.58 bar

Specific Impulse = 2073.438 N.s/kg

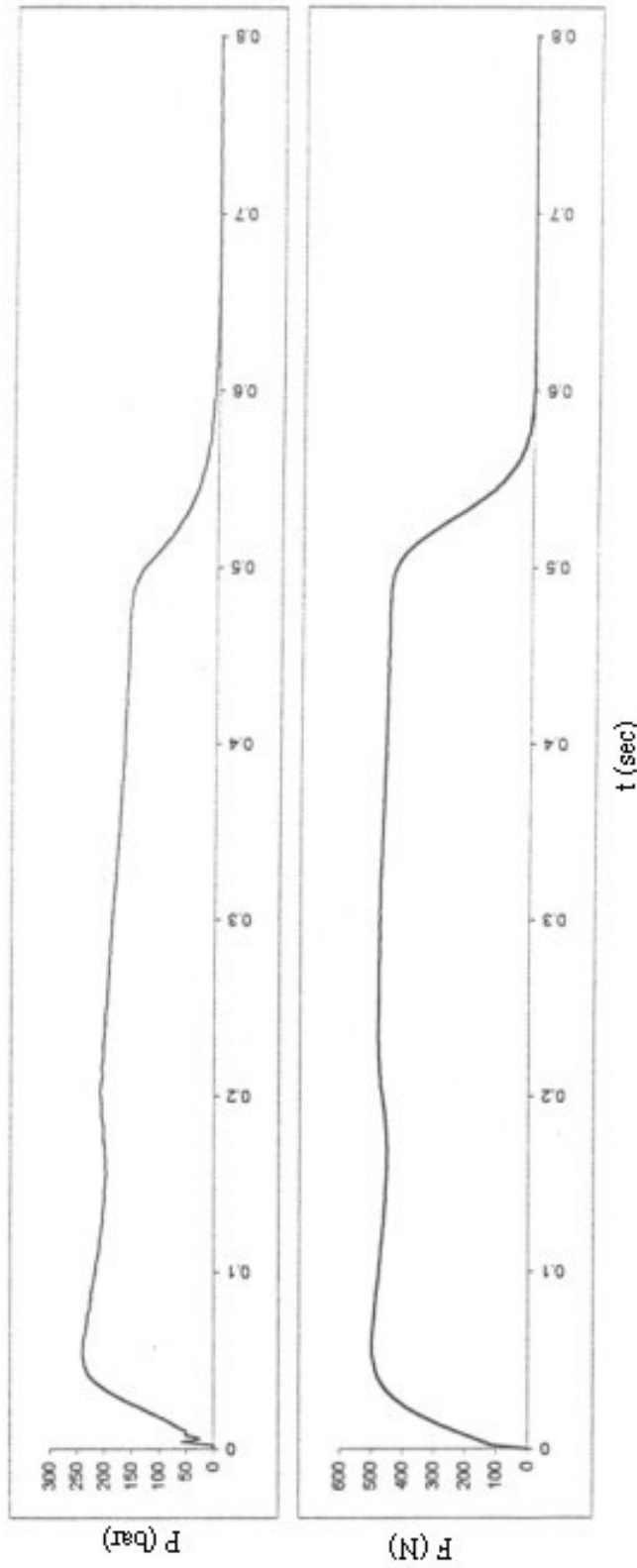


Figure 6.4: Results for DB4, as pressure-time curve and thrust-time curve

Action Time = 0.588 sec

Maximum Pressure = 241.5035 bar

Total Impulse = 2361.741 N.s

Burning time = 0.478 sec

Average Pressure = 179.9897 bar

Specific Impulse = 1968.117 N.s/kg

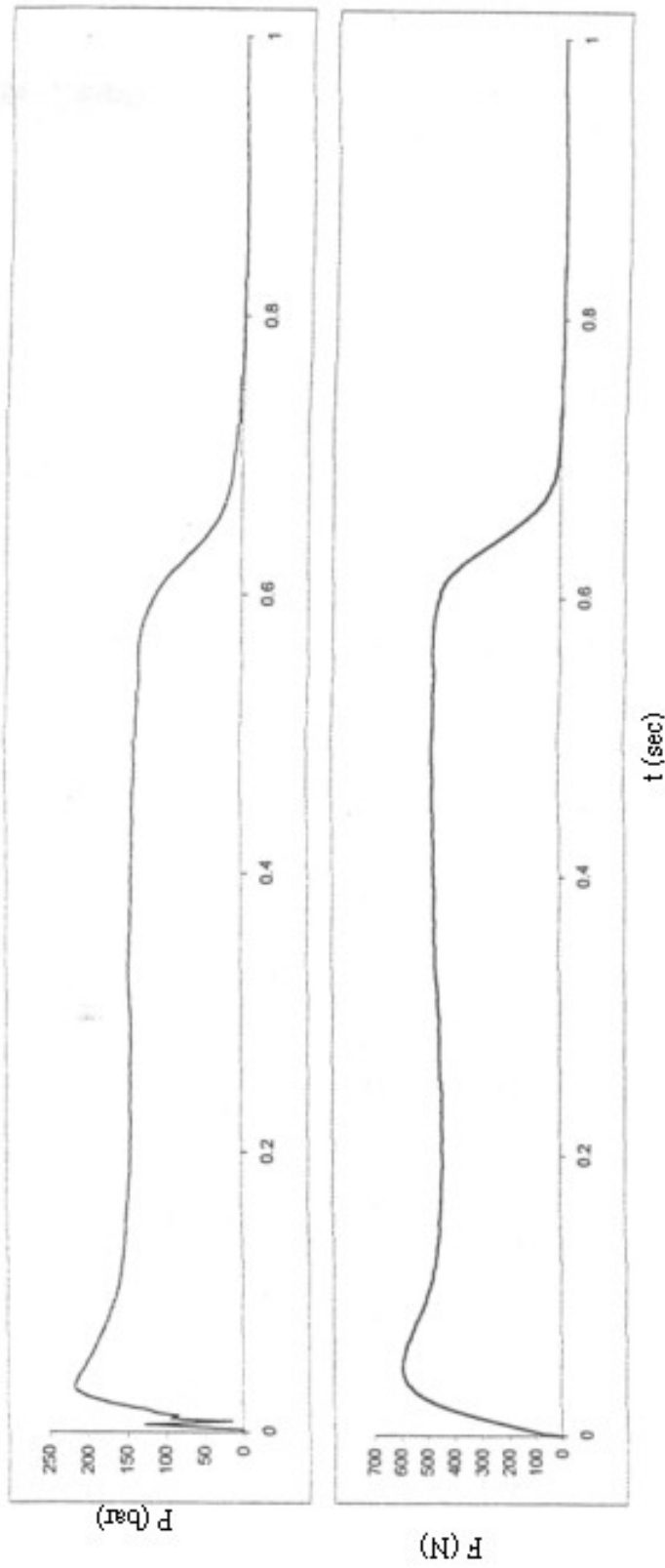


Figure 6.5: Results for DB5, as pressure-time curve and thrust-time curve

Action Time = 0.694 sec

Burning time = 0.578 sec

Maximum Pressure = 216.7384 bar

Average Pressure = 142.1172 bar

Total Impulse = 2874.206 N.s

Specific Impulse = 2395.172 N.s/kg

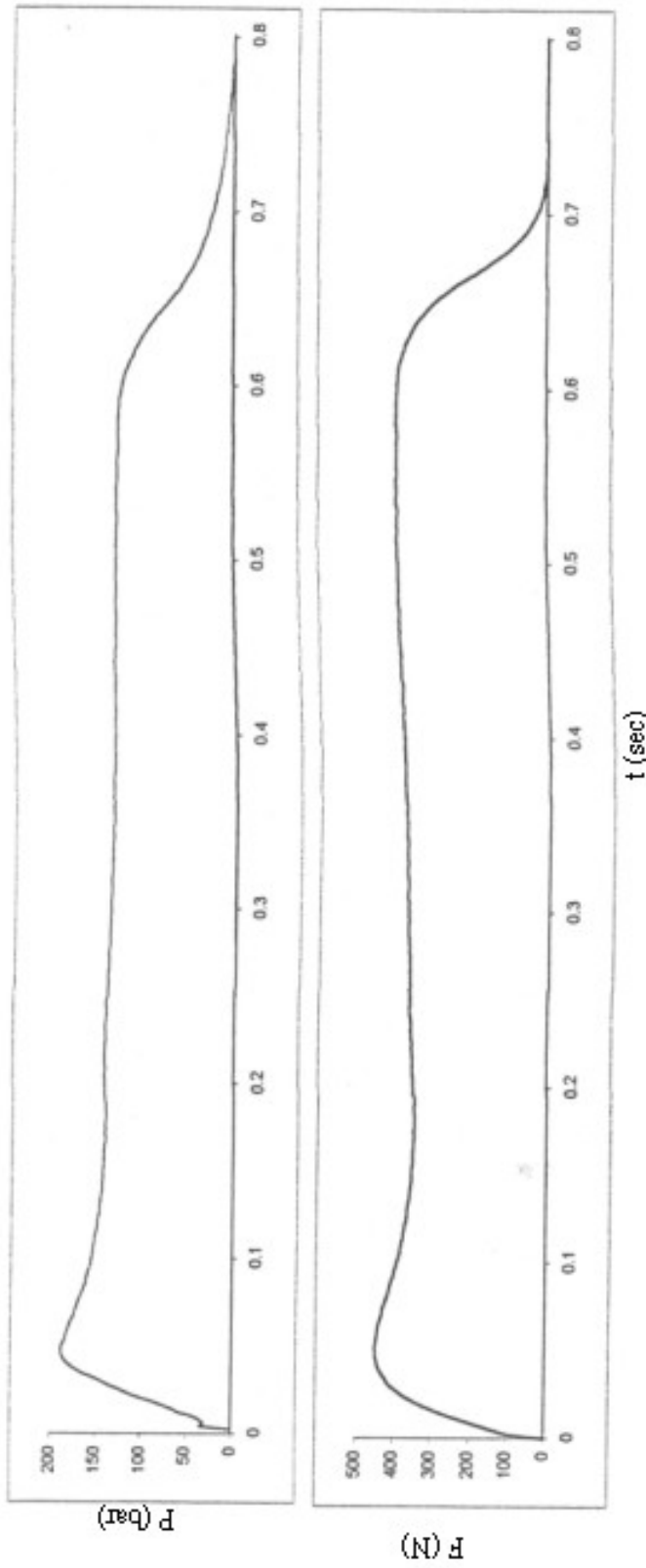


Figure 6.6: Results for DB6, as pressure-time curve and thrust-time curve

Action Time = 0.74 sec

Maximum Pressure = 189.02 bar

Total Impulse = 2444.324 N.s

Burning time = 0.596 sec

Average Pressure = 132.70 bar

Specific Impulse = 2036.937 N.s/kg

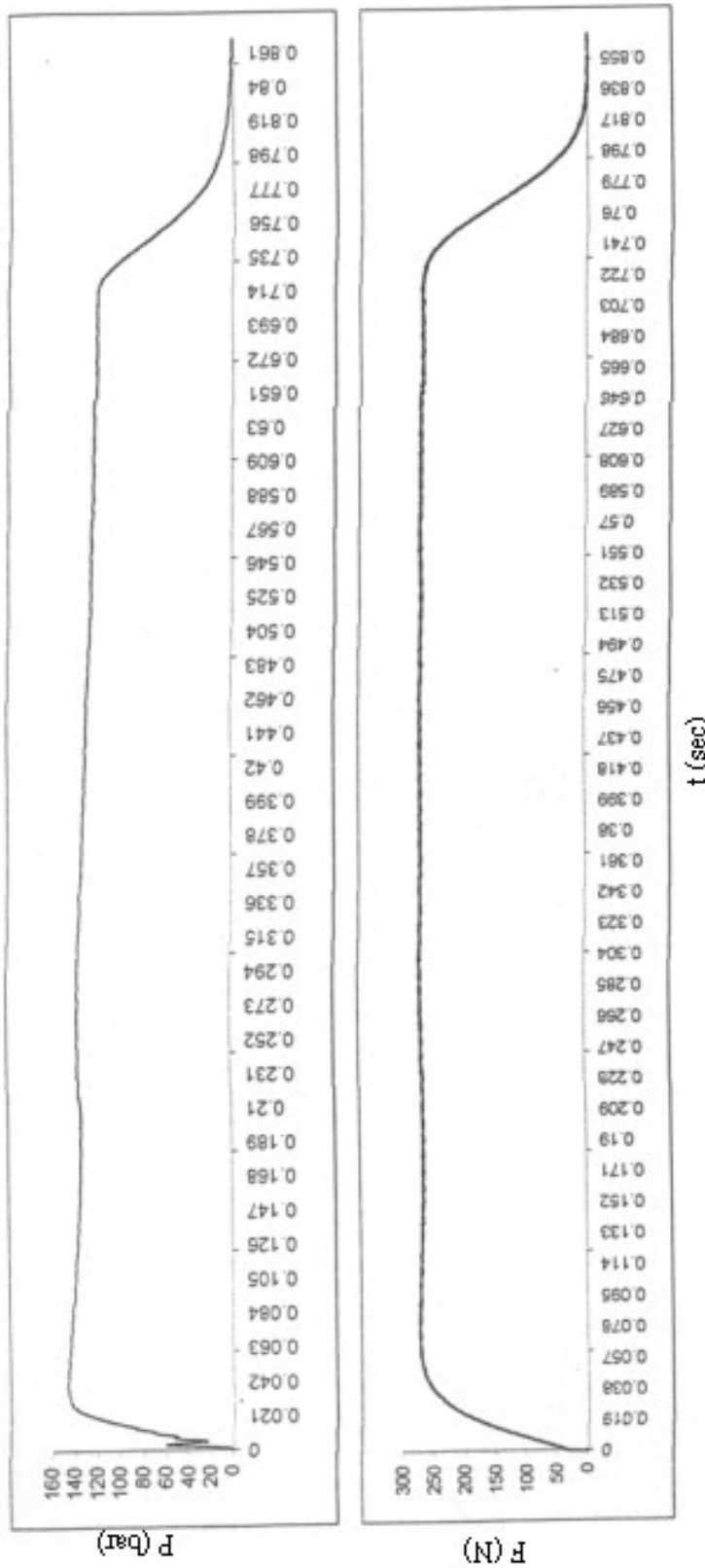


Figure 6.7: Results for DB7, as pressure-time curve and thrust-time curve

Action Time = 0.834 sec	Burning time = 0.636 sec
Maximum Pressure = 154.45 bar	Average Pressure = 121.26 bar
Total Impulse = 2305.684 N.s	Specific Impulse = 1921.404 N.s/kg

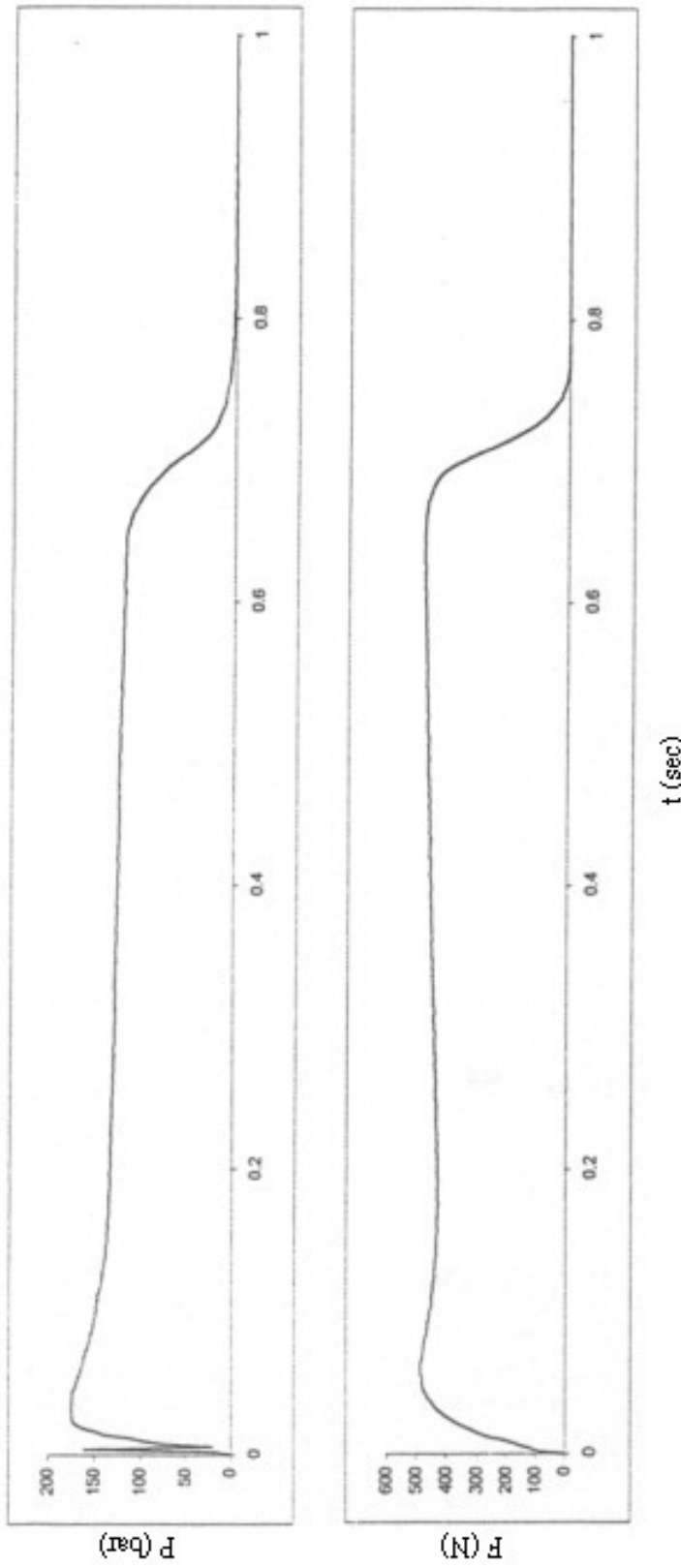


Figure 6.8: Results for DB8, as pressure-time curve and thrust-time curve

Action Time = 0.752 sec

Burning time = 0.653 sec

Maximum Pressure = 175.77 bar

Average Pressure = 130.08 bar

Total Impulse = 3082.511 N.s

Specific Impulse = 2568.759 N.s/kg

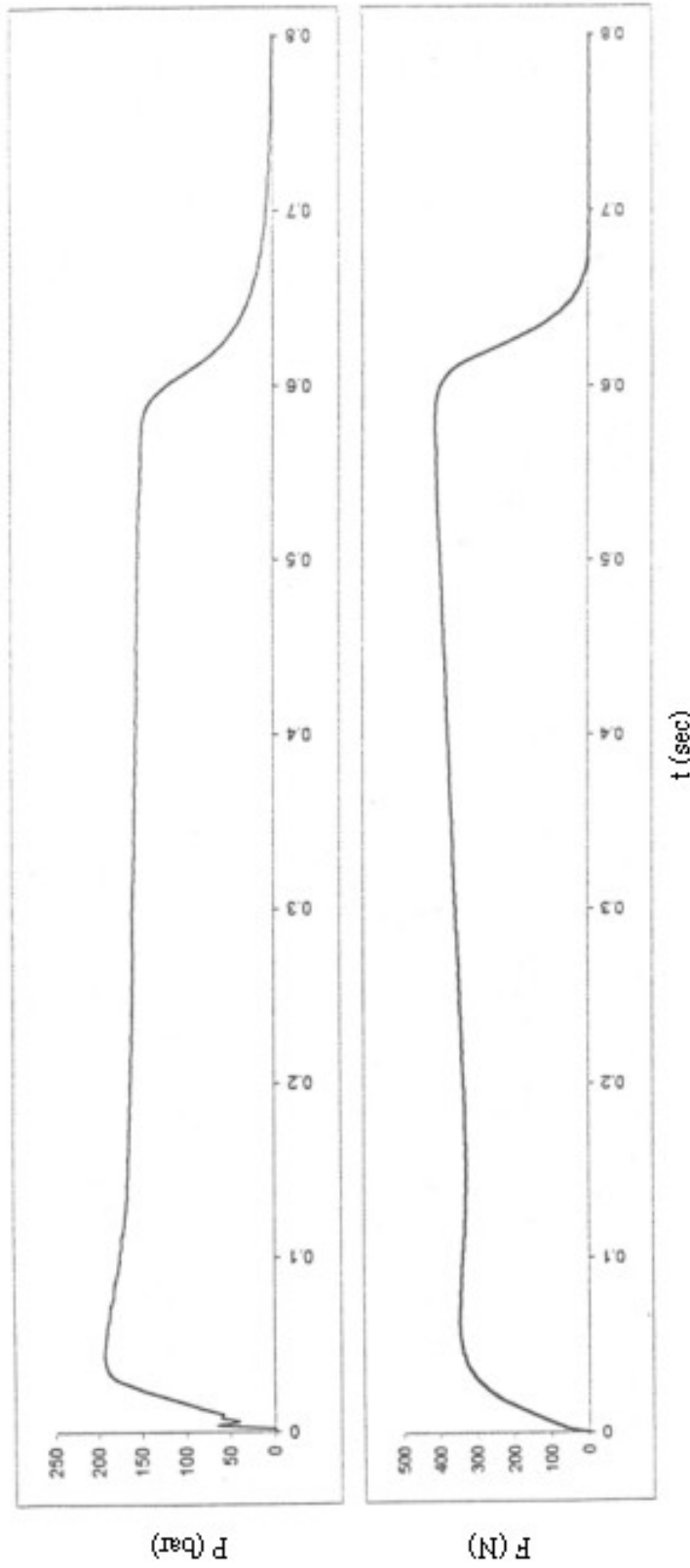


Figure 6.9: Results for DB9, as pressure-time curve and thrust-time curve

Action Time = 0.694 sec

Burning time = 0.583 sec

Maximum Pressure = 194.1 bar

Average Pressure = 152.73 bar

Total Impulse = 2195.95 N.s

Specific Impulse = 1829.958 N.s/kg

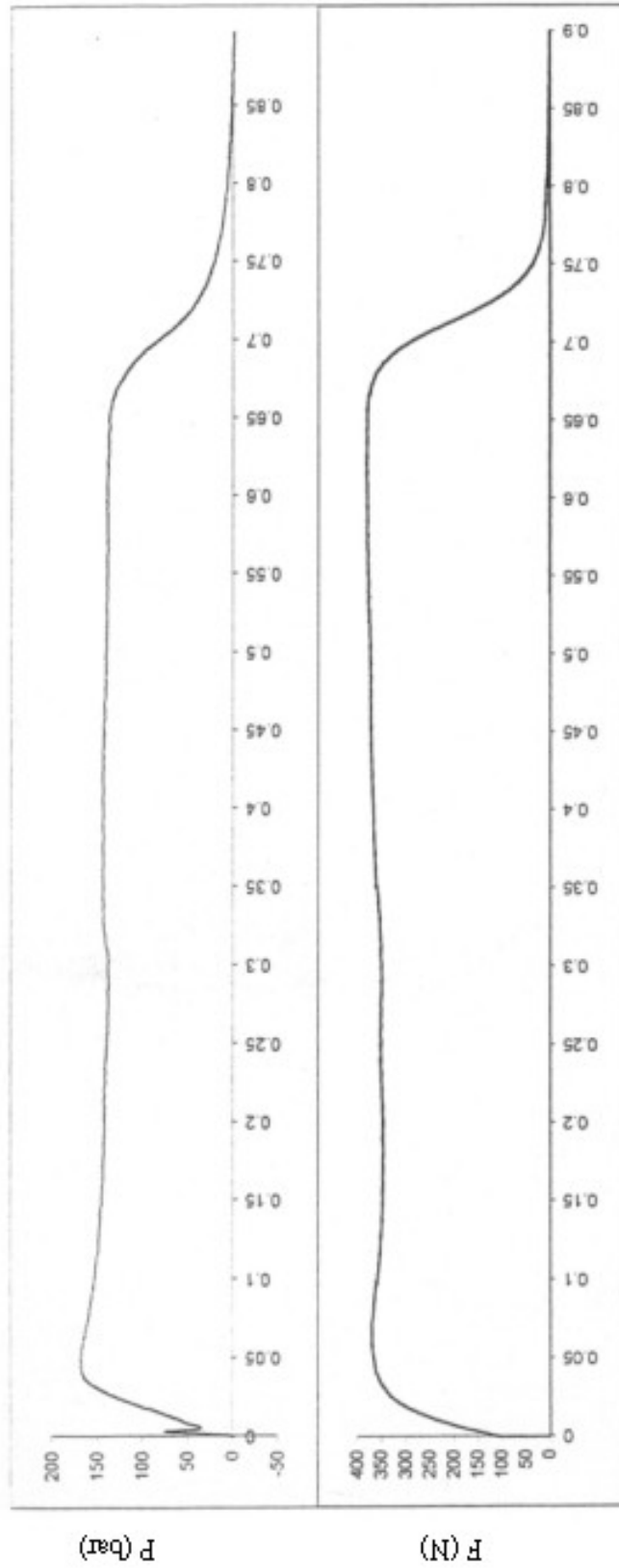


Figure 6.10: Results for Comp. 1, as pressure-time curve and thrust-time curve

Action Time = 0.796 sec

Maximum Pressure = 148.30 bar

Total Impulse = 2820.61 N.s

Burning time = 0.6555 sec

Average Pressure = 120.76 bar

Specific Impulse = 2089.34 N.s/kg

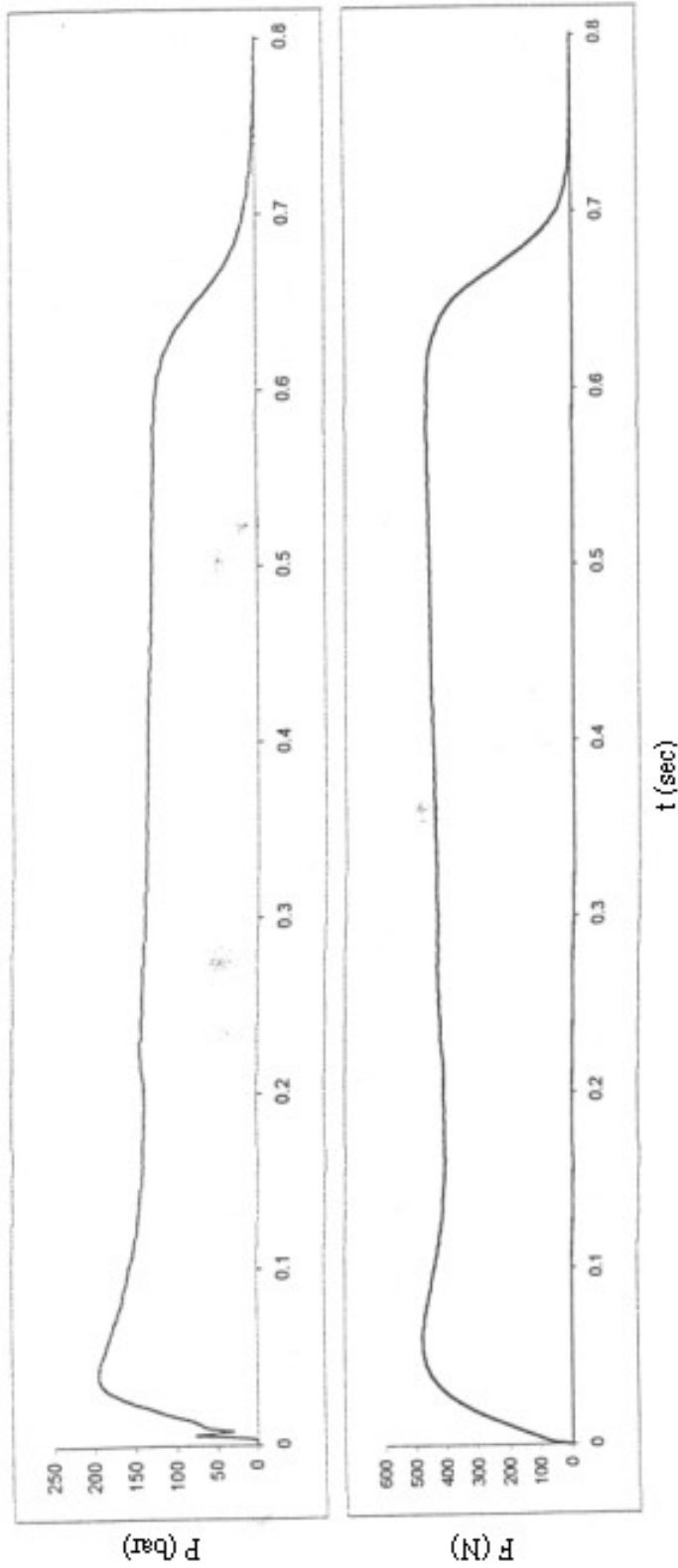


Figure 6.11: Results for Comp. 2, as pressure-time curve and thrust-time curve

Action Time = 0.694 sec

Maximum Pressure = 199.44 bar

Total Impulse = 2900.556 N.s

Burning time = 0.568 sec

Average Pressure = 140.68 bar

Specific Impulse = 2148.56 N.s/kg

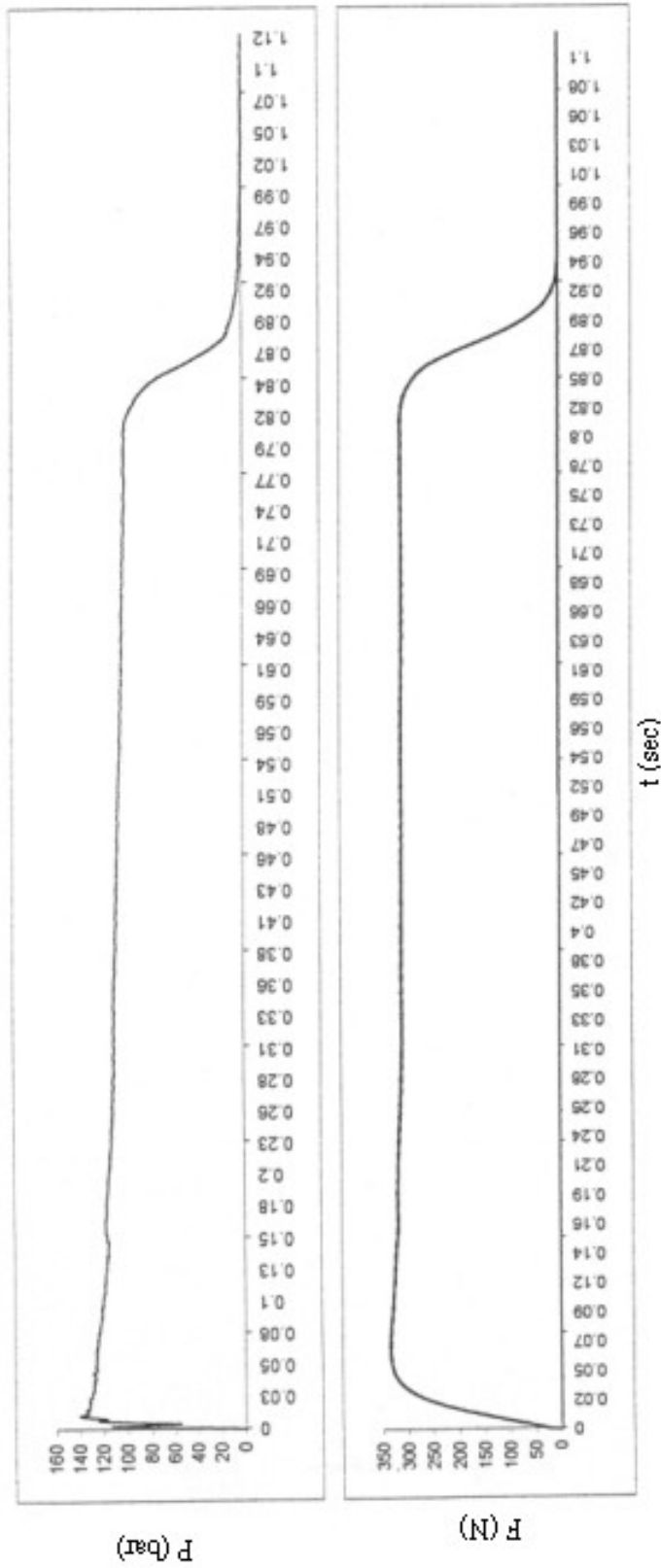


Figure 6.12: Results for Comp. 3, as pressure-time curve and thrust-time curve

Action Time = 0.907 sec	Burning time = 0.809 sec
Maximum Pressure = 140.95 bar	Average Pressure = 108.6 bar
Total Impulse = 2925.33 N.s	Specific Impulse = 2166.911 N.s/kg

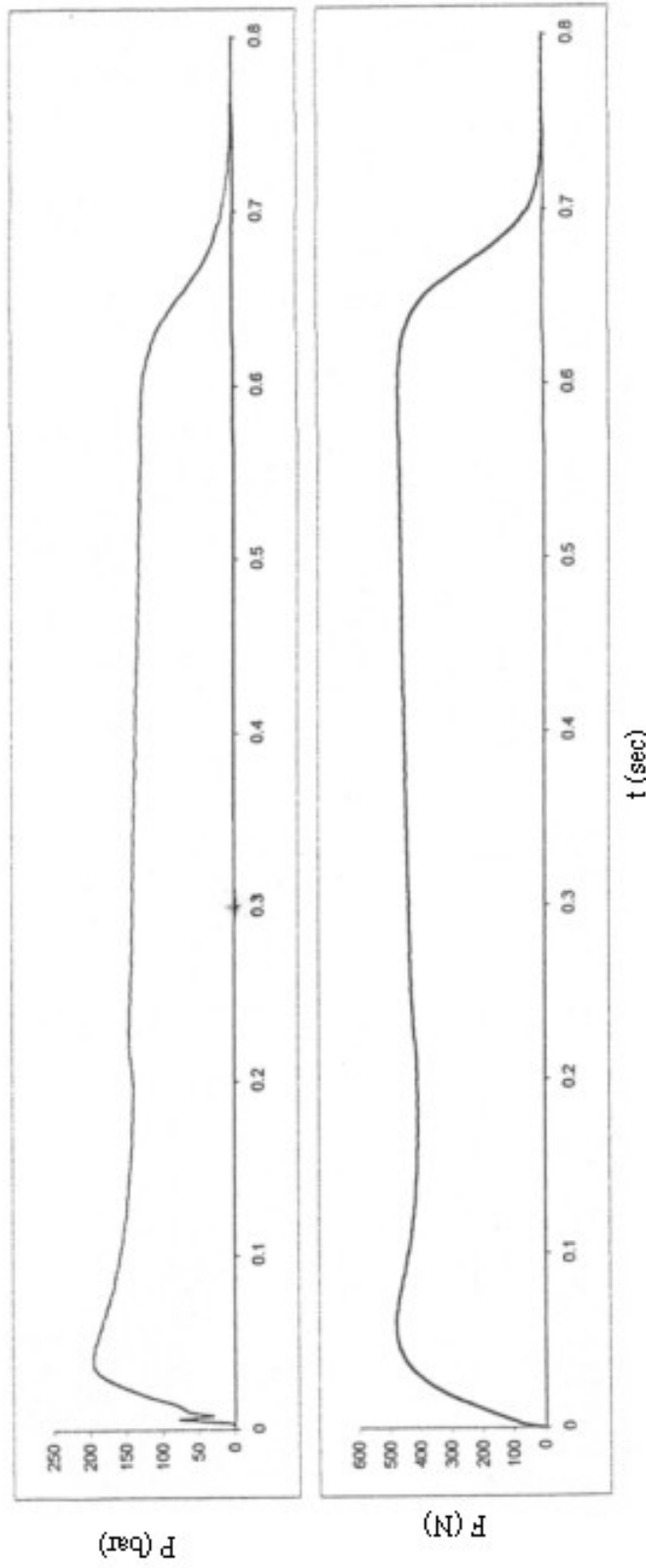


Figure 6.13: Results for Comp. 4, as pressure-time curve and thrust-time curve

Action Time = 0.714 sec

Maximum Pressure = 196.53 bar

Total Impulse = 3148.321 N.s

Burning time = 0.606 sec

Average Pressure = 137.15 bar

Specific Impulse = 2332.089 N.s/kg

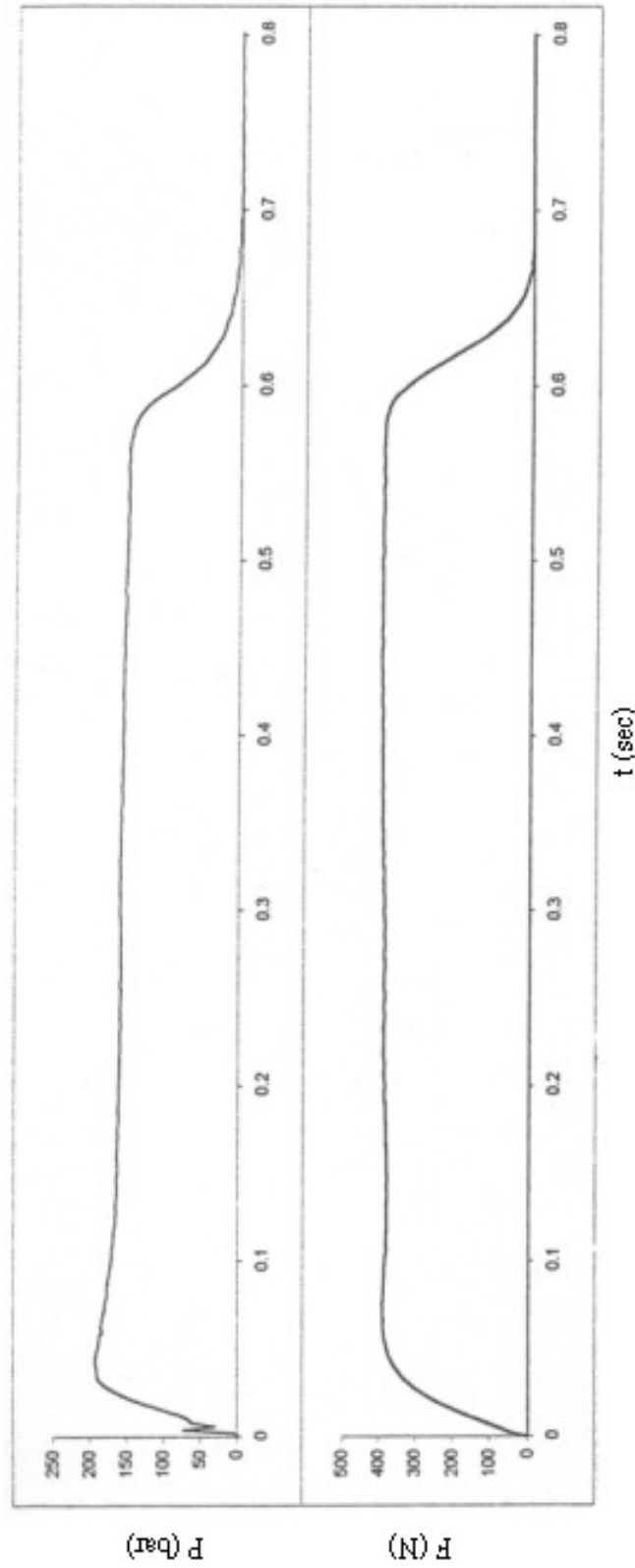


Figure 6.14: Results for Comp. 5, as pressure-time curve and thrust-time curve

Action Time = 0.656 sec

Maximum Pressure = 194.30 bar

Total Impulse = 2270.067 N.s

Burning time = 0.568 sec

Average Pressure = 156.96 bar

Specific Impulse = 1891.722 N.s/kg

6.2. Combustion Simulation & Motor Performance Prediction

The results obtained from the computer program are as follows:

6.2-1 Results of Double Base Propellants

As all the double base propellants used in the experiments (table 5.1) consist of nitrocellulose, nitroglycerine (except DB9) and centralite, their combustion have the same expected species⁽⁷³⁾, which are:

Table (6.1): The Expected Species From DB Propellants

C	CH	CNH	CNHO	CHO	CH ₂	CH ₂ O	CH ₃
CH ₄	CN	CO	CO ₂	C ₂	C ₂ H ₂	C ₂ H ₄	C ₂ H ₄ O
C ₂ N ₂	C ₃	C ₃ O ₂	C ₄	C ₄ N ₂	C ₅	H ⁻	H
NH	HO	H ₂	NH ₂	H ₂ O	H ₂ O ₂	NH ₃	N ₂ H ₄
N	NO	NO ₂	N ₂	N ₂ O	N ₂ O ₃	N ₂ O ₄	N ₂ O ₅
O	O ₂	O ₃	C ⁻	NHO	NHO ₂	NHO ₂	NHO ₃
HO ₂	NO ₃	O ⁻	N ₂ H ₂	NO ₂ ⁻	HO ⁺	HO ⁻	CHO ⁺
CN ₂	CO ₂ ⁻	C ₂ ⁻	C ₂ O	H ⁺	H ₃ O ⁺	NO ⁺	O ₂ ⁻
C ₂ H	C ₂ N	CN ₊	CN ⁻	CNO	N ₂ O ⁺	N ₃	CH ⁺
N ⁺	N ⁻	O ⁺	H ₂ ⁺	H ₂ ⁻	N ₂ ⁺	N ₂ ⁻	O ₂ ⁺
C ⁺	C _(s)	N ₂ O _{4 (s)}	N ₂ O _{4 (l)}	N ₂ H _{4 (l)}	H ₂ O _(l)	C _(s)	

As stated in the program, any species with number of moles less than 1×10^{-7} will be ignored from the results.

6.2-1-1 Results for DB1:

Fuel Type	Nitrocellulose	Nitroglycerine	Centralite
DB Fuel No.1	56.0 %	42.0 %	2.0 %

Results are based on 100 gm of DB1

Propellant density $\rho_p = 1571.0 \text{ kg/m}^3$

Number of gram atoms of each element present in ingredients

(2.528254) H, (1.826121) C, (1.079489) N, (3.774781) O

A) Chamber Results

Temperature = 3176 K, Pressure = 85 atm = 8615.66475 kPa

Enthalpy = - 219.3671 kJ, Entropy = 0.9752905 kJ/K

$c_p/c_v = \gamma = 1.2090$

Number of moles of gas = 3.6879

Number of moles of condensed species = 0.0000

Table (6.2): Number of moles of expected products in the combustion chamber

1.05152 (H ₂ O)	1.01779 (CO)	0.80828 (CO ₂)
0.53426 (N ₂)	0.17428 (H ₂)	0.05356 (HO)
0.02294 (H)	0.01092 (NO)	0.01002 (O ₂)
4.18×10^{-03} (O)	6.00×10^{-04} (HO ₂)	3.00×10^{-04} (CHO)
1.02×10^{-05} (NHO)	7.79×10^{-06} (NH ₃)	6.0×10^{-06} (N)
$5. \times 10^{-06}$ (NO ₂)	3.62×10^{-06} (NH ₂)	2.30×10^{-06} (CH ₂ O)
2.20×10^{-06} (N ₂ O)	2.18×10^{-06} (NH)	2.07×10^{-06} (CNH)
2.07×10^{-06} (CNHO)	8.84×10^{-07} (NHO ₂)	1.56×10^{-07} (CNO)

The molecular weight of the mixture is = 27.116

B) Exhaust Results

Temperature = 1560 K, Pressure = 1.00 atm = 101.325 kPa

Enthalpy = - 532.3723 kJ, Entropy = 0.9752905 kJ/K

$c_p/c_v = \gamma = 1.2286$

Number of moles of gas = 3.6300

Number of moles of condensed species = 0.0000

Table (6.3): Number of moles of expected products at the exhaust

0.98021 (CO ₂)	0.96844 (H ₂ O)	0.84591 (CO)
0.53974 (N ₂)	0.29566 (H ₂)	0.00004 (H)

The molecular weight of the mixture is = 27.548

C) Throat and Rocket Performance Result

Temperature = 2930 K,

Pressure = 47.64 atm = 4827.123 kPa

Characteristic velocity $c^* = 1,506.322$ m/s, $\gamma^s = 1.2220$

Optimum expansion = 10.47, Isp = 255.2 sec

Table (6.4): DB1 Results For Different Expansion Ratio

Expansion Ratio	Exit Pressure		Exit Temperature K	Specific Impulse	
	atm	kPa		sec	N.s/kg
1	48.355	4898.4	2930	105.0	1029
2	16.118	1632.8	2533	173.0	1696
3	5.672	574.6	2111	212.6	2084
4	3.740	378.9	1963	224.8	2204
5	2.732	276.7	1858	233.0	2285
6	2.123	215.0	1778	239.2	2345
7	1.719	174.1	1714	244.0	2392
8	1.434	145.3	1661	247.9	2431
9	1.224	124.0	1615	251.2	2463
10	1.063	107.6	1576	254.0	2491
11	0.936	94.8	1542	256.4	2515
12	0.834	84.4	1511	258.6	2536
13	0.750	76.0	1483	260.5	2555
14	0.680	68.9	1458	262.2	2572
15	0.621	62.9	1435	263.8	2587

6.2-1-2 Results for DB2:

Fuel Type	Nitrocellulose	Nitroglycerine	Centralite
DB Fuel No.2	56.3 %	42.1 %	1.6 %

Results are based on 100 gm of DB2

Propellant density $\rho_p = 1571.0 \text{ kg/m}^3$

Number of gram atoms of each element present in ingredients

(2.527399) H, (1.824799) C, (1.080122) N, (3.775274) O

A) Chamber Results

Temperature = 3178 K, Pressure = 85 atm = 8615.66475 kPa

Enthalpy = - 219.2416 kJ, Entropy = 0.9752068 kJ/K

$c_p/c_v = \gamma = 1.2090$

Number of moles of gas = 3.6869

Number of moles of condensed species = 0.0000

Table (6.5): Number of moles of expected products in the combustion chamber

1.05154 (H ₂ O)	1.01551 (CO)	0.80924 (CO ₂)
0.53452 (N ₂)	0.17363 (H ₂)	0.05392 (HO)
0.02299 (H)	0.01103 (NO)	0.01018 (O ₂)
4.24×10^{-03} (O)	6.00×10^{-04} (HO ₂)	3.00×10^{-04} (CHO)
1.03×10^{-05} (NHO)	7.75×10^{-06} (NH ₃)	6.25×10^{-06} (N)
5.24×10^{-06} (NO ₂)	3.61×10^{-06} (NH ₂)	2.29×10^{-06} (CH ₂ O)
2.22×10^{-06} (N ₂ O)	2.19×10^{-06} (NH)	2.06×10^{-06} (CNH)
2.06×10^{-06} (CNHO)	8.96×10^{-07} (NHO ₂)	1.56×10^{-07} (CNO)

The molecular weight of the mixture is = 27.123

B) Exhaust Results

Temperature = 1561 K, Pressure = 1.00 atm = 101.325 kPa

Enthalpy = - 532.4141 kJ, Entropy = 0.9752068 kJ/K

$c_p/c_v = \gamma = 1.2285$

Number of moles of gas = 3.6286

Number of moles of condensed species = 0.0000

Table (6.6): Number of moles of expected products at the exhaust

0.98098 (CO ₂)	0.96949 (H ₂ O)	0.84381 (CO)
0.54006 (N ₂)	0.29418 (H ₂)	0.00004 (H)

The molecular weight of the mixture is = 27.559

C) Throat and Rocket Performance Result

Temperature = 2931 K,

Pressure = 47.64 atm = 4827.123 kPa

Characteristic velocity $c^* = 1,506.505$ m/s, $\gamma^s = 1.2219$

Optimum expansion = 10.47, Isp = 255.2 sec

Table (6.7): DB2 Results For Different Expansion Ratio

Expansion Ratio	Exit Pressure		Exit Temperature K	Specific Impulse	
	atm	kPa		sec	N.s/kg
1	48.324	4895.2	2931	105.0	1030
2	16.108	1631.7	2535	173.1	1697
3	5.674	574.8	2113	212.6	2085
4	3.742	379.1	1965	224.8	2205
5	2.733	276.9	1861	233.1	2286
6	2.124	215.1	1781	239.2	2346
7	1.720	174.2	1716	244.0	2393
8	1.435	145.4	1663	247.9	2431
9	1.224	124.0	1618	251.2	2464
10	1.063	107.7	1578	254.0	2491
11	0.936	94.8	1544	256.5	2515
12	0.834	84.5	1513	258.7	2536
13	0.750	76.0	1485	260.6	2555
14	0.680	68.9	1460	262.3	2572
15	0.621	62.9	1437	263.9	2588

6.2-1-3 Results for DB3:

Fuel Type	Nitrocellulose	Nitroglycerine	Centralite
DB Fuel No.3	58.8 %	39.0 %	2.2 %

Results are based on 100 gm of DB3

Propellant density $\rho_p = 1569.6 \text{ kg/m}^3$

Number of gram atoms of each element present in ingredients

(2.544100) H, (1.850631) C, (1.067769) N, (3.765645) O

A) Chamber Results

Temperature = 3148 K, Pressure = 85 atm = 8615.66475 kPa

Enthalpy = - 221.9194 kJ, Entropy = 0.976211 kJ/K

$c_p/c_v = \gamma = 1.2102$

Number of moles of gas = 3.7063

Number of moles of condensed species = 0.0000

Table (6.8): Number of moles of expected products in the combustion chamber

1.06047 (CO)	1.05068 (H ₂ O)	0.79011 (CO ₂)
0.52934 (N ₂)	0.18678 (H ₂)	0.04701 (HO)
0.02203 (H)	9.05×10^{-03} (NO)	7.38×10^{-03} (O ₂)
3.30×10^{-03} (O)	4.73×10^{-05} (HO ₂)	3.53×10^{-05} (CHO)
8.74×10^{-06} (NHO)	8.71×10^{-06} (NH ₃)	5.25×10^{-06} (N)
3.72×10^{-06} (NO ₂)	3.61×10^{-06} (NH ₂)	2.56×10^{-06} (CH ₂ O)
2.37×10^{-06} (CNH)	2.20×10^{-06} (CNHO)	1.98×10^{-06} (NH)
1.81×10^{-06} (N ₂ O)	6.83×10^{-07} (NHO ₂)	1.46×10^{-07} (CNO)

The molecular weight of the mixture is = 26.981

B) Exhaust Results

Temperature = 1524 K, Pressure = 1.00 atm = 101.325 kPa

Enthalpy = - 531.6191 kJ, Entropy = 0.976211 kJ/K

$c_p/c_v = \gamma = 1.2314$

Number of moles of gas = 3.6566

Number of moles of condensed species = 0.0000

Table (6.9): Number of moles of expected products at the exhaust

0.96656 (CO ₂)	0.94845 (H ₂ O)	0.88406 (CO)
0.53388 N ₂	0.32358 (H ₂)	0.00003 (H)

The molecular weight of the mixture is = 27.348

C) Throat and Rocket Performance Result

Temperature = 2896 K,

Pressure = 47.64 atm = 4827.123 kPa

Characteristic velocity $c^* = 1,502.634$ m/s, $\gamma^s = 1.2234$

Optimum expansion = 10.39, Isp = 253.8 sec

Table (6.10): DB3 Results For Different Expansion Ratio

Expansion Ratio	Exit Pressure		Exit Temperature K	Specific Impulse	
	atm	kPa		sec	N.s/kg
1	48.290	4891.7	2896	104.8	1028
2	16.097	1630.6	2486	172.5	1691
3	5.628	570.1	2066	211.9	2078
4	3.710	375.9	1920	224.0	2196
5	2.709	274.5	1817	232.1	2276
6	2.105	213.2	1738	238.2	2336
7	1.704	172.6	1674	242.9	2382
8	1.421	144.0	1622	246.8	2420
9	1.213	122.8	1577	250.1	2452
10	1.053	106.7	1538	252.8	2479
11	0927	93.9	1504	255.3	2503
12	0.826	83.6	1474	257.4	2524
13	0.743	75.2	1447	259.3	2543
14	0.673	68.2	1422	261.0	2559
15	0.615	62.3	1399	262.6	2575

6.2-1-4 Results for DB4:

Fuel Type	Nitrocellulose	Nitroglycerine	Centralite
DB Fuel No.4	59.7 %	37.3 %	3.0 %

Results are based on 100 gm of DB4

Propellant density $\rho_p = 1568.9 \text{ kg/m}^3$

Number of gram atoms of each element present in ingredients

(2.552479) H, (1.863591) C, (1.061571) N, (3.760813) O

A) Chamber Results

Temperature = 3132 K, Pressure = 85.00 atm = 8615.66475 kPa

Enthalpy = - 53.35 kJ, Entropy = 233.43 kJ/K

$c_p/c_v = \gamma = 1.2108$

Number of moles of gas = 3.7163

Number of moles of condensed species = 0.0000

Table (6.11): Number of moles of expected products in the combustion chamber

1.08335 (CO)	1.04982 (H ₂ O)	0.78019 (CO ₂)
0.52669 (N ₂)	0.19378 (H ₂)	0.04366 (HO)
0.02148 (H)	8.14×10^{-03} (NO)	6.22×10^{-03} (O ₂)
2.88×10^{-03} (O)	4.06×10^{-05} (HO ₂)	3.56×10^{-05} (CHO)
9.24×10^{-06} (NH ₃)	7.99×10^{-06} (NHO)	4.78×10^{-06} (N)
3.60×10^{-06} (NH ₂)	3.10×10^{-06} (NO ₂)	2.71×10^{-06} (CH ₂ O)
2.55×10^{-06} (CNH)	2.27×10^{-06} (CNHO)	1.87×10^{-06} (NH)
1.62×10^{-06} (N ₂ O)	5.92×10^{-07} (NHO ₂)	3.49×10^{-07} (HO ⁻)
1.41×10^{-07} (CNO)		

The molecular weight of the mixture is = 26.908

B) Exhaust Results

Temperature = 1506 K, Pressure = 1.00 atm = 101.325 kPa

Enthalpy = -126.95 kJ, Entropy = 233.43 kJ/K

$c_p/c_v = \gamma = 1.2328$

Number of moles of gas = 3.6706

Number of moles of condensed species = 0.0000

Table (6.12): Number of moles of expected products at the exhaust

0.95982 (CO ₂)	0.93740 (H ₂ O)	0.90376 (CO)
0.53078 (N ₂)	0.33883 (H ₂)	3.00×10^{-05} (H)

The molecular weight of the mixture is = 27.243

C) Throat and Rocket Performance Result

Temperature = 2877 K, Pressure = 48.25 atm = 4888.931 kPa

Characteristic velocity $c^* = 1,520.586$ m/s, $\gamma^s = 1.2242$

Optimum expansion = 10.36, $I_{sp} = 253.1$ sec

Table (6.13): DB4 Results For Different Expansion Ratio

Expansion Ratio	Exit Pressure		Exit Temperature K	Specific Impulse	
	atm	kPa		sec	N.s/kg
1	48.246	4887.3	2877	104.7	1027
2	16.082	1629.1	2461	172.2	1688
3	5.606	567.9	2043	211.5	2074
4	3.696	374.4	1897	223.5	2192
5	2.698	273.3	1795	231.6	2271
6	2.096	212.3	1716	237.6	2330
7	1.697	171.9	1654	242.4	2377
8	1.415	143.4	1601	246.2	2414
9	1.207	122.3	1557	249.4	2446
10	1.048	106.2	1519	252.2	2473
11	0.923	93.5	1485	254.6	2497
12	0.822	83.2	1455	256.7	2517
13	0.739	74.9	1428	258.6	2536
14	0.670	67.9	1403	260.3	2553
15	0.612	62.0	1381	261.9	2568

6.2-1-5 Results for DB5:

Fuel Type	Nitrocellulose	Nitroglycerine	Centralite
DB Fuel No.5	60.0 %	36.8 %	3.2 %

Results are based on 100 gm of DB5

Propellant density $\rho_p = 1568.6 \text{ kg/m}^3$

Number of gram atoms of each element present in ingredients

(2.554987) H, (1.867471) C, (1.059716) N, (3.759367) O

A) Chamber Results

Temperature = 4052 K, Pressure = 85 atm = 8615.66475 kPa

Enthalpy = 51.61 kJ, Entropy = 262.35 kJ/K

$c_p/c_v = \gamma = 1.2427$

Number of moles of gas = 4.2246

Number of moles of condensed species = 0.0000

Table (6.14): Number of moles of expected products in the combustion chamber

1.45614 (CO)	0.71836 (H ₂ O)	0.49192 (N ₂)
0.41109 (CO ₂)	0.31804 (HO)	0.29395 (H ₂)
0.21094 (H)	0.12714 (O)	0.12000 (O ₂)
0.07522 (NO)	9.00×10^{-04} (HO ₂)	3.33×10^{-04} (N)
2.12×10^{-04} (CHO)	9.07×10^{-05} (NHO)	7.19×10^{-05} (NO ₂)
5.97×10^{-05} (NH)	2.53×10^{-05} (NH ₂)	1.43×10^{-05} (N ₂ O)
9.66×10^{-06} (NH ₃)	8.41×10^{-06} (CNH)	6.51×10^{-07} (NHO ₂)
4.79×10^{-06} (CH ₂ O)	3.84×10^{-06} (CNHO)	2.11×10^{-06} (CNO)
1.51×10^{-06} (CN)	1.08×10^{-06} (NO ⁺)	8.51×10^{-07} (CO ₂ ⁻)
8.20×10^{-07} (O ₃)	5.67×10^{-07} (HO ⁻)	3.09×10^{-07} (H ₃ O)
2.16×10^{-07} (O ⁻)	1.19×10^{-07} (C)	

The molecular weight of the mixture is = 23.671

B) Exhaust Results

Temperature = 2706 K, Pressure = 1.00 atm = 101.325 kPa

Enthalpy = - 65.55 kJ, Entropy = 262.35 kJ/K

$c_p/c_v = \gamma = 1.2180$

Number of moles of gas = 3.7657

Number of moles of condensed species = 0.0000

Table (6.15): Number of moles of expected products at the exhaust

1.09865 (CO)	1.00364 (H ₂ O)	0.76881 (CO ₂)
0.52577 (N ₂)	0.21547 (H ₂)	0.06428 (OH)
0.05246 (H)	0.01858 (O ₂)	9.81×10^{-03} (O)
8.16×10^{-03} (NO)	1.39×10^{-05} (HO ₂)	2.40×10^{-06} (N)
1.62×10^{-06} (CHO)	8.72×10^{-07} (NHO)	8.18×10^{-07} (NO ₂)
2.01×10^{-07} (NH)	1.72×10^{-07} (N ₂ O)	1.71×10^{-07} (NH ₃)
1.41×10^{-07} (NH ₂)		

The molecular weight of the mixture is = 26.556

C) Throat and Rocket Performance Result

Temperature = 3849 K, Pressure = 49.02 atm = 4966.952 kPa

Characteristic velocity $c^* = 1,876.958$ m/s, $\gamma^s = 1.2562$

Optimum expansion = 12.26, $I_{sp} = 319.3$ sec

Table (6.16): DB5 Results For Different Expansion Ratio

Expansion Ratio	Exit Pressure		Exit Temperature K	Specific Impulse	
	atm	kPa		sec	N.s/kg
1	49.001	4963.8	3849	125.5	1230
2	16.334	1654.6	3469	201.0	2059
3	6.233	631.4	3184	257.2	2522
4	4.218	427.2	3076	272.8	2675
5	3.139	318.0	2996	283.6	2781
6	2.476	250.8	2933	291.8	2861
7	2.030	205.7	2882	298.3	2925
8	1.712	173.4	2839	303.6	2978
9	1.474	149.4	2801	308.2	3022
10	1.291	130.8	2768	312.1	3060
11	1.145	116.0	2739	315.5	3094
12	1.027	104.0	2713	318.6	3124
13	0.929	94.2	2689	321.3	3151
14	0.848	85.9	2667	323.8	3175
15	0.778	78.8	2647	326.1	3198

6.2-1-6 Results for DB6:

Fuel Type	Nitrocellulose	Nitroglycerine	Centralite
DB Fuel No.6	60.6 %	37.5 %	1.9 %

Results are based on 100 gm of DB6

Propellant density $\rho_p = 1568.7 \text{ kg/m}^3$

Number of gram atoms of each element present in ingredients

(2.553961) H, (1.865884) C, (1.060475) N, (3.759959) O

A) Chamber Results

Temperature = 3148 K, Pressure = 85 atm = 8615.66475 kPa

Enthalpy = - 221.9194 kJ, Entropy = 0.976211 kJ/K

$c_p/c_v = \gamma = 1.2102$

Number of moles of gas = 3.7063

Number of moles of condensed species = 0.0000

Table (6.17): Number of moles of expected products in the combustion chamber

1.08742 (CO)	1.04963 (H ₂ O)	0.77842 (CO ₂)
0.52622 (N ₂)	0.19505 (H ₂)	0.04308 (HO)
0.02138 (H)	7.99×10^{-03} (NO)	6.03×10^{-03} (O ₂)
2.81×10^{-03} (O)	3.94×10^{-05} (HO ₂)	3.56×10^{-05} (CHO)
9.33×10^{-06} (NH ₃)	7.85×10^{-06} (NHO)	4.69×10^{-06} (N)
3.60×10^{-06} (NH ₂)	3.00×10^{-06} (NO ₂)	2.73×10^{-06} (CH ₂ O)
2.58×10^{-06} (CNH)	2.28×10^{-06} (CNHO)	1.85×10^{-06} (NH)
1.59×10^{-06} (N ₂ O)	5.76×10^{-07} (NHO ₂)	5.14×10^{-07} (CNO)

The molecular weight of the mixture is = 26.895

B) Exhaust Results

Temperature = 1503 K, Pressure = 1.00 atm = 101.325 kPa

Enthalpy = - 126.93 kJ, Entropy = 0.976211 kJ/K

$c_p/c_v = \gamma = 1.2331$

Number of moles of gas = 3.6731

Number of moles of condensed species = 0.0000

Table (6.18): Number of moles of expected products at the exhaust

0.96656 (CO ₂)	0.93541 (H ₂ O)	0.90721 (CO)
0.53023 N ₂	0.34156 (H ₂)	0.00002 (H)

The molecular weight of the mixture is = 27.225

C) Throat and Rocket Performance Result

Temperature = 2873 K,

Pressure = 47.64 atm = 4827.123 kPa

Characteristic velocity $c^* = 1,520.068$ m/s, $\gamma^s = 1.2244$

Optimum expansion = 10.35, $I_{sp} = 253.0$ sec

Table (6.19): DB6 Results For Different Expansion Ratio

Expansion Ratio	Exit Pressure		Exit Temperature K	Specific Impulse	
	atm	kPa		sec	N.s/kg
1	48.238	4886.6	2873	104.7	1027
2	16.079	1628.9	2456	172.1	1688
3	5.602	567.5	2038	211.4	2073
4	3.693	374.1	1893	223.4	2191
5	2.696	273.1	1791	231.5	2270
6	2.094	212.1	1713	237.5	2329
7	1.695	171.7	1950	242.3	2376
8	1.414	143.2	1598	246.1	2413
9	1.206	122.2	1553	249.3	2445
10	1.047	106.1	1515	252.1	2472
11	0.922	93.4	1481	254.5	2496
12	0.821	83.2	1451	256.6	2516
13	0.738	74.8	1424	258.5	2535
14	0.669	67.8	1400	260.2	2552
15	0.611	61.9	1377	261.7	2567

6.2-1-7 Results for DB7:

Fuel Type	Nitrocellulose	Nitroglycerine	Centralite
DB Fuel No.7	62.0 %	37.6 %	0.4 %

Results are based on 100 gm of DB7

Propellant density $\rho_p = 1568.6 \text{ kg/m}^3$

Number of gram atoms of each element present in ingredients

(2.556070) H, (1.869146) C, (1.058915) N, (3.758743) O

A) Chamber Results

Temperature = 3125 K, Pressure = 85 atm = 8615.66475 kPa

Enthalpy = - 223.8022 kJ, Entropy = 0.9768386 kJ/K

$c_p/c_v = \gamma = 1.2111$

Number of moles of gas = 3.7207

Number of moles of condensed species = 0.0000

Table (6.20): Number of moles of expected products in the combustion chamber

1.09321 (CO)	1.04936 (H ₂ O)	0.77588 (CO ₂)
0.52555 (N ₂)	0.19687 (H ₂)	0.04225 (HO)
0.02123 (H)	7.77×10^{-03} (NO)	5.77×10^{-03} (O ₂)
2.72×10^{-03} (O)	3.79×10^{-05} (HO ₂)	3.57×10^{-05} (CHO)
9.48×10^{-06} (NH ₃)	7.67×10^{-06} (NHO)	4.58×10^{-06} (N)
3.59×10^{-06} (NH ₂)	2.86×10^{-06} (NO ₂)	2.77×10^{-06} (CH ₂ O)
2.63×10^{-06} (CNH)	2.30×10^{-06} (CNHO)	1.82×10^{-06} (NH)
1.54×10^{-06} (N ₂ O)	5.55×10^{-07} (NHO ₂)	1.38×10^{-07} (CNO)

The molecular weight of the mixture is = 26.876

B) Exhaust Results

Temperature = 1498 K, Pressure = 1.00 atm = 101.325 kPa

Enthalpy = -530.9497 kJ, Entropy = 0.9768386 kJ/K

$c_p/c_v = \gamma = 1.2334$

Number of moles of gas = 3.6766

Number of moles of condensed species = 0.0000

Table (6.21): Number of moles of expected products at the exhaust

0.95703 (CO ₂)	0.93256 (H ₂ O)	0.91211 (CO)
0.52945 (N ₂)	0.34546 (H ₂)	0.00002 (H)

The molecular weight of the mixture is = 27.199

C) Throat and Rocket Performance Result

Temperature = 2984 K,

Pressure = 47.64 atm = 4827.123 kPa

Characteristic velocity $c^* = 1,499.433$ m/s, $\gamma^s = 1.2246$

Optimum expansion = 10.34 , Isp = 252.8 sec

Table (6.22): DB7 Results For Different Expansion Ratio

Expansion Ratio	Exit Pressure		Exit Temperature K	Specific Impulse	
	atm	kPa		sec	N.s/kg
1	48.211	4883.8	2868	104.7	1027
2	16.070	1627.9	2450	172.0	1687
3	5.597	566.9	2032	211.3	2072
4	3.689	373.7	1888	223.3	2190
5	2.693	272.8	1786	231.4	2269
6	2.092	211.9	1707	237.4	2328
7	1.693	171.5	1645	242.1	2374
8	1.412	143.1	1593	246.0	2412
9	1.205	122.0	1548	249.2	2443
10	1.046	105.9	1510	251.9	2470
11	0.921	93.3	1476	254.3	2494
12	0.820	83.1	1447	256.4	2515
13	0.737	74.7	1420	258.3	2533
14	0.669	67.7	1395	260.0	2550
15	0.610	61.8	1373	261.6	2565

6.2-1-8 Results for DB8:

Fuel Type	Nitrocellulose	Nitroglycerine	Centralite
DB Fuel No.8	62.6 %	34.3 %	3.1 %

Results are based on 100 gm of DB8

Propellant density $\rho_p = 1567.4 \text{ kg/m}^3$

Number of gram atoms of each element present in ingredients

(2.569921) H, (1.890570) C, (1.048671) N, (3.750757) O

A) Chamber Results

Temperature = 4049 K, Pressure = 85 atm = 8615.66475 kPa

Enthalpy = 51.04 kJ, Entropy = 262.63 kJ/K

$c_p/c_v = \gamma = 1.2429$

Number of moles of gas = 4.2340

Number of moles of condensed species = 0.0000

Table (6.23): Number of moles of expected products in the combustion chamber

1.48301 (CO)	0.71912 (H ₂ O)	0.48783 (N ₂)
0.40730 (CO ₂)	0.31210 (HO)	0.30256 (H ₂)
0.21311 (H)	0.12248 (O)	0.11243 (O ₂)
0.07236 (NO)	8.50×10^{-03} (HO ₂)	3.30×10^{-03} (N)
2.18×10^{-04} (CHO)	8.84×10^{-05} (NHO)	6.69×10^{-05} (NO ₂)
5.98×10^{-05} (NH)	2.58×10^{-05} (NH ₂)	1.37×10^{-05} (N ₂ O)
1.00×10^{-05} (NH ₃)	8.87×10^{-06} (CNH)	6.16×10^{-06} (NHO ₂)
5.01×10^{-06} (CH ₂ O)	2.12×10^{-06} (CNO)	1.56×10^{-06} (CN)
1.06×10^{-06} (NO ⁺)	8.09×10^{-07} (CO ₂ ⁻)	7.40×10^{-07} (O ₃)
5.32×10^{-07} (HO ⁻)	3.20×10^{-07} (H ₃ O ⁺)	2.00×10^{-07} (O ⁻)
1.23×10^{-07} (C)		

The molecular weight of the mixture is = 23.618

B) Exhaust Results

Temperature = 2688 K, Pressure = 1.00 atm = 101.325 kPa

Enthalpy = - 66.16 kJ, Entropy = 262.63 kJ/K

$c_p/c_v = \gamma = 1.2188$

Number of moles of gas = 3.7798

Number of moles of condensed species = 0.0000

Table (6.24): Number of moles of expected products at the exhaust

1.13484 (CO)	1.00319 (H ₂ O)	0.75573 (CO ₂)
0.52085 N ₂	0.22775 (H ₂)	0.05752 (HO)
0.05051 (H)	0.01438 (O ₂)	8.01×10^{-03} (O)
6.96×10^{-03} (NO)	1.10×10^{-05} (HO ₂)	2.07×10^{-06} (N)
1.64×10^{-06} (CHO)	7.62×10^{-07} (NHO)	6.22×10^{-07} (NO ₂)
1.87×10^{-07} (NH ₃)	1.84×10^{-07} (NH)	1.45×10^{-07} (N ₂ O)
1.40×10^{-07} (NH ₂)		

The molecular weight of the mixture is = 26.457

C) Throat and Rocket Performance Result

Temperature = 3845 K, Pressure = 49.02 atm = 4966.952 kPa

Characteristic velocity $c^* = 1,878.025$ m/s, $\gamma^s = 1.2564$

Optimum expansion = 12.22, $I_{sp} = 319.4$ sec

Table (6.25): DB8 Results For Different Expansion Ratio

Expansion Ratio	Exit Pressure		Exit Temperature K	Specific Impulse	
	atm	kPa		sec	N.s/kg
1	49.005	4964.2	3845	125.5	1231
2	16.335	1654.7	3465	210.1	2061
3	6.221	630.2	3174	257.4	2524
4	4.207	426.2	3063	273.0	2677
5	3.130	317.1	2982	283.8	2783
6	2.468	250.0	2918	292.0	2863
7	2.023	204.9	2866	298.5	2927
8	1.706	172.8	2822	303.8	2980
9	1.469	148.8	2784	308.4	3024
10	1.286	130.2	2750	312.3	3062
11	1.140	115.5	2721	315.7	3096
12	1.022	103.6	2694	318.8	3126
13	0.925	93.7	2670	321.5	3153
14	0.844	85.5	2647	324.0	3177
15	0.774	78.4	2627	326.3	3199

6.2-1-9 Results for DB9:

Fuel Type	Nitrocellulose	Nitroglycerine	Centralite
DB Fuel No.9	98.6 %	00.0 %	1.4 %

Results are based on 100 gm of DB9

Propellant density $\rho_p = 1550.1 \text{ kg/m}^3$

Number of gram atoms of each element present in ingredients

(2.771700) H, (2.202676) C, (0.899426) N, (3.634415) O

A) Chamber Results

Temperature = 2526 K, Pressure = 85 atm = 8615.66475 kPa

Enthalpy = - 61.70 kJ, Entropy = 234.57 kJ/K

$c_p/c_v = \gamma = 1.2348$

Number of moles of gas = 4.0412

Number of moles of condensed species = 0.0000

Table (6.26): Number of moles of expected products in the combustion chamber

1.68208 (CO)	0.90929 (H ₂ O)	0.52055 (CO ₂)
0.47345 (H ₂)	0.44962 (N ₂)	4.23×10^{-03} (H)
1.77×10^{-03} (HO)	1.20×10^{-04} (NO)	4.81×10^{-05} (NH ₃)
2.01×10^{-05} (CHO)	1.45×10^{-05} (CNH)	1.02×10^{-05} (O)
9.93×10^{-06} (CH ₂ O)	8.06×10^{-06} (O ₂)	4.00×10^{-06} (CNHO)
1.42×10^{-06} (NH ₂)	2.37×10^{-07} (CH ₄)	1.63×10^{-07} (NHO)

The molecular weight of the mixture is = 24.745

B) Exhaust Results

Temperature = 1088 K, Pressure = 1.00 atm = 101.325 kPa

Enthalpy = - 122.65 kJ, Entropy = 234.57 kJ/K

$c_p/c_v = \gamma = 1.2720$

Number of moles of gas = 4.0375

Number of moles of condensed species = 0.0000

Table (6.27): Number of moles of expected products at the exhaust

1.31713 (CO)	0.88518 (CO ₂)	0.83812 (H ₂)
0.54693 (H ₂ O)	0.44969 (N ₂)	3.70×10 ⁻⁰⁴ (CH ₄)
4.00×10 ⁻⁰⁵ (NH ₃)	3.32×10 ⁻⁰⁷ (CH ₂ O)	

The molecular weight of the mixture is = 24.768

C) Throat and Rocket Performance Result

Temperature = 2264 K,

Pressure = 47.46 atm = 4808.885 kPa

Characteristic velocity $c^* = 1,407.201$ m/s, $\gamma^s = 1.2556$

Optimum expansion = 9.77, $I_{sp} = 230.3$ sec

Table (6.28): DB9 Results For Different Expansion Ratio

Expansion Ratio	Exit Pressure		Exit Temperature K	Specific Impulse	
	atm	kPa		sec	N.s/kg
1	47.463	4808.0	2264	98.7	968
2	15.821	1602.7	1841	159.5	1564
3	5.274	534.2	1493	195.4	1916
4	3.462	350.7	1378	205.9	2019
5	2.520	255.3	1297	213.0	2089
6	1.953	197.8	1236	218.2	2140
7	1.577	189.8	1187	222.3	2180
8	1.313	133.0	1146	225.7	2213
9	1.118	113.3	1111	228.4	2240
10	0.969	98.2	1082	230.8	2264
11	0.852	86.3	1055	232.9	2284
12	0.758	76.8	1032	234.7	2302
13	0.681	69.0	1011	236.4	2318
14	0.617	62.5	992	237.8	2332
15	0.562	57.0	975	239.1	2345

6.2-2 Results of Composite Propellants

The first four types composite propellants used in the experiments (table 5.2) consist of aluminum powder (Al), ammonium perchlorate (AP), iron oxide (Fe_2O_3), and Hydroxy Terminated Polybutadiene (HTPB), and they have the same expected species in the reaction⁽⁷³⁾, which are:

Table (6.29): The Expected Species From Composite Propellants

Al	AlC	AlCl	AlOCl	AlCl ₂	AlCl ₃
AlH	AlHO	AlHO ₂	AlN	AlO	Al ₂ Cl ₆
Al ₂ O	Al ₂ O ₂	C	CCl	CNCl	COCl ₂
CCl ₄	CH	CHCl ₃	CNH	CNHO	CHO
CH ₂	CH ₂ Cl ₂	CH ₂ O	CH ₃	CH ₃ Cl	CH ₄
CN	CO	CO ₂	C ₂	C ₂ H ₂	C ₂ H ₄
C ₂ H ₄ O	C ₂ N ₂	C ₃	C ₃ O ₂	C ₄	C ₄ N ₂
C ₅	Cl	HCl	HOCl	NOCl	OCl
O ₂ Cl	Cl ₂	OCl ₂	H ⁻	H	NH
HO	H ₂	NH ₂	H ₂ O	H ₂ O ₂	NH ₃
N ₂ H ₄	N	NO	NO ₂	N ₂	N ₂ O
N ₂ O ₃	N ₂ O ₄	N ₂ O ₅	O	O ₂	O ₃
COCl	C ⁻	NO ₂ Cl	NHO	NHO ₂	NHO ₃
AlHO	HO ₂	NO ₃	Fe	CCl ₂	CCl ₃
Al ⁺	Cl ⁺	Cl ⁻	FeCl	FeCl ₂	FeCl ₃
Fe ₂ Cl ₆	FeO	O ⁻	N ₂ H ₂	NO ₂ ⁻	HO ⁺
HO ⁻	CN ₂	CO ₂ ⁻	C ₂ ⁻	C ₂ O	FeH ₂ O ₂
H ⁺	H ₃ O ⁺	NO ⁺	O ₂ ⁻	C ₂ H	C ₂ N
C ₂ Cl ₄	C ₂ Cl ₆	AlHO ⁺	AlHO ⁻	AlCl ⁺	AlCl ₂ ⁺
AlCl ₂ ⁻	AlO ⁺	AlO ₂	AlO ₂ ⁻	Al ₂ O ⁺	Al ₂ O ₂ ⁺
C ₂ Cl ₂	C ₂ HCl	CN ⁺	CN ⁻	CHCl	CNO
Fe ₂ Cl ₄	N ₂ O ⁺	N ₃	CH ⁺	AlO ⁻	N ⁺
N ⁻	O ⁺	H ₂ ⁺	H ₂ ⁻	N ₂ ⁺	N ₂ ⁻
O ₂ ⁺	C ⁺	FeC ₅ O ₅	Fe ⁺	Fe ⁻	Al ⁻
Al ₂	Al _(s)	Al _(l)	AlCl _{3(s)}	AlCl _{3(l)}	AlN _(s)
Al ₂ O _{3(s)}	Al ₂ O _{3(l)}	Al ₄ C _{3(s)}	C _(s)	NH ₄ Cl _(s)	NH ₄ O ₄ Cl _(s)
N ₂ O _{4(s)}	N ₂ O _{4(l)}	AlOCl _(s)	Fe _(s)	Fe _(l)	FeCl _{2(s)}
FeCl _{2(l)}	FeCl _{3(s)}	FeCl _{3(l)}	FeO _(s)	FeO _(l)	Fe ₂ O _{3(s)}
Fe ₃ O _{4(s)}	N ₂ H _{4(l)}	FeH ₂ O _{2(s)}	Al ₂ O _{3(s)}	FeC ₅ O _{5(l)}	H ₂ O _(l)

As stated in the program, the species with number of moles less than 1×10^{-7} is ignored from the results.

6.2-2-1 Results for Comp.1:

Fuel Type	Al	AP	Fe ₂ O ₃	binder
Comp. Fuel No.1	15.9 %	72.2 %	2.0 %	9.9 %

Results are based on 100 gm of Comp.1

Propellant density $\rho_p = 1848.4 \text{ kg/m}^3$

Number of gram atoms of each element present in ingredients

(3.511585) H, (0.697456) C, (0.623015) N, (2.516834) O

(0.589325) Al, (0.614484) Cl, (0.025047) Fe

A) Chamber Results

Temperature = 3484 K, Pressure = 85 atm = 8615.66475 kPa

Enthalpy = - 179.3263 kJ, Entropy = 0.9471741 kJ/K

$c_p/c_v = \gamma = 1.1749$

Number of moles of gas = 3.5031

Number of moles of condensed species = 0.2580

Table (6.30): Number of moles of expected products in the combustion chamber

0.76583 (H ₂ O)	0.63889 (H ₂)	0.60872 (CO)
0.49747 (HCl)	0.30752 (N ₂)	0.28218 (Al ₂ O ₃ (l))
0.12246 (H)	0.08856 (CO ₂)	0.07452 (HO)
0.06273 (Cl)	0.01497 (FeCl ₂)	0.00835 (AlCl)
8.16×10^{-03} (O)	7.81×10^{-03} (NO)	6.72×10^{-03} (Fe)
6.34×10^{-03} (AlOCl)	4.06×10^{-03} (AlHO ₂)	3.82×10^{-03} (O ₂)
3.26×10^{-03} (AlCl ₂)	1.32×10^{-03} (FeO)	1.18×10^{-03} (AlHO)
1.05×10^{-03} (FeCl)	9.67×10^{-04} (FeH ₂ O ₂)	9.22×10^{-04} (AlO)
4.37×10^{-04} (AlCl ₃)	1.98×10^{-04} (Al)	1.88×10^{-04} (Cl ₂)
1.47×10^{-04} (OCl)	1.04×10^{-04} (HOCl)	8.76×10^{-05} (CHO)
6.13×10^{-05} (COCl)	5.32×10^{-05} (Al ₂ O)	4.82×10^{-05} (HO ₂)
4.34×10^{-05} (N)	3.76×10^{-05} (NH ₃)	3.17×10^{-05} (AlH)
2.75×10^{-05} (Cl ⁻)	2.62×10^{-05} (AlO ₂)	2.59×10^{-05} (NH ₂)
1.89×10^{-05} (NH)	1.85×10^{-05} (FeCl ₃)	1.55×10^{-05} (NHO)
1.54×10^{-05} (Al ₂ O ₂)	1.45×10^{-05} (AlHO)	1.06×10^{-05} (CNH)

7.39×10^{-06} (Al ⁺)	5.68×10^{-06} (CH ₂ O)	5.59×10^{-06} (Fe ⁺)
2.26×10^{-06} (CNHO)	1.85×10^{-06} (NO ₂)	1.72×10^{-06} (NOCl)
1.31×10^{-06} (N ₂ O)	4.55×10^{-07} (AlO ⁻)	4.07×10^{-07} (CN)
4.00×10^{-07} (NHO ₂)	3.91×10^{-07} (Fe ₂ Cl ₄)	3.60×10^{-07} (NHO ₂)
3.19×10^{-07} (AlCl ₂ ⁺)	2.93×10^{-07} (CNO)	1.42×10^{-07} (HO ⁻)
1.29×10^{-07} (CO ₂ ⁻)		

The molecular weight of the mixture is = 28.414

B) Exhaust Results

Temperature = 2328 K, Pressure = 1.00 atm = 101.325 kPa

Enthalpy = - 526.6401 kJ, Entropy = 0.9471741 kJ/K

$c_p/c_v = \gamma = 1.1608$

Number of moles of gas = 3.0877

Number of moles of condensed species = 0.2945

Table (6.31): Number of moles of expected products at the exhaust

0.80755 (H ₂ O)	0.66009 (H ₂)	0.57322 (CO)
0.55674 (HCl)	0.31144 (N ₂)	0.15572 (Al ₂ O _{3 (l)})
0.13882 (Al ₂ O _{3 (s)})	0.12422 (CO ₂)	0.02385 (FeCl ₂)
0.01598 (H)	9.64×10^{-03} (Cl)	3.34×10^{-03} (HO)
9.60×10^{-04} (Fe)	1.26×10^{-04} (NO)	1.05×10^{-04} (FeH ₂ O ₂)
8.76×10^{-05} (AlOCl)	7.31×10^{-05} (FeCl)	6.31×10^{-05} (AlCl)
5.38×10^{-05} (O)	4.63×10^{-05} (FeO)	3.40×10^{-05} (AlCl ₂)
2.75×10^{-05} (O ₂)	2.56×10^{-05} (AlHO ₂)	2.02×10^{-05} (AlCl ₃)
6.40×10^{-06} (Cl ₂)	5.15×10^{-06} (AlHO)	4.95×10^{-06} (FeCl ₃)
1.26×10^{-06} (NH ₃)	8.23×10^{-07} (HOCl)	5.40×10^{-07} (CHO)
4.57×10^{-07} (COCl)	3.51×10^{-07} (OCl)	2.89×10^{-07} (AlO)
1.44×10^{-07} (Fe ₂ Cl ₄)	1.17×10^{-07} (CNH)	

The molecular weight of the mixture is = 29.566

C) Throat and Rocket Performance Result

Temperature = 3425 K, Pressure = 49.13 atm = 4978.10 kPa

Characteristic velocity $c^* = 1,553.200$ m/s, $\gamma^s = 1.1687$

Optimum expansion = 12.55, $I_{sp} = 266.0$ sec

Table (6.32): comp.1 Results For Different Expansion Ratio

Expansion Ratio	Exit Pressure		Exit Temperature K	Specific Impulse	
	atm	kPa		sec	N.s/kg
1	49.134	4977.2	3425	104.1	1021
2	16.378	1659.1	3049	174.8	1714
3	6.249	633.0	2753	214.2	2100
4	4.218	427.3	2641	227.2	2228
5	3.134	317.5	2559	236.3	2317
6	2.469	250.1	2495	243.1	2384
7	2.022	204.8	2443	248.5	2437
8	1.703	172.6	2399	252.9	2480
9	1.466	148.5	2361	256.7	2517
10	1.283	130.0	2329	259.9	2549
11	1.155	117.1	2329	262.5	2574
12	1.050	106.1	2328	264.8	2597
13	0.962	97.4	2328	266.9	2617
14	0.887	89.8	2328	268.8	2636
15	0.822	83.3	2327	270.6	2654

6.2-2-2 Results for Comp.2:

Fuel Type	Al	AP	Fe ₂ O ₃	binder
Comp. Fuel No.2	14.9 %	72.1 %	1.1 %	11.9 %

Results are based on 100 gm of Comp.2

Propellant density $\rho_p = 1796.0 \text{ kg/m}^3$

Number of gram atoms of each element present in ingredients

(3.721039) H, (0.838357) C, (0.623888) N, (2.500832) O
 (0.552261) Al, (0.613633) Cl, (0.013776) Fe

A) Chamber Results

Temperature = 3515 K, Pressure = 85 atm = 8615.66475 kPa

Enthalpy = - 181.1254 kJ, Entropy = 0.9388479 kJ/K

$c_p/c_v = \gamma = 1.1721$

Number of moles of gas = 3.4402

Number of moles of condensed species = 0.2649

Table (6.33): Number of moles of expected products in the combustion chamber

0.80318 (H ₂)	0.75524 (CO)	071405 (H ₂ O)
0.52452 (HCl)	0.30980 (N ₂)	0.26492 (Al ₂ O ₃ (l))
0.11023 (H)	0.08292 (CO ₂)	0.04758 (Cl)
0.04677 (HO)	9.07×10^{-03} (FeCl ₂)	8.64×10^{-03} (AlCl)
5.02×10^{-03} (AlOCl)	4.13×10^{-03} (NO)	3.70×10^{-03} (O)
3.55×10^{-03} (AlCl ₂)	3.33×10^{-03} (Fe)	2.72×10^{-03} (AlHO ₂)
1.29×10^{-03} (O ₂)	1.05×10^{-03} (AlHO)	5.66×10^{-04} (AlO)
5.32×10^{-04} (AlCl ₃)	5.16×10^{-04} (FeCl)	4.48×10^{-04} (FeO)
3.93×10^{-04} (FeH ₂ O ₂)	1.64×10^{-04} (Al)	1.35×10^{-04} (Cl ₂)
1.00×10^{-04} (CHO)	6.49×10^{-05} (OCl)	6.07×10^{-05} (HOCl)
5.91×10^{-05} (COCl)	5.27×10^{-05} (NH ₃)	4.62×10^{-05} (Al ₂ O)
3.09×10^{-05} (AlH)	2.66×10^{-05} (N)	2.59×10^{-05} (NH ₂)
1.86×10^{-05} (CNH)	1.79×10^{-05} (Cl ⁻)	1.77×10^{-05} (HO ₂)
1.41×10^{-05} (NH)	1.07×10^{-05} (AlO ₂)	1.04×10^{-05} (FeCl ₃)
1.00×10^{-05} (AlHO ⁺)	9.78×10^{-06} (Al ₂ O ₂)	8.84×10^{-06} (NHO)
8.35×10^{-06} (CH ₂ O)	5.58×10^{-06} (Al ⁺)	2.90×10^{-06} (CNHO)

2.07×10^{-06} (Fe ⁺)	1.49×10^{-06} (AlHO)	7.70×10^{-07} (NOCl)
6.69×10^{-07} (N ₂ O)	5.88×10^{-06} (NO ₂)	4.78×10^{-07} (CN)
2.59×10^{-07} (CNO)	2.57×10^{-07} (AlCl ₂ ⁺)	2.39×10^{-07} (AlO ⁻)
1.56×10^{-07} (Fe ₂ Cl ₄)	1.54×10^{-07} (NHO ₂)	1.45×10^{-07} (CH ₃)
1.28×10^{-07} (CNCl)		

The molecular weight of the mixture is = 26.990

B) Exhaust Results

Temperature = 2176 K, Pressure = 1.00 atm = 101.325 kPa

Enthalpy = - 526.6401 kJ, Entropy = 0.9388479 kJ/K

$c_p/c_v = \gamma = 1.1915$

Number of moles of gas = 3.3245

Number of moles of condensed species = 0.2761

Table (6.34): Number of moles of expected products at the exhaust

0.84915 (H ₂)	0.72080 (CO)	0.71558 (H ₂ O)
0.58228 (HCl)	0.31193 (N ₂)	0.27609 (Al ₂ O _{3 (s)})
0.11754 (CO ₂)	0.01353 (FeCl ₂)	8.27×10^{-03} (H)
4.12×10^{-03} (Cl)	9.57×10^{-04} (HO)	1.89×10^{-04} (Fe)
2.64×10^{-05} (FeH ₂ O ₂)	2.62×10^{-05} (NO)	2.10×10^{-05} (AlOCl)
1.94×10^{-05} (AlCl)	1.66×10^{-05} (FeCl)	1.61×10^{-05} (AlCl ₃)
1.49×10^{-05} (AlCl ₂)	6.40×10^{-06} (O)	4.70×10^{-06} (FeO)
4.53×10^{-06} (AlHO ₂)	2.73×10^{-06} (Cl ₂)	2.64×10^{-06} (FeCl ₃)
2.29×10^{-06} (O ₂)	2.07×10^{-06} (NH ₃)	1.23×10^{-06} (AlHO)
4.28×10^{-07} (CHO)	3.01×10^{-07} (COCl)	2.26×10^{-07} (CNH)
2.26×10^{-07} (HOCl)	1.16×10^{-07} (CH ₂ O)	

The molecular weight of the mixture is = 27.773

C) Throat and Rocket Performance Result

Temperature = 3321 K, Pressure = 49.25 atm = 4990.26 kPa

Characteristic velocity $c^* = 1,598.310$ m/s, $\gamma^s = 1.1785$

Optimum expansion = 12.18, $I_{sp} = 268.1$ sec

Table (6.35): comp.2 Results For Different Expansion Ratio

Expansion Ratio	Exit Pressure		Exit Temperature K	Specific Impulse	
	atm	kPa		sec	N.s/kg
1	49.164	4980.3	3321	104.3	1023
2	16.388	1660.1	2963	175.5	1721
3	6.322	640.4	2684	214.9	2108
4	4.275	433.1	2577	228.2	2237
5	3.181	322.2	2499	237.3	2327
6	2.508	254.1	2438	244.2	2395
7	2.056	208.3	2388	249.7	2449
8	1.734	175.6	2346	254.2	2493
9	1.488	150.7	2303	258.2	2532
10	1.294	131.1	2258	261.8	2567
11	1.142	115.7	2218	264.9	2598
12	1.019	103.2	2182	267.6	2625
13	0.918	93.0	2150	270.1	2649
14	0.834	84.5	2121	272.3	2670
15	0.763	77.3	2094	274.3	2690

6.2-2-3 Results for Comp.3:

Fuel Type	Al	AP	Fe ₂ O ₃	Binder
Comp. Fuel No.3	14.4 %	72.2 %	1.0 %	12.4 %

Results are based on 100 gm of Comp.3

Propellant density $\rho_p = 1783.5 \text{ kg/m}^3$

Number of gram atoms of each element present in ingredients

(3.777658) H, (0.873582) C, (0.625170) N, (2.503435) O
 (0.533729) Al, (0.614484) Cl, (0.012523) Fe

A) Chamber Results

Temperature = 3475 K, Pressure = 85 atm = 8615.66475 kPa

Enthalpy = - 180.6233 kJ, Entropy = 0.9449984 kJ/K

$c_p/c_v = \gamma = 1.1748$

Number of moles of gas = 3.4938

Number of moles of condensed species = 0.2566

Table (6.36): Number of moles of expected products in the combustion chamber

0.83400 (H ₂)	0.78936 (CO)	071424 (H ₂ O)
0.53184 (HCl)	0.31075 (N ₂)	0.25661 (Al ₂ O ₃ (l))
0.10347 (H)	0.08402 (CO ₂)	0.04369 (Cl)
0.04136 (HO)	8.56×10^{-03} (FeCl ₂)	7.98×10^{-03} (AlCl)
4.51×10^{-03} (AlOCl)	3.52×10^{-03} (NO)	3.40×10^{-03} (AlCl ₂)
2.97×10^{-03} (O)	2.81×10^{-03} (Fe)	2.38×10^{-03} (AlHO ₂)
9.97×10^{-04} (O ₂)	9.47×10^{-04} (AlHO)	5.42×10^{-04} (AlCl ₃)
4.55×10^{-04} (AlO)	4.42×10^{-04} (FeCl)	3.53×10^{-04} (FeO)
3.42×10^{-04} (FeH ₂ O ₂)	1.37×10^{-04} (Al)	1.24×10^{-04} (Cl ₂)
9.95×10^{-05} (CHO)	5.76×10^{-05} (COCl)	5.60×10^{-05} (NH ₃)
5.34×10^{-05} (HOCl)	5.26×10^{-05} (OCl)	3.78×10^{-05} (Al ₂ O)
2.69×10^{-05} (AlH)	2.49×10^{-05} (NH ₂)	2.22×10^{-05} (N)
2.03×10^{-05} (CNH)	1.51×10^{-05} (Cl ⁻)	1.39×10^{-05} (HO ₂)
1.24×10^{-05} (NH)	9.80×10^{-06} (FeCl ₃)	8.94×10^{-06} (CH ₂ O)
8.55×10^{-05} (AlHO ⁺)	7.97×10^{-05} (AlO ₂)	7.68×10^{-06} (Al ₂ O ₂)

7.59×10^{-06} (NHO)	4.66×10^{-06} (Al ⁺)	3.02×10^{-06} (CNHO)
1.62×10^{-06} (Fe ⁺)	1.23×10^{-06} (AlHO)	6.30×10^{-07} (NOCl)
5.65×10^{-07} (N ₂ O)	4.58×10^{-07} (CN)	4.46×10^{-06} (NO ₂)
2.41×10^{-07} (CNO)	2.28×10^{-07} (AlCl ₂ ⁺)	2.39×10^{-07} (AlO ⁻)
1.45×10^{-07} (CH ₃)	1.56×10^{-07} (Fe ₂ Cl ₄)	1.28×10^{-07} (CNCl)
1.54×10^{-07} (NHO ₂)		

The molecular weight of the mixture is = 26.664

B) Exhaust Results

Temperature = 2104 K, Pressure = 1.00 atm = 101.325 kPa

Enthalpy = - 526.0544 kJ, Entropy = 0.9449984 kJ/K

$c_p/c_v = \gamma = 1.1957$

Number of moles of gas = 3.3867

Number of moles of condensed species = 0.2668

Table (6.37): Number of moles of expected products at the exhaust

0.88544 (H ₂)	0.75173 (CO)	0.70688 (H ₂ O)
0.58689 (HCl)	0.31257 (N ₂)	0.26684 (Al ₂ O _{3 (s)})
0.12184 (CO ₂)	0.01240 (FeCl ₂)	5.54×10^{-03} (H)
2.69×10^{-03} (Cl)	5.41×10^{-04} (HO)	9.13×10^{-05} (Fe)
1.80×10^{-05} (FeH ₂ O ₂)	1.31×10^{-05} (NO)	1.27×10^{-05} (AlCl ₃)
9.40×10^{-06} (AlOCl)	9.00×10^{-06} (FeCl)	8.54×10^{-06} (AlCl)
8.25×10^{-06} (AlCl ₂)	2.44×10^{-06} (FeCl ₃)	2.40×10^{-06} (NH ₃)
2.36×10^{-06} (O)	1.85×10^{-06} (FeO)	1.85×10^{-06} (Cl ₂)
1.84×10^{-06} (AlHO ₂)	8.04×10^{-07} (O ₂)	5.06×10^{-07} (AlHO)
3.38×10^{-07} (CHO)	2.53×10^{-07} (Cl ⁻)	2.50×10^{-07} (CNH)
2.32×10^{-07} (COCl)	1.30×10^{-07} (HOCl)	1.26×10^{-07} (CH ₂ O)

The molecular weight of the mixture is = 27.371

C) Throat and Rocket Performance Result

Temperature = 3251 K, Pressure = 48.86 atm = 4950.74 kPa

Characteristic velocity $c^* = 1,570.573$ m/s, $\gamma^s = 1.1816$

Optimum expansion = 12.20, $I_{sp} = 268.1$ sec

Table (6.38): comp.3 Results For Different Expansion Ratio

Expansion Ratio	Exit Pressure		Exit Temperature K	Specific Impulse	
	atm	kPa		sec	N.s/kg
1	48.828	4946.3	3251	106.2	1042
2	16.276	1648.8	2847	177.2	1737
3	6.081	616.0	2529	217.1	2129
4	4.088	414.1	2410	230.0	2256
5	3.029	306.9	2325	239.0	2343
6	2.406	243.7	2278	245.5	2408
7	1.983	200.9	2238	250.8	2460
8	1.680	170.2	2205	255.2	2503
9	1.452	147.1	2176	258.9	2539
10	1.276	129.2	2151	262.2	2571
11	1.135	115.0	2128	265.0	2599
12	1.021	103.4	2108	267.6	2624
13	0.926	93.8	2090	269.9	2646
14	0.846	85.7	2073	271.9	2667
15	0.778	78.9	2057	273.8	2685

6.2-2-4 Results for Comp.4:

Fuel Type	Al	AP	Fe ₂ O ₃	binder
Comp. Fuel No.4	14.5 %	72.5 %	0.6 %	12.4 %

Results are based on 100 gm of Comp.4

Propellant density $\rho_p = 1779.9 \text{ kg/m}^3$

Number of gram atoms of each element present in ingredients

(3.787871) H, (0.873582) C, (0.627723) N, (2.506134) O
 (0.537435) Al, (0.617037) Cl, (0.007514) Fe

A) Chamber Results

Temperature = 3484 K, Pressure = 85 atm = 8615.66475 kPa

Enthalpy = - 179.3263 kJ, Entropy = 0.9471741 kJ/K

$c_p/c_v = \gamma = 1.1749$

Number of moles of gas = 3.5031

Number of moles of condensed species = 0.2580

Table (6.39): Number of moles of expected products in the combustion chamber

0.83608 (H ₂)	0.78988 (CO)	0.71215 (H ₂ O)
0.53888 (HCl)	0.31197 (N ₂)	0.25796 (Al ₂ O ₃ (l))
0.10588 (H)	0.08350 (CO ₂)	0.04517 (Cl)
0.04231 (HO)	0.00842 (AlCl)	0.00310 (O)
2.46×10^{-03} (AlHO ₂)	1.70×10^{-03} (Fe)	1.04×10^{-03} (O ₂)
9.85×10^{-04} (AlHO)	5.68×10^{-04} (AlCl ₃)	4.84×10^{-04} (AlO)
2.68×10^{-04} (Fecl)	2.14×10^{-04} (FeO)	2.01×10^{-04} (FeH ₂ O ₂)
1.47×10^{-04} (Al)	1.29×10^{-04} (Cl ₂)	1.01×10^{-04} (CHO)
5.90×10^{-05} (COCl)	5.59×10^{-05} (NH ₃)	5.51×10^{-05} (OCl)
5.51×10^{-05} (HOCl)	4.09×10^{-05} (Al ₂ O)	2.86×10^{-05} (AlH)
2.54×10^{-05} (NH ₂)	2.33×10^{-05} (N)	2.04×10^{-05} (CNH)
1.56×10^{-05} (Cl ⁻)	1.44×10^{-05} (HO ₂)	1.29×10^{-05} (NH)
9.20×10^{-06} (AlHO)	8.94×10^{-06} (CH ₂ O)	8.52×10^{-06} (AlO ₂)
8.28×10^{-06} (Al ₂ O ₂)	7.81×10^{-06} (NHO)	5.91×10^{-06} (FeCl ₃)
5.09×10^{-06} (Al ⁺)	3.03×10^{-06} (CNHO)	1.02×10^{-06} (Fe ⁺)
6.59×10^{-07} (NOCl)	5.82×10^{-07} (N ₂ O)	4.74×10^{-07} (CN)

4.65×10^{-07} (NO ₂)	2.50×10^{-07} (AlCl ₂ ⁺)	2.47×10^{-07} (CNO)
1.87×10^{-07} (AlO ⁻)	1.63×10^{-07} (CH ₃)	1.34×10^{-07} (CNCl)
1.27×10^{-07} (NHO ₂)		

The molecular weight of the mixture is = 26.588

B) Exhaust Results

Temperature = 2113 K, Pressure = 1.00 atm = 101.325 kPa

Enthalpy = - 526.6401 kJ, Entropy = 0.9471741 kJ/K

$c_p/c_v = \gamma = 1.2314$

Number of moles of gas = 3.3946

Number of moles of condensed species = 0.2687

Table (6.40): Number of moles of expected products at the exhaust

0.88609 (H ₂)	0.75276 (CO)	0.70502 (H ₂ O)
0.59915 (HCl)	0.31385 (N ₂)	0.26869 (Al ₂ O _{3 (s)})
0.12082 (CO ₂)	0.00743 (FeCl ₂)	5.88×10^{-03} (H)
2.91×10^{-03} (Cl)	5.81×10^{-04} (HO)	5.77×10^{-05} (Fe)
1.43×10^{-05} (NO)	1.40×10^{-05} (AlCl ₃)	1.07×10^{-05} (AlOCl)
1.06×10^{-05} (FeH ₂ O ₂)	9.88×10^{-06} (AlCl)	9.42×10^{-06} (AlCl ₂)
5.69×10^{-06} (FeCl)	2.68×10^{-06} (O)	2.37×10^{-06} (NH ₃)
2.08×10^{-06} (AlHO ₂)	2.02×10^{-06} (Cl ₂)	1.48×10^{-06} (FeCl ₃)
1.19×10^{-06} (FeO)	9.09×10^{-07} (O ₂)	8.22×10^{-07} (Cl ⁺)
5.76×10^{-07} (AlHO)	3.52×10^{-07} (CHO)	2.51×10^{-07} (CNH)
4.61×10^{-07} (COCl)	1.41×10^{-07} (HOCl)	1.26×10^{-07} (CH ₂ O)

The molecular weight of the mixture is = 27.298

C) Throat and Rocket Performance Result

Temperature = 3287 K, Pressure = 49.20 atm = 4985.19 kPa

Characteristic velocity $c^* = 1,604.101$ m/s, $\gamma^s = 1.1817$

Optimum expansion = 12.00, $I_{sp} = 268.8$ sec

Table (6.41): comp.4 Results For Different Expansion Ratio

Expansion Ratio	Exit Pressure		Exit Temperature K	Specific Impulse	
	atm	kPa		sec	N.s/kg
1	49.136	4977.4	3286	104.9	1028
2	16.379	1659.1	2923	176.2	1728
3	6.290	637.1	2640	215.8	2117
4	4.250	430.5	2532	229.1	2246
5	3.160	320.1	2453	238.2	2336
6	2.491	252.3	2392	245.1	2404
7	2.041	206.8	2341	250.6	2458
8	1.711	173.3	2287	255.4	2504
9	1.462	1.481	2235	259.5	2545
10	1.271	128.7	2189	263.0	2579
11	1.121	113.5	2149	266.1	2609
12	1.000	101.3	2113	268.8	2636
13	0.900	91.2	2081	271.2	2660
14	0.817	82.8	2052	273.4	2681
15	0.747	75.7	2025	275.4	2700

6.2-2-5 Results for Comp.5:

Fuel Type	Mg	AP	Fe ₂ O ₃	binder
Comp. Fuel No.5	5.3 %	74.6 %	2.1 %	18.0 %

The expected species from this propellant are:

Table (6.42): The Expected Species From Comp.5 Propellants

C	CCl	CNCl	COCl ₂	CCl ₄	CH
CHCl ₃	CNH	CNHO	CHO	CH ₂	CH ₂ Cl ₂
CH ₂ O	CH ₃	CH ₃ Cl	CH ₄	CN	CO
CO ₂	C ₂	C ₂ H ₂	C ₂ H ₄	C ₂ H ₄ O	C ₂ N ₂
C ₃	C ₃ O ₂	C ₄	C ₄ N ₂	C ₅	Cl
HCl	HOCl	MgCl	NOCl	OCl	O ₂ Cl
Cl ₂	MgCl ₂	Ocl ₂	H ⁻	H	MgH
MgHO	NH	HO	H ₂	NH ₂	H ₂ O
H ₂ O ₂	NH ₃	N ₂ H ₄	Mg	MgO	N
NO	NO ₂	N ₂	N ₂ O	N ₂ O ₃	N ₂ O ₄
N ₂ O ₅	O	O ₂	O ₃	COCl	C ⁻
NO ₂ Cl	NHO	NHO ₂	NHO ₃	HO ₂	MgN
NO ₃	Fe	CCl ₂	CCl ₃	Cl ⁺	Cl ⁻
FeCl	FeCl ₂	FeCl ₃	Fe ₂ Cl ₆	FeO	O ⁻
N ₂ H ₂	NO ₂ ⁻	HO ⁺	HO ⁻	CHO ⁺	CN ₂
CO ₂ ⁻	C ₂ ⁻	C ₂ O	FeH ₂ O ₂	H ⁺	H ₃ O ⁺
NO ⁺	O ₂ ⁻	C ₂ H	C ₂ N	MgH ₂ O ₂	C ₂ Cl ₄
C ₂ Cl ₆	Mg ⁺	MgCl ⁺	MgHO ⁺	C ₂ Cl ₂	C ₂ HCl
CN ⁺	CN ⁻	CHCl	Mg ₂ Cl ₄	CNO	Fe ₂ Cl ₄
N ₂ O ⁺	N ₃	CH ⁺	Mg ₂	N ⁺	N ⁻
O ⁺	H ₂ ⁺	H ₂ ⁻	N ₂ ⁺	N ₂ ⁻	O ₂ ⁺
C ⁺	FeC ₅ O ₅	Fe ⁺	Fe ⁻	C _(s)	MgCO ₃ (s)
MgC ₂ (s)	Mg ₂ C ₃ (s)	NH ₄ Cl (s)	NH ₄ O ₄ Cl (s)	MgCl ₂ (s)	MgCl ₂ (l)
MgH ₂ (s)	MgH ₂ O ₂ (s)	Mg (s)	Mg (l)	MgO (s)	Mg ₃ N ₂ (s)
N ₂ O ₄ (s)	N ₂ O ₄ (l)	Fe (s)	Fe (l)	FeCl ₂ (s)	FeCl ₂ (l)
FeCl ₃ (s)	FeCl ₃ (l)	FeO (s)	FeO (l)	Fe ₂ O ₃ (s)	Fe ₃ O ₄ (s)
N ₂ H ₄ (l)	MgO (l)	FeH ₂ O ₂ (s)	FeH ₃ O ₃ (s)	FeC ₅ O ₅ (l)	Fe ₂ O ₃ (s)
H ₂ O (l)					

Results are based on 100 gm of Comp.5

Propellant density $\rho_p = 1630.5 \text{ kg/m}^3$

Number of gram atoms of each element present in ingredients

(4.455366) H, (1.268102) C, (0.650422) N, (2.617868) O
(0.217928) Mg, (0.634910) Cl, (0.026299) Fe

A) Chamber Results

Temperature = 2706 K, Pressure = 85 atm = 8615.66475 kPa

Enthalpy = - 45.28 kJ, Entropy = 240.37 kJ/K

$c_p/c_v = \gamma = 1.2284$

Number of moles of gas = 4.1517

Number of moles of condensed species = 0.1167

Table (6.43): Number of moles of expected products in the combustion chamber

1.09204 (CO)	1.04477 (H ₂ O)	0.97434 (H ₂)
0.39190 (HCl)	0.32506 (N ₂)	0.17597 (CO ₂)
0.11668 (MgO _(s))	0.09390 (MgCl ₂)	0.02450 (FeCl ₂)
0.01268 (H)	3.57×10^{-03} (HO)	3.53×10^{-03} (Cl)
2.60×10^{-03} (MgH ₂ O ₂)	1.95×10^{-03} (MgCl)	1.33×10^{-03} (MgHO)
1.09×10^{-03} (Mg)	9.78×10^{-04} (FeH ₂ O ₂)	6.15×10^{-04} (Fe)
1.68×10^{-04} (NO)	1.27×10^{-04} (FeCl)	1.20×10^{-04} (Mg ₂ Cl ₄)
1.05×10^{-04} (MgH)	9.97×10^{-05} (NH ₃)	4.58×10^{-05} (FeO)
3.00×10^{-05} (CHO)	2.91×10^{-05} (O)	2.73×10^{-05} (MgO)
2.08×10^{-05} (FeCl ₃)	2.01×10^{-05} (CNH)	1.27×10^{-05} (O ₂)
1.27×10^{-05} (CH ₂ O)	1.16×10^{-05} (COCl)	8.57×10^{-06} (Cl ₂)
4.39×10^{-06} (NH ₂)	3.65×10^{-06} (Fe ₂ Cl ₄)	3.51×10^{-06} (HOCl)
3.24×10^{-06} (CNHO)	5.76×10^{-07} (OCl)	5.70×10^{-07} (Cl ⁻)
5.52×10^{-07} (CH ₄)	4.56×10^{-07} (MgN)	3.65×10^{-07} (MgCl ⁺)
3.35×10^{-07} (NH)	3.35×10^{-07} (NHO)	2.14×10^{-07} (N)
1.78×10^{-07} (HO ₂)	1.67×10^{-07} (CH ₃)	

The molecular weight of the mixture is = 23.428

B) Exhaust Results

Temperature = 1220 K, Pressure = 1.00 atm = 101.325 kPa

Enthalpy = - 114.46 kJ, Entropy = 240.37 kJ/K

$$c_p/c_v = \gamma = 1.2634$$

Number of moles of gas = 4.1382

Number of moles of condensed species = 0.2177

Table (6.44): Number of moles of expected products at the exhaust

1.18892 (H ₂)	0.88369 (CO)	0.74769 (H ₂ O)
0.58192 (HCl)	0.38437 (CO ₂)	0.32519 (N ₂)
0.21773 (MgO _(s))	0.02612 (FeCl ₂)	1.91×10 ⁻⁰⁴ (MgCl ₂)
8.65×10 ⁻⁰⁵ (Fe ₂ Cl ₄)	3.25×10 ⁻⁰⁵ (CH ₄)	3.13×10 ⁻⁰⁵ (NH ₃)
7.47×10 ⁻⁰⁶ (FeCl ₃)	6.30×10 ⁻⁰⁷ (H)	4.03×10 ⁻⁰⁷ (CNH)
2.66×10 ⁻⁰⁷ (Cl)	2.64×10 ⁻⁰⁷ (CH ₂ O)	2.14×10 ⁻⁰⁷ (FeH ₂ O ₂)

The molecular weight of the mixture is = 22.957

C) Throat and Rocket Performance Result

Temperature = 2457 K,

Pressure = 47.93 atm = 4856.51 kPa

Characteristic velocity $c^* = 1,487.576$ m/s,

$\gamma^s = 1.2491$

Optimum expansion = 9.97,

$I_{sp} = 245.4$ sec

Table (6.45): comp.5 Results For Different Expansion Ratio

Expansion Ratio	Exit Pressure		Exit Temperature K	Specific Impulse	
	atm	kPa		sec	N.s/kg
1	47.917	4854.0	2457	103.1	1011
2	15.972	1618.0	2053	168.2	1649
3	5.419	549.0	1676	206.7	2027
4	3.558	360.4	1549	218.2	2140
5	2.590	262.4	1459	226.0	2216
6	2.007	203.3	1391	231.7	2272
7	1.621	164.2	1336	236.2	2316
8	1.350	136.7	1291	239.8	2352
9	1.149	116.4	1253	242.9	2381
10	0.996	100.9	1219	245.5	2407
11	0.876	88.8	1190	247.7	2429
12	0.779	79.0	1164	249.7	2449
13	0.700	70.9	1141	251.5	2466
14	0.634	64.2	1120	253.1	2482
15	0.578	58.6	1101	254.5	2496

6.3. Output Data from Experiment

Referring to section 6.1, the experimental results are shown in table 6.46 below

Table 6.46: The Experimental Results

Fuel type	Fuel weight (kg)	Total Impulse (N.s)	I_{sp} (N.s/kg)	I_{sp} (s)
DB.1	1.2	2294 ± 12	1911.7	195.07
DB.2	1.2	2301 ± 10	1917.5	195.68
DB.3	1.2	2488 ± 12	2073.3	211.56
DB.4	1.2	2361 ± 13	1967.5	200.77
DB.5	1.2	2874 ± 6	2395.0	244.39
DB.6	1.2	2444 ± 8	2036.7	207.83
DB.7	1.2	2305 ± 12	1920.8	196.00
DB.8	1.2	3082 ± 3	2568.3	262.07
DB.9	1.2	2195 ± 8	1829.2	186.65
Comp.1	1.35	2900 ± 3	2148.2	219.20
Comp.2	1.35	2925 ± 11	2166.7	221.09
Comp.3	1.35	3148 ± 10	2331.9	237.95
Comp.4	1.35	2820 ± 2	2089.9	213.26
Comp.5	1.2	2270 ± 7	1891.7	193.03

6.4. Comparison Between Experimental & Theoretical Results

From section 5.4-1, one can get the expansion ratio of the experimental rocket motor, which has the value of (3.16). By interpolating this value in results obtained in section 6.2, one can get the third column in table 6.47. Second column is obtained from table 6.46. The Absolute Percent Deviation (A%D) is calculated using equation (6.3-1) below:

$$A\%D = \frac{|Experimental I_{sp} - Theoretical I_{sp}|}{Experimental I_{sp}} \times 100\% \quad (6.3-1)$$

Table 6.47: Comparison Between Experimental and Theoretical Results

Fuel type	Experimental I_{sp} (s)	Theoretical I_{sp} (s)	Deviation A%D
DB.1	195.07	214.552	9.99
DB.2	195.68	214.552	9.64
DB.3	211.56	222.236	5.05
DB.4	200.77	213.42	6.30
DB.5	244.39	259.696	6.26
DB.6	207.83	213.32	2.64
DB.7	196.00	213.22	8.79
DB.8	262.07	259.896	0.83
DB.9	186.65	197.08	5.59
Comp.1	219.20	216.28	1.33
Comp.2	221.09	217.028	1.84
Comp.3	237.95	219.164	7.90
Comp.4	213.26	217.928	2.19
Comp.5	193.03	208.54	8.04

6.4. Discussion

NASA had published some examples, and their results as NASA-Lewis program produced. Those examples were subjected to the program obtained by this work, and the results were compared with those of NASA. This comparison gives good agreements with a deviation of less than 4%, as shown in table 6.48 below. This gives confidence to use the program, to obtain either complex chemical equilibrium composition and/or rocket motor performance.

Table 6.48: Comparison Between NASA and This work

Fuel	Optimum Impulse (sec)		A%D
	NASA result	This work	
H ₂ = 2.83% wt. Air = 97.17% wt.	224.3	221.4	1.29
H ₂ = 2.00% wt. Air = 98.00% wt.	200.0	193.6	3.20
Li = 33.4%wt. F = 66.6% wt.	355.5	369.0	3.80
Hydrazine = 14.26% wt. Dimethylhydrazine = 14.26% wt. F = 71.48% wt.	382.5	370.7	3.08
O ₂ = 50%wt. H ₂ = 50% wt.	426.1	412.2	3.26
Average A%D			2.926

Contrary to expectations, the performance of the composite propellants was slightly higher (except for comp.5) than that of the double base propellants, delivering an average specific impulse within about 3.5 percent for both theoretical and experimental results. It was expected that the composite propellant, as a high energetic fuel (higher than the double base propellant), would give much higher rocket performance; but neither experiments nor the prediction program gave the expected results. This is due to the formation of condensed species occurred in the composite propellants, which affected the throat as can be seen from the discussion of thrust coefficient.

An extra examination of the results was done by comparing the theoretical thrust coefficient with that obtained from experimental results. The characteristic velocity can be obtained from the experimental results by using equation (3.8-3). Then from equation (3.8-2), thrust coefficient can be obtained, using experimental results for specific impulse. Experimental thrust coefficients were compared with the theoretical ones and the results are shown in table 6.49.

From table 6.49, the deviations of the double base propellant are acceptable, except that of DB5 and DB8. Those propellants gave unexpected experimental results for both specific impulse and thrust coefficient. The only logical explanation is that there was inaccurate composition in manufacturing these grains

While for composite propellant the deviation is higher than 10% for all Al propellants. This is because aluminum formed condensed species, which were deposited on throat.

Table 6.49: Comparison Between Experimental and Theoretical thrust Coefficient

Fuel type	Experimental C_f (s)	Theoretical C_f (s)	Deviation A%D
DB.1	1.2903	1.3900	7.75
DB.2	1.3277	1.3957	5.12
DB.3	1.4094	1.4494	2.84
DB.4	1.3046	1.3755	5.43
DB.5	1.6197	1.3559	16.29
DB.6	1.3880	1.3753	0.92
DB.7	1.3057	1.3936	6.73
DB.8	1.7307	1.3562	21.64
DB.9	1.2056	1.3725	13.84
Comp.1	1.5198	1.3646	10.21
Comp.2	1.6366	1.3307	18.69
Comp.3	1.6187	1.3675	15.52
Comp.4	1.4651	1.3314	19.59
Comp.5	1.2533	1.3738	9.62

To study the effect of O/F ratio, the program was applied to different percent of oxidizer ranging from 1% to 99%, for both propellant types, and the variation of chamber temperature and specific impulse with the percent oxidizer, which were obtained from the program, were tabulated and drawn. The results are shown in tables 6.50 and 6.51 and figures 6.15 to 6.16

Table 6.50: Effect of varying percent oxidizer ratio on chamber temperature and specific impulse of double base propellant

Percent Oxidizer	Chamber Temperature K	Specific Impulse Sec
1	3971	316.8
10	3999	318.2
20	4023	319.1
30	4041	319.4
40	4054	319.3
50	4063	318.8
60	4067	318.0
70	4068	317.0
80	4066	315.9
90	4061	314.7
95	4057	314.0
99	4054	313.5

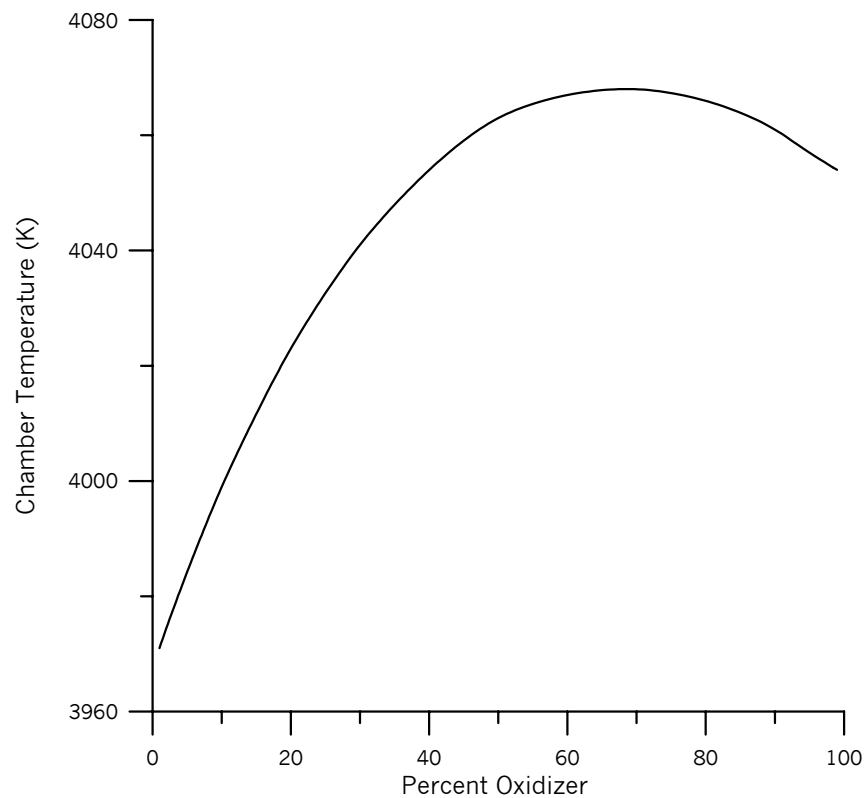


Figure 6.15: Effect of Varying O/F Ratio on Temperature of Double Base Propellant

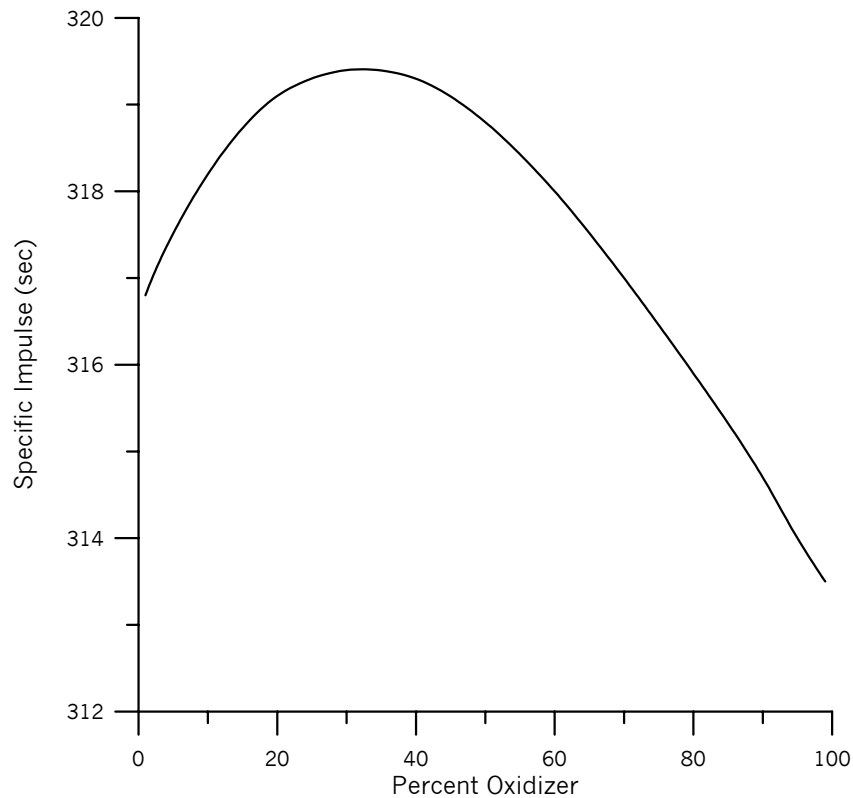


Figure 6.16: Effect of Varying O/F Ratio on Specific Impulse of Double Base propellant

Table 6.51: Effect of varying O/F ratio on chamber temperature and specific impulse of composite propellant

Percent Oxidizer	Chamber Temperature K	Specific Impulse Sec
1	546	9.4
10	1790	55.2
20	2868	110.9
30	2988	160.1
40	3148	198.8
50	4000	228.6
60	4000	273.8
70	4000	277.5
80	3805	249.1
90	2923	229.3
95	2315	202.4
99	1598	169.1

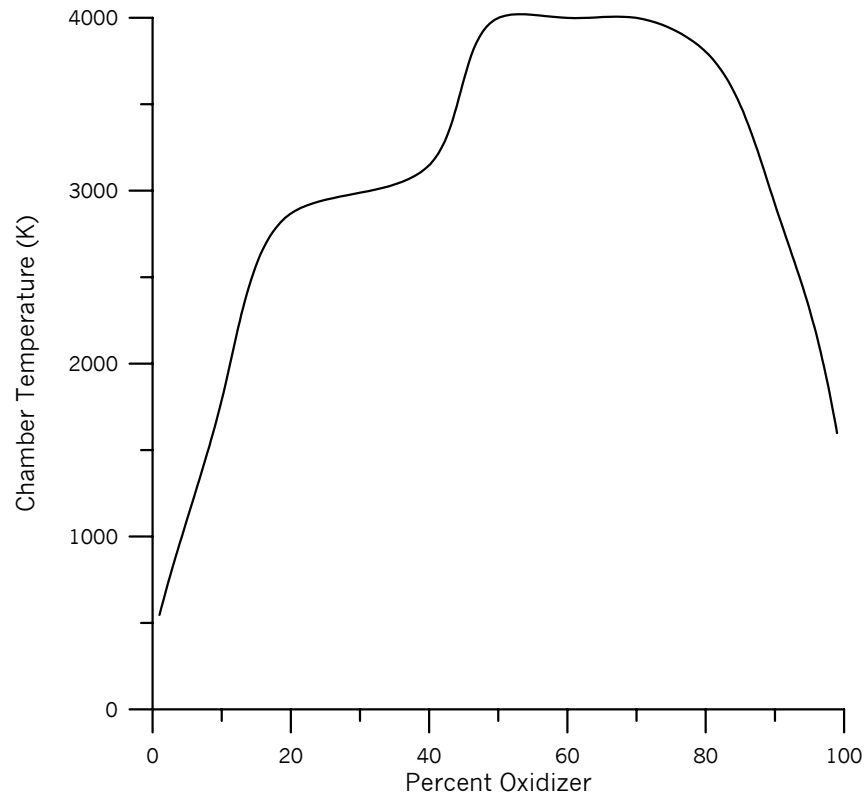


Figure 6.17: Effect of varying O/F ratio on chamber temperature of composite propellant

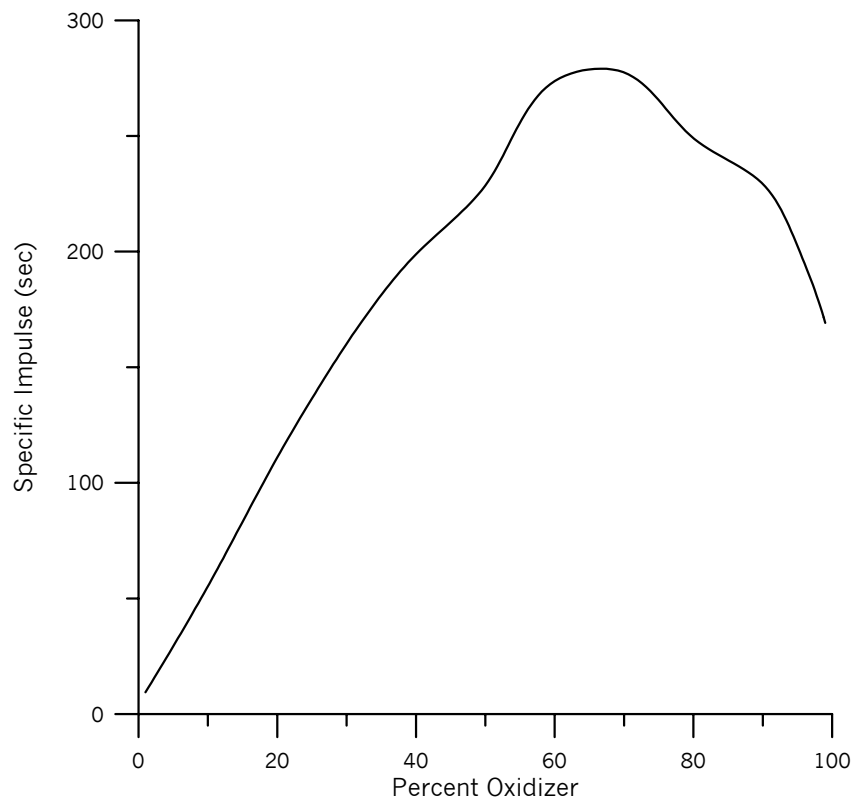


Figure 6.18: Effect of varying O/F ratio on specific impulse of composite propellant

From the above figures (6.15 and 6.16), maximum performance for double base propellant can be achieved with a moderately O/F ratio, that the specific impulse is highest in the range of 40 percent, tapering off with a lower oxidizer percentage, and being drastically lowered at high oxidizer ratio.

Combustion temperature (chamber temperature) is ranging within 70 K only, increasing with oxidizer percentage, due to complete combustions. It is important to notice that these figures are based on theoretical result obtained from the computer program.

In the case of composite propellant in figures (6.17 and 6.18), maximum performance can be achieved at higher oxidizer percentage. The specific impulse is highest in the range of 60 to 75 percent oxidizer, tapering off with a lower oxidizer percentage, and being drastically lowered at high oxidizer ratio. Again here these figures were based on theoretical results, which were obtained from the computer program

Chamber temperatures are highest in the range 50 to 80 oxidizer percentage. From 20 to 50 percent, the temperature is lowered because of the decomposition reactions of high fuel percentages. Under 20 percent oxidizer, the low temperature is due to the limited combustion process.

The chamber temperatures for the applied composition of the double base propellant were theoretically calculated and drawn versus the variation of oxidizer to fuel ratio, on figure 6.19. From this figure, it is noticed that the optimum (higher) combustion temperature occurred at a moderate oxidizer ratio of about 36% where the temperature is 4052 K.

The value of expansion ratio and the obtained specific impulse were drawn in figures 6.20, and 6.21, and they fitted the theoretical figures.

Table 6.52: Effect of oxidizer percentage ratio on chamber temperature and specific impulse for double base propellant (applied compositions)

Fuel type	Oxidizer	Chamber Temperature (K)	Specific Impulse	
			sec	N.s/kg
DB.1	42.0 %	3176	214.552	2102.61
DB.2	42.1 %	3178	214.552	2102.61
DB.3	39.0 %	3148	222.236	2177.913
DB.4	37.3 %	3132	213.42	2091.516
DB.5	36.8 %	4052	259.696	2545.021
DB.6	37.5 %	3148	213.32	2090.536
DB.7	37.6 %	3125	213.22	2089.556
DB.8	34.3 %	4049	259.896	2546.981
DB.9	00.0 %	2526	197.08	1931.384

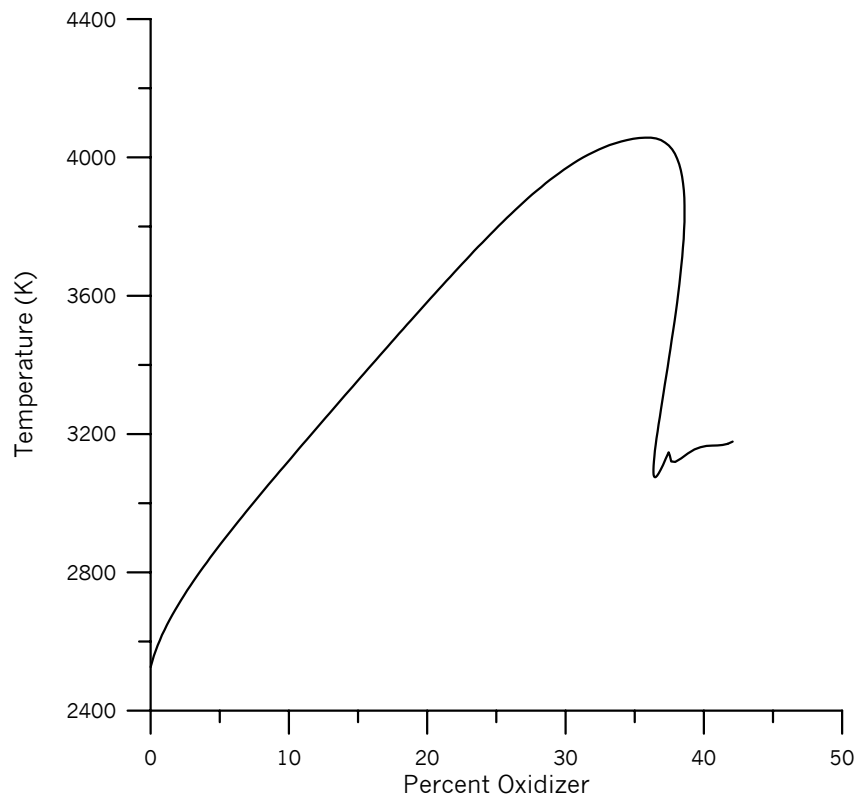


Figure 6.19: Effect of Varying O/F Ratio on the Temperature of Double Base Propellant

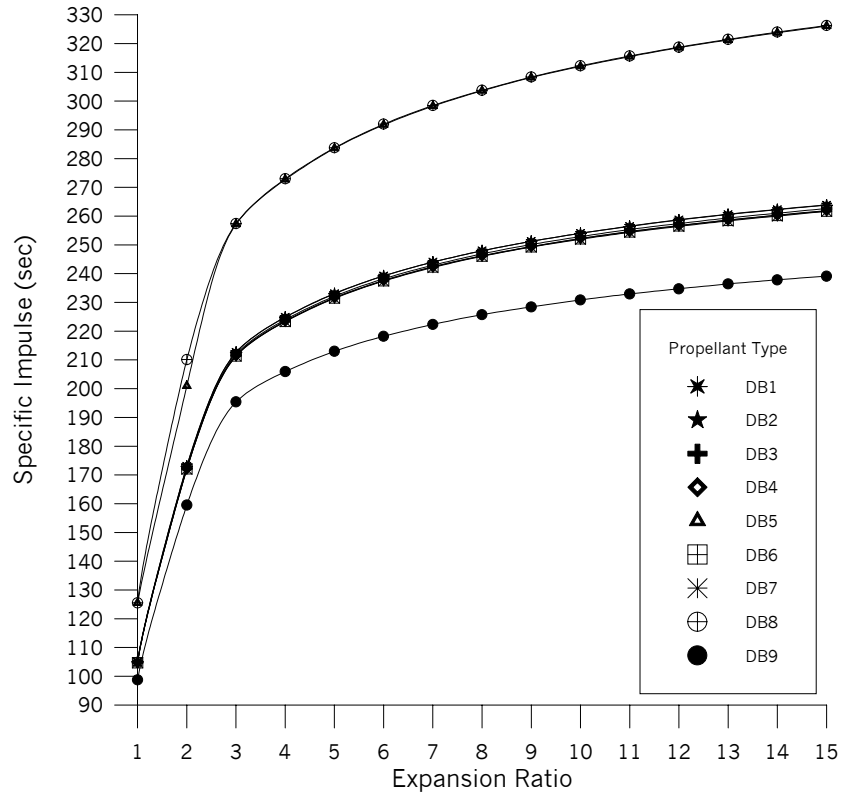


Figure 6.20: Specific Impulse versus Expansion Ratio for Double Base Propellant

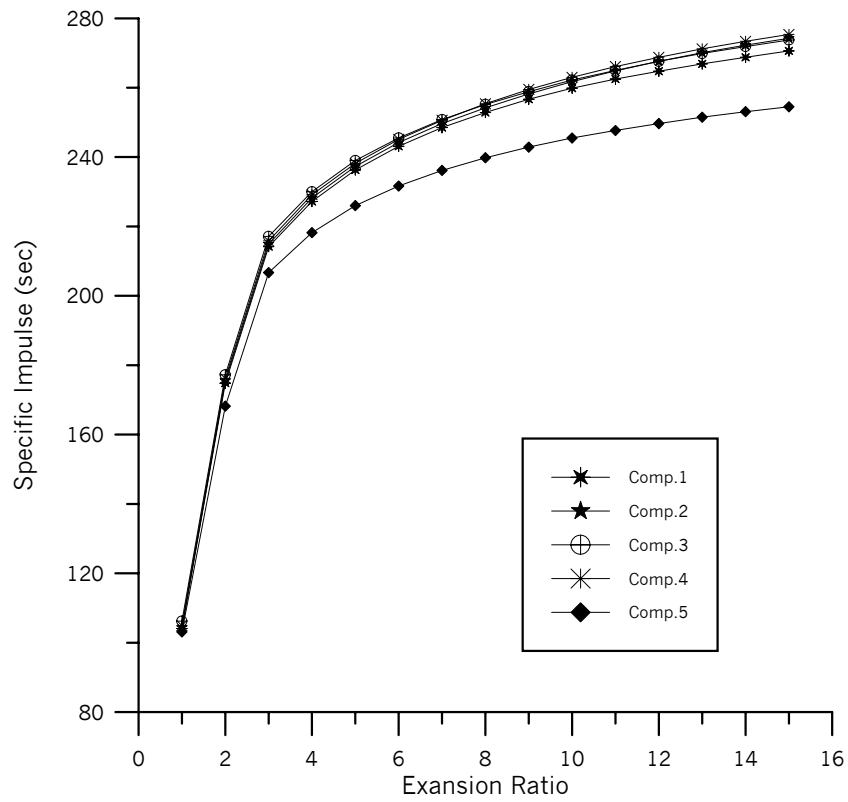


Figure 6.21: Specific Impulse versus Expansion Ratio for Composite Propellant

6.6. Conclusion

- 1- In describing complex system at equilibrium, minimizing Gibbs free energy technique (non-stoichiometric technique) has been proved to be more reliable than the equilibrium constant technique (stoichiometric technique).
- 2- A very successful algorithm has been developed to calculate the composition of chemical equilibrium in complex system. The model is based on the minimization of Gibbs free energy technique.
- 3- To extend the application of the algorithm to more practical application, an algorithm for the computation of theoretical rocket performance, has been introduced, and a computer program has been build for this purpose. This program is supplied with a huge data base file in which, as much as possible, the newer thermodynamic properties of propellants and reaction products have been introduced.
- 4- The results of this program has been compared with those obtained from NASA algorithm, and the comparison gave a very satisfactory agreement, with a percentage deviation of less than 4%.
- 5- A set of fourteen successful experiments has been achieved, for both type of propellants, double base and composite. The results obtained from these experiments were compared with the results obtained from the program. The comparison gives good agreement, with an average deviation of about 5%.

6.7. Recommendation

For those who would carry future studies on related subject, the following recommendations may be considered:

1. Studying the constant volume algorithms, i.e., the use of Helmholtz free energy, with appropriate experimental model.
2. Introduction of actual gas laws and the two-phase flow calculations, to obtain general-purpose program.
3. Studying the effect of different inlet temperature on the results, and the use of multi-nozzles.



References

References

1. Albery, Physical Chemistry, McGraw Hill, Singapore, 1987.
2. AMCP 706-285, Engineering Design Handbook, Elements of Aircraft and Missile Propulsion, 1969.
3. AMCP 706-175, Engineering Design Handbook, Explosive Series Solid Propellants, 1964.
4. Austin, G.T., Shreve's Chemical Process Industries, 5th edition, McGraw Hill, Singapore, 1985
5. Bedard, A, Composite Solid Propellants, at the Site:-
<http://www.friends-partners.org/partners/mwade/articles/comlants.htm>.
6. Bedard, A, Composite Solid Propellants, at the Site:- <http://www.space-ship.com/articles/comlants.htm>.
7. Bedard, A, Double Base Solid Propellants, at the site:-
<http://www.astronautix.com/articles/doulants.htm>
8. Bishnu, P.S., D. Hamiroune, M. Metghalchi, and J. C. Keck. Constrained equilibrium calculations for chemical systems subject to generalized linear constraints using the NASA and STANJAN equilibrium programs. *Combust. Theory Modeling*, 1:295–312, 1997.
9. Braeunig, R.A., Rocket and Space Technology, Rocket Propellants, 1996, at the site: <http://users.commkey.net/Braeunig/space/propell1.htm>
10. Brinkly, S.R., "Calculation of Equilibrium Composition of Systems of Many Constituents", *The Journal of Chemical Physics*, vol. 15, No.2, 1947, pp.107-110.
11. Chase, M.W., Jr., Davies, C.A., Downey, J.R., Jr., Frurip, D.J., McDonald, R.A., and Syverud, A.N., "JANAF Thermochemical Tables", 3rd edition, American Chemical Society, Washington, 1985.

12. Cohen, N.S., "Review of Composite Propellant Burn Rate Modeling", AIAA 277-93, 1980.
13. Cohen, E.R., and Taylor, B.N., "The 1986 CODATA Recommended Values of the Fundamental Physical Constants," National Bureau of Standards, Journal of Research, Vol. 92, 1987, pp.85-95.
14. Complex Chemical Equilibrium Compositions, a web site at: members.aol.com/engware/cec.htm
15. Cormier, T.A., "PHATCAT: Power-Head And Thrust Chamber Analysis Tool", M.Sc. thesis, Georgia Institute of Technology, USA, 2001.
16. Cox, J.D., "Notation of States and Processes, Significance of the Word 'Standard' in Chemical Thermodynamics, and Remarks on Commonly Tabulated Forms of Thermodynamic Functions", Pure and Applied Chemistry, Vol. 54, 1982, pp.1239-1250.
17. Daubert, T.E.; Chemical Engineering Thermodynamics, McGraw Hill, Singapore, (1985).
18. Douglass, H.W., Solid Rocket Motor Nozzles, NASA SP 8115, Ohio USA, 1975.
19. Elliott, J.R., C.T., Lira, A Workbook for Chemical Reaction Equilibria, 2002.
20. Elliott, J.R., Lira, C.T., Introductory Chemical Engineering Thermodynamics, at the site: - www.egr.msu.edu/~lira/supp/
21. Eriksson, L., Documentation for the CHEMICAL Equilibrium Program Package (CHEPP), Linköping University, 2000.
22. Filipović, M., Kilibarda, N., Calculation of Complex Chemical Equilibrium Compositions of Composite Rocket Propellants Combustion Products, Journal of Serbian Chemical Society, Vol. 65, No. 11, 2000, pp.803-810.

23. Fogler, H.S., Elements of Chemical Reaction Engineering, 3rd edition, Printice-Hall International, USA, 1999.
24. Gaithersburg, M.D., Computational Chemistry and Reaction Engineering, 2001, at the site: -
www.mines.edu/research/ccre/Presentations/
25. Garvin, D., Parker, V.B., and White, H.J., "CODATA Thermodynamic Tables", Hemisphere Publishing Corp, New York, 1987.
26. General Gibbs Minimization as an Approach to Equilibrium, at the site:- www.me.washington.edu/~kramlich/me524/handouts/gibbs_minim.pdf
27. Germain, B.D., Technique for the Optimization of the Powerhead Configuration and Performance of Liquid Rocket Engines, PhD Thesis, School of Aerospace Engineering, Georgia Institute of Technology, USA, 2003.
28. Gordon, S. and McBride, B. J., "Computer Program for Computation of Complex Chemical Equilibrium Compositions, Rocket Performance, Incident and Reflected Shocks, and Chapman-Jouguet Detonations", NASA SP-273, 1976.
29. Gordon, S. and Zeleznik, F. J., 1971, NASA SP-273, "Computer Program for Computation of Complex Chemical Equilibrium Compositions, Rocket Performance, Incident and Reflected Shocks, and Chapman-Jouguet Detonations".
30. Gordon, S. and Zeleznik, F. J., Oct 1962, NASA TN D-1454, "A General IBM 704 or 7090 Computer Program for Computation of Chemical Equilibrium Compositions, Rocket Performance, and Chapman-Jouguet Detonations".

31. Gordon, S., "Calculation of Theoretical Equilibrium Nozzle Throat Conditions when Velocity of Sound is Discontinuous", American Institute of Aeronautics and Astronautics Journal, Vol.9 No.1, 1970, pp.179-182.
32. Gordon, S., "Thermodynamic and Transport Combustion Properties of Hydrocarbons with Air, I-Properties in SI Units", NASA TP-1906, 1982.
33. Gordon, S., and McBride, B.J., "Finite Area Combustor Theoretical Rocket Performance", NASA TM-100785, 1988.
34. Gordon, S., and Zeleznik, F.J., "A General IBM 704 or 7090 Computer Program for Computation of Chemical Equilibrium Compositions, Rocket Performance, and Chapman-Jouguet Detonations, Suppl. 1: Assigned Area-Ratio Performance", NASA TN D-1737, 1963.
35. Gordon, S., and Zeleznik, F.J., "Thermodynamic Extrapolation of Rocket Performance Parameters", American Rocket Society Journal, Vol.32, No.8, 1962, pp.1195-1202.
36. Gordon, S., B.J., McBride. Computer program for calculations of complex chemical equilibrium compositions, rocket performances, incident and reflected shocks, and Chapman-Jouguet detonations. Technical report, NASA SP-273, 1971.
37. Gordon, S., McBride, B.J., and Zeleznik, F.J., "Computer Program for Calculation of Complex Chemical Equilibrium Compositions and Applications, Supplement I-Transport Properties", NASA TM-86885, 1984.
38. Gordon, S., Zeleznik, F.J., and Huff, V.N., "A General Method for Automatic Computation of Equilibrium Compositions and Theoretical Rocket Performance of Propellants", NASA TN D-132, 1959.
39. Hill, P.G., and Peterson, C.R., Mechanics and Thermodynamics of Propulsion, Addison-Wesley Publishing Company, Madison, 1965.

40. Huff, V.N., Gordon, S., and Morrell, V.E., "General Method and Thermodynamic Tables for Computation of Equilibrium Composition and Temperature of Chemical Reactions", NACA Report 1037, 1951.
41. Keck, J.C., and D. Gillespie, Rate-controlled partial-equilibrium method for treating reacting gas-mixtures. *Combust. Flame*, 17:237, 1971.
42. Keck, J.C., Rate-controlled constrained-equilibrium theory of chemical reactions in complex systems. *Prog. Energy Combust. Sci.*, 16:125–154, 1990.
43. Khalaf, H.J., Modeling and Experimental Analysis of Losses in Solid Propellant Rocket Motors, PhD Thesis, Military College of Engineering, IRAQ, 2002.
44. Kishore, K., "Comprehensive View of the Combustion Models of Composite Solid Propellants", AIAA 1216, 1979.
45. Kruse, R.B., *Modern-Materials-Solid Propellants*, Vol.6, Academic Press., New York, 1968.
46. Lewis, G.N., Randall, M., *Thermodynamics*, 2nd edition, McGraw Hill, 1961.
47. McBride, B.J., and Gordon S., "Thermodynamic Functions of Several Triatomic Molecules in the Ideal Gas State", *Journal of Chemical Physics*, Vol.35, No. 6, 1961, pp.2198-2206.
48. McBride, B.J., and Gordon, S., "Computer Program for Calculating and Fitting Thermodynamic Functions" NASA RP-1271, 1992.
49. McBride, B.J., Gordon, S., and Reno, M.A., "Thermodynamic Data of Fifty Reference Elements", NASA TP-3287, 1993.
50. McBride, B.J., Gordon, S., and Reno, M.A., "Coefficients for Calculating Thermodynamic and Transport Properties of Individual Specie", NASA TM-4513, 1993.

51. McBride, B. J. and Gordon, S. and Reno, M. A., Oct 1993, NASA TM 4516, "Coefficients for Calculating Thermodynamic and Transport Properties of Pure and Combined Species".
52. McBride, B.J., Heibel, S., Ehlers, J.G., and Gordon, S., "Thermodynamic Properties to 6000 K for 210 Substances Involving the First 18 Elements", NASA SP-3001, 1963.
53. MIL-HDBK-762, Military Handbook, Propulsion, 1980.
54. Negus, C.H., "An Interactive Chemical Equilibrium Solver For The Personal Computer" M.Sc. Thesis, Virginia, 1997, from the web site <http://scholar.lib.vt.edu/theses/available/etd-595410211975510/unrestricted/>
55. Noltingk, B.E., Instrumentation Reference Book, 2nd edition, Butterworth-Heinemann, Great Britain, 2000.
56. - Nozzle, at the site:-
<http://www.engapplets.vt.edu/fluids/CDnozzle/cdinfo.html>
57. Nozzle Theory, at the site:-
<http://thermal.sdsu.edu/profs/Bhattacharjee/sooby/classes/s99/me696s99/rockets/>
58. Pope, S.B. CEQ: A Fortran library to compute equilibrium compositions using Gibbs function continuation. <http://mae.cornell.edu/~pope/CEQ>, 2003.
59. Pope, S.B. The computation of constrained and unconstrained equilibrium compositions of ideal gas mixtures using gibbs function continuation. FDA 03-02, Cornell University, 2003.
60. Pope, S.B., Gibbs Function Continuation for the Stable Computation of Chemical Equilibrium, Cornell University, NY, 2004, at the site: mae.cornell.edu/~pope/Reports/Pope04_CEQ.pdf

61. Quarteroni, A., R., Sacco, F., Saleri, Numerical Mathematics, Springer, USA, 2000.
62. Ramette, R.W., Exploring Practical Thermodynamic and Equilibrium Calculations, at the site:-
http://jchemed.chem.wisc.edu/JCESoft/Issues/Series_B/8B1/prog1-8B1.html
63. Reynolds, W.C., The element potential method for chemical equilibrium analysis: implementation in the interactive program STANJAN. Technical report, Stanford University, 1986.
64. Richard, L., Bogart, D., Constant Pressure Combustion Charts Including Effects of Diluents Addition, NACA RP-973, at the site:
<http://naca.larc.nasa.gov/reports/1949/naca-report-937/naca-report-937.pdf>
65. Richard Nakka's Experimental Rocketry Web Site, at the site:-
<http://members.aol.com/ricnakk/rtheory.html>
66. Saad, M.A., Thermodynamic, Principle and Practice, Prentice Hall, USA, 1997.
67. Smith J.M., Van Ness H.C.; Introduction to Chemical Engineering Thermodynamics, McGraw Hill, Singapore, (1987).
68. Smith, W.R., "Some Remarks on the Calculation of Complex Chemical Equilibria by General Method", Industrial and Engineering Chemistry Fundamentals, vol. 17, No.1, (1978), pp.69-70.
69. Smith, W.R., "The Computation of Chemical Equilibria in Complex Systems", Industrial and Engineering Chemistry Fundamentals, vol. 19, No.1, (1980), pp.1-10.
70. Smith, W.R., R.W. Missen, Chemical Reaction Equilibrium Analysis: Theory and Algorithms. John Wiley & Sons. USA, 1982.

71. Smith, W.R., R.W. Missen, Chemical Reaction Stoichiometry (CRS), Canada, 1998, from the web site: www.mathstat.uoguelph.ca/faculty/smith/crs
72. Stephen R. Turns, An Introduction to Combustion, Concepts and Applications, 2nd edition, McGraw Hill, Singapore, 2000.
73. Stull, D.R., Prophet, H., JANAF Thermochemical Tables, 2nd edition, United State Department of Commerce ,Michigan, USA, 1971.
74. Sutton G.P., and D.M. Ross, Rocket Propulsion Elements, 4th edition, John Wiley & Sons, USA, 1976.
75. Sutton, G.P., Rocket propulsion Nozzle theory, at the site:- http://www.tfd.chalmers.se/~ulfh/raket_motor_h/gsut3-03_files/
76. Tang, Q., S.B., Pope. Implementation of combustion chemistry by in situ adaptive tabulation of rate-controlled constrained equilibrium manifolds. Proc. Combust. Inst, 29:1411–1417, 2002. 14
77. Teasdale, D., Solid Propellant Microrockets, MSc thesis, University of California, USA, 2000
78. Van Zeggeren, F., S.H. Storey, The Computation of Chemical Equilibria, Cambridge University Press, 1970.
79. Voňka, P., J. Leitner, “Calculation of Chemical Equilibrium in Complex Systems: System Restrictions” Collect. Czech. Chem. Commun., Vol. 65, 2000, at the web site: www.vscht.cz/ipL/en/osobni/leitner/_FulltextPDF/A-10.pdf.
80. Way, D.W., Olds, J.R., “SCORES: Web-Based Rocket Propulsion Analysis Tool for Space Transportation System Design”, AIAA 99-2353, 35th AIAA/ASME/SAE/ASEE Joint Propulsion Conference, Los Angeles, CA, June 20-24, 1999.From the web site: <http://atlas.cad.gatech.edu/~dwway/SCORES>

81. White, W.B., S.M. Johnson, G.B. Dantzig, "Chemical Equilibrium in Complex Mixtures", *The Journal of Chemical Physics*, vol. 28, No.5, 1958, pp.751-755.
82. Winnick, J., *Chemical Engineering Thermodynamics*, John Wiley & Sons, Canada, 1997.
83. Zeleznik, F.J., S. Gordon, "simultaneous Least-Square Approximation of a Function and Its First Integrals With Application to Thermodynamic Data", NASA TN D-767, 1961.
84. Zeleznik, F.J., S. Gordon, "Calculation of Complex Chemical Equilibria", *Industrial and Engineering Chemistry*, vol. 60, June 1968, pp.27-57.
85. Zucrow, M.J., *Aircraft and Missile Propulsion, Vol.I & II*, John Wiley & Sons. New York, 1958.



A. Solid Propellant Burn Rate^(12, 65)

A.1 Introduction

The burning surface of a rocket propellant grain recedes in a direction perpendicular to this burning surface. The rate of regression, typically measured in inches per second (or mm per second), is termed burning rate (or burn rate). This rate can differ significantly for different propellants, or for one particular propellant, depending on various operating conditions as well as formulation. Knowing quantitatively the burning rate of a propellant, and how it changes under various conditions, is of fundamental importance in the successful design of a solid rocket motor. This appendix discusses the factors that influence burn rate, how it may be modified, how the burn rate can be determined experimentally, and the physical processes that occur at the burning surface of a propellant that governs the burning rate.

A.2 Factors That Influence Burning Rate

An illustration of the concept of burning surface regression is given in Figure A.1, for a section of a hollow cylindrical grain, with an inhibited outer surface (“inhibited” means that the propellant surface is protected from the heat of combustion and as such, burning does not occur). Burning commences along the length of the central core, with the burning surface receding radially outward (shown at arbitrary times t_1 , t_2 , t_3). Note that the burning surface area is continually increasing. Also note that the surface regression rate (burn rate) is not constant. These two events are, in fact, directly related, as will be discussed shortly.

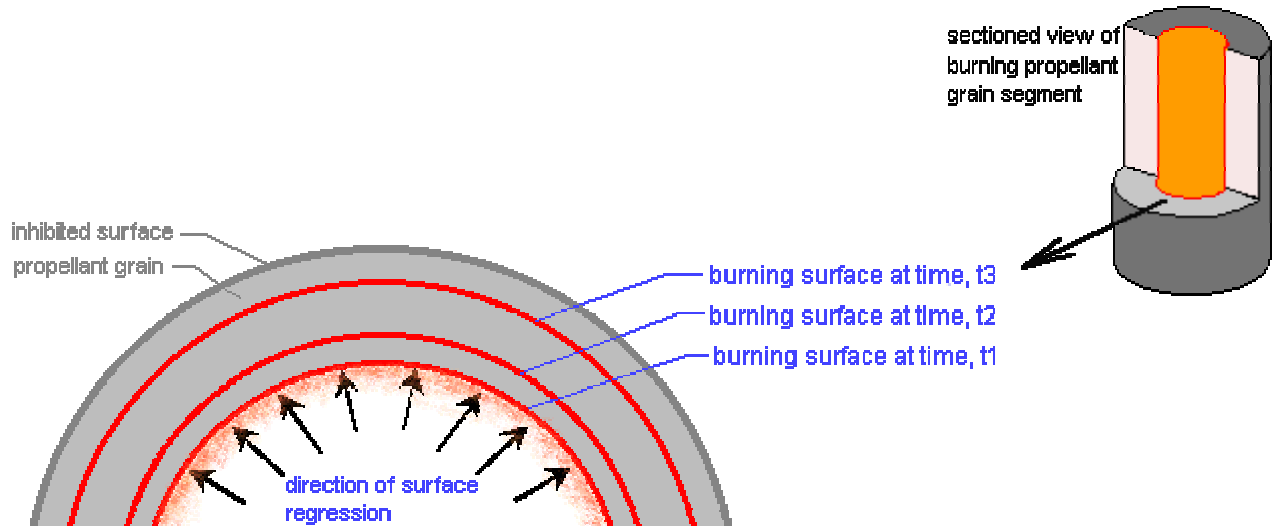


Figure A.1: Burning surface regression

Propellant burning rate is influenced by certain factors, the most significant of which being:

1. Combustion chamber pressure,
2. Initial temperature of the propellant grain,
3. Velocity of the combustion gases flowing parallel to the burning surface,
4. Local static pressure, and
5. Motor acceleration.

These factors are discussed below.

A.2-1 Chamber Pressure

Burn rate is strongly affected by chamber pressure. The usual representation of the pressure dependence on burn rate is the Saint Robert's Law (Vieille's Law):

$$r = r_o + a P_c^n \quad (\text{A.2-1})$$

where r = the burn rate,

r_o = a constant (usually taken as zero),

a = the burn rate coefficient, and

n = the pressure exponent.

The values of a and n are determined empirically for a particular propellant formulation, and cannot be theoretically predicted. Various means may be employed to determine these parameters, such as a Strand Burner or Ballistic Evaluation Motor (BEM). It is important to realize that a single set of a , n values are typically valid over a distinct pressure range. More than one set may be necessary to accurately represent the full pressure regime of interest, as illustrated in Figure A.2.

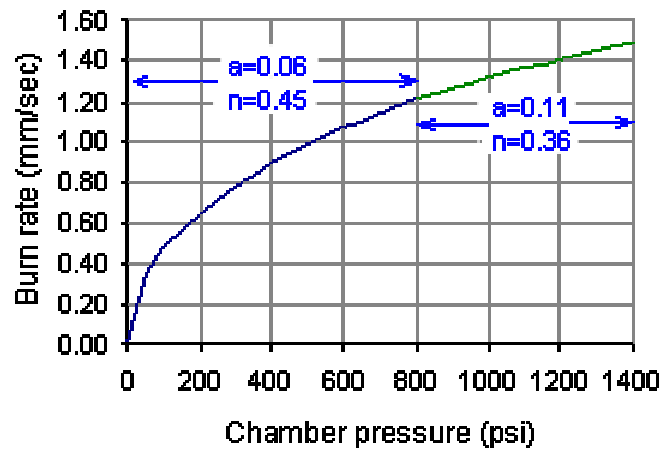


Figure A.2: Saint Robert's model of burn rate vs. pressure

When plotted on log-log scales, the Saint Robert's function is a straight line. Certain propellants (or with additives) deviate from this behavior, and exhibit sharp changes in burn rate behavior. These types of propellants are termed plateau or mesa propellants, as illustrated in Figure A.3. Plateau and mesa effects may be the result of different rates of surface regression (as a function of pressure) of the binder compared to the oxidizer particles. Another explanation is that the condensed phase combustion products may pool and retard heat transfer to the surface at elevated pressure levels.

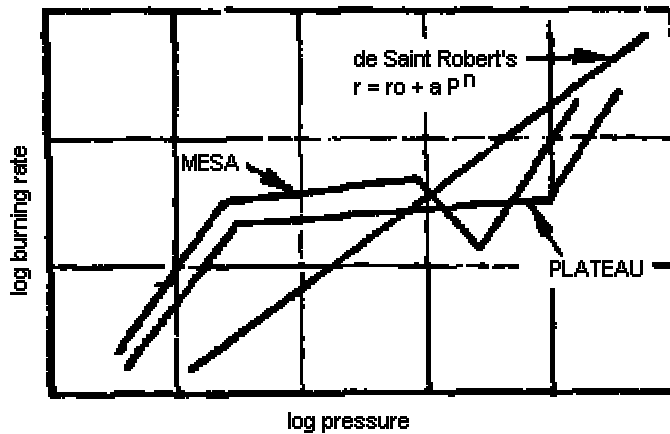


Figure A.3: Plateau and mesa behavior

Burning rate can be particularly sensitive to the value of the pressure exponent, n (the slope of the log-log curve in Figure A.3). High values of n can produce large changes in burning rate with relatively small changes in chamber pressure, with potentially catastrophic consequences, as higher burning rate leads to even greater chamber pressure. Another reason why a high-pressure exponent may be undesirable is due to the low sensitivity of burn rate, due to pressure, at the low end of the pressure regime. This can result in difficult starting, with the motor simply refusing to come up to pressure. This low sensitivity to pressure, for high pressure exponents, becomes more clear if a pressure exponent of unity is considered ($n=1$). This implies burn rate being directly, or linearly, proportional to chamber pressure. The slope of the burn rate vs. pressure curve is a straight line. Figure A.4 illustrates the pressure profile for various values of n . It can be seen that with a low value of pressure exponent, for example $n=0.2$, the burn rate changes very rapidly at low pressure, providing excellent motor start-up capability.

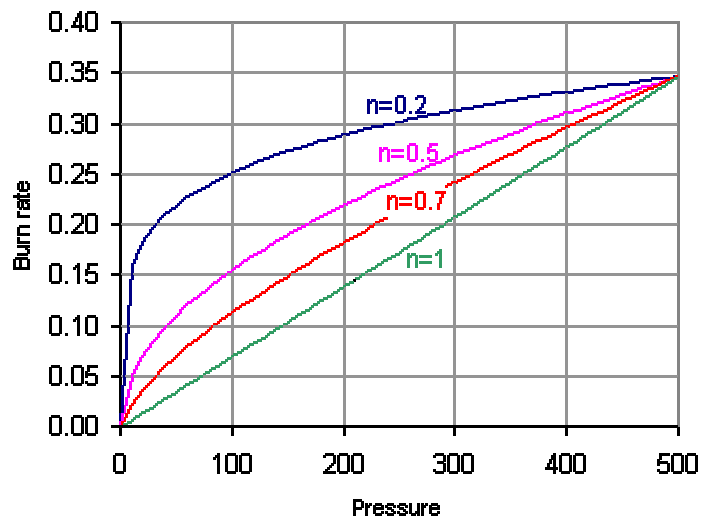


Figure A.4: Effect of various pressure exponents on burning rate sensitivity to pressure

If the value of the exponent is close to zero, the burning rate is largely insensitive to pressure, and unstable combustion may result. For these reasons, the pressure exponent for a practical propellant should have a value between 0.3 and 0.6 in the regime of the motor steady-state operating condition.

A.2-2 Initial Temperature

Temperature affects the rate of chemical reactions and thus the initial temperature of the propellant grain influences burning rate. If a particular propellant shows significant sensitivity to initial grain temperature, operation at temperature extremes will affect the time-thrust profile of the motor. This is a factor to consider for winter launches, for example, when the grain temperature may be 20°C or more lower than normal launch conditions.

A.2-3 Velocity of the Combustion Gases

For most propellants, certain levels of local combustion gas velocity (or mass flux) flowing parallel to the burning surface leads to an increased

burning rate. This augmentation (growth) of burn rate is referred to as erosive burning, with the extent varying with propellant type and chamber pressure. The mechanism of increased convective heat transfer to the propellant surface due to turbulence is most likely responsible for this augmentation. For many propellants, a threshold flow velocity exists. Below this flow level, either no augmentation occurs, or a decrease in burn rate is experienced (negative erosive burning). This is illustrated in Figure A.5.

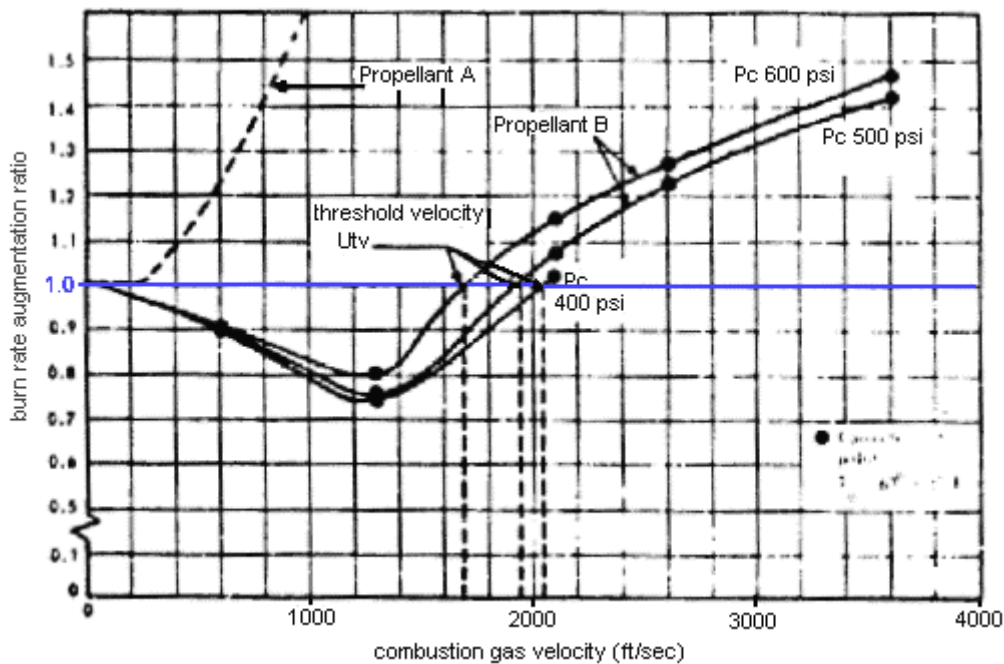


Figure A.5: Erosive burning phenomenon

In Figure A.5, propellant “A” exhibits a threshold flow velocity of about 240 ft/sec. Propellant “B” exhibits a lower threshold velocity with higher chamber pressures. Below this threshold level, an interesting phenomenon occurs, the burn rate decreases relative to the zero flow level. This is referred to as negative erosive burning, and is possibly the result of changing physical processes of heat transfer that controls the burning rate. At low flow velocity, mass transfer dominates, but as the flow velocity increases,

the mechanism of convection becomes increasingly more significant (Figure A.6).

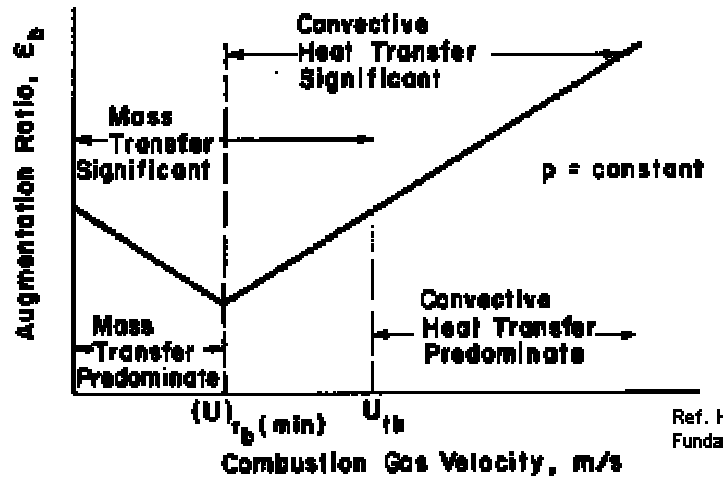


Figure A.6: Heat transfer processes that influence burning rate

An alternative explanation suggests that this effect may be due to partial coverage of the oxidizer (particle) surfaces by the melted binder under the effect of shear stresses in the boundary layer of combustion flow.

The effects of erosive burning can be minimized by designing the motor with a sufficiently large port-to-throat area ratio (A_{port}/A_t). The port area is the cross-section area of the flow channel(s) in a motor. For a hollow-cylindrical grain, this is the cross-sectional area of the core. As a rule of thumb, the ratio should be a minimum of 2, for a typical grain L/D ratio of 6. A greater A_{port}/A_t ratio should be used for grains with larger L/D ratios.

To relate the erosive burning rate to the gas flow in the combustion chamber, various empirical laws are used:

$$r = a P_c^n [1 + k(G - G^*)] \quad \text{multiplicative law} \quad (\text{A.2-2})$$

where k = a constant,

G = the specific mass flow rate of the main flow, and

G^* = a threshold flow rate.

$$r = a P_c^n + k u \quad \text{additive law} \quad (\text{A.2-3})$$

where k = a constant, and

u = the velocity of the main flow.

A.2-4 Local Static Pressure

In an operating rocket motor, there is a pressure drop along the axis of the combustion chamber, a drop which is physically necessary to accelerate the increasing mass flow of combustion products toward the nozzle. The static pressure is greatest where gas flow is zero, that is, at the front (bulkhead) of the motor. Since burn rate is dependant upon the local pressure, the rate should be greatest at this location. However, this effect is relatively minor and is usually offset by the countereffect of erosive burning.

A.2-5 Motor Acceleration

Burning rate is enhanced by acceleration of the motor. Whether the acceleration is a result of longitudinal force (e.g. thrust) or spin, burning surfaces, that form an angle of about 60-90° with the acceleration vector, are prone to increase burn rate. As the majority of the burning surfaces of most grain configurations are perpendicular to the motor axis, spin (rather than longitudinal acceleration) has a far more profound effect on burning rate.

There are three main reasons why spin increases burn rate:

1. Rotation reduces the mass flux (flow) at the nozzle throat. This reduction in mass flux has the same effect as a decrease in throat area, thus increased chamber pressure (and consequently higher burning rate) may result.
2. Viscous flow patterns are set up in the motor, increasing heat transfer to the propellant surface through greater mass transfer.

3. The radial acceleration forces can cause greater retention of the solid phase combustion products near the propellant surface.

A.3 Modification of Burning Rate

It is sometimes desirable to modify the burning rate such that it is more suitable to a certain grain configuration. For example, if one wished to design an end burner grain, which has a relatively small burning area, it is necessary to have a fast burning propellant. In other circumstances, a reduced burning rate may be preferred. For example, a motor may have a large L/D ratio to generate sufficiently high thrust, or it may be necessary for a particular design to restrict the diameter of the motor. The web would consequently be thin, resulting in a short burn duration. Reducing the burning rate would be beneficial. There are a number of ways to modify the burning rate, they are:

1. Decreasing the oxidizer particle size.
2. Increasing or reducing the percentage of oxidizer (greater O/F ratio).
3. Addition of a burn rate catalyst or suppressant.
4. Operating the motor at a lower or higher chamber pressure.

These factors are discussed below.

A.3-1 Particle Size

The effect of the oxidizer particle size on burn rate seems to be influenced by the type of oxidizer. Propellants that use AP as the oxidizer have a burn rate that is significantly affected by AP particle size. This most likely results from the decomposition of AP being the rate-determining step in

the combustion process. Propellants that use KN as the oxidizer, however, have a burn rate that is not strongly influenced by the KN particle size.

A.3-2 Oxidizer

The burn rate of most propellants is strongly influenced by the oxidizer/fuel ratio (O/F). Unfortunately, modifying the burn rate by this means is quite restrictive, as the performance of the propellant, as well as mechanical properties, are also greatly affected by the O/F ratio.

A.3-3 Catalyst

Certainly the best and most effective means of increasing the burn rate is the addition of a catalyst to the propellant mixture. A catalyst's action is possibly due to a number of means (or combination of means) and probably varies with specific propellant and catalyst type:

- Enhancing fuel decomposition.
- Enhancing oxidizer decomposition.
- Accelerating vaporized fuel reactions in the gas phase in the combustion zone.
- Increasing heat transfer at the propellant surface layer.

Some catalysts increase the burn rate by increasing the burn rate coefficient, others tend to increase the pressure exponent (making the propellant more sensitive to pressure changes).

Some examples of burn rate catalysts are:

- Ferric Oxide (Fe_2O_3), copper oxide (CuO), Manganese Dioxide (MnO_2) are commonly used catalysts in AP based composite propellants, as is copper chromate ($\text{Cu}_2\text{Cr}_2\text{O}_5$ or $2\text{CuO Cr}_2\text{O}_3$).

- Potassium dichromate $K_2Cr_2O_7$ or ammonium dichromate $(NH_4)_2Cr_2O_7$ for AN based mixtures.
- Ferric Oxide (Fe_2O_3), Iron sulphate ($FeSO_4$) and potassium dichromate for KN-Sugar propellants
- Lampblack (carbon) may slightly increase the burn rate of most propellants through increasing heat transfer from the combustion flame to the propellant surface.

The effect of iron compounds on the burning rate of an AP propellant is shown in Figure A.7.

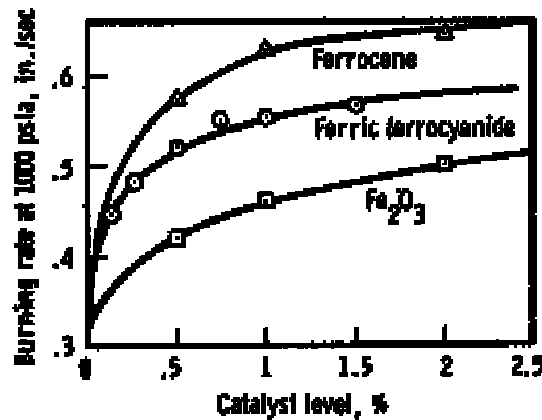


Figure A.7: Increase in burn rate from catalyst additives

It should be noted that the addition of a burn rate catalyst not only makes a propellant burn more rapidly, but it also makes it easier to ignite. This is a double-edged sword, as motor start-up is enhanced, which leads to more efficient use of propellant, and a thrust-time profile more closely matching design curve. However, greater care and precautions must be taken when handling a propellant with a significant amount of catalyst to avoid inadvertent ignition.

A burn rate suppressant is an additive that has the opposite effect to that of a catalyst, it is used to decrease the burn rate. For AP based propellants,

oxamide $(\text{NH}_2\text{CO}_2)_2$ is particularly effective in reducing burn rate, without sacrificing performance. Other potential burn rate suppressants include calcium carbonate, calcium phosphate, ammonium chloride, and ammonium sulphate. All burn rate suppressants make the grain more difficult to ignite, necessitating an enhanced pyrotechnic or pyrogen ignition system.

A.3-4 Chamber Pressure

For a propellant that follows the Saint Robert's burn rate law, designing a rocket motor to operate at a lower chamber pressure will provide for a lower burning rate (see Figure A.2). This effect is more pronounced for a propellant with a higher pressure exponent. If a propellant exhibits plateau or mesa behavior, this means of obtaining a lower burning rate that would be less effective. Due to the nonlinearity of the pressure-burn rate relationship, it may be necessary to reduce significantly the operating pressure to get the desired burning rate.

A.4 Combustion Process

Solid propellant combustion is a very complex phenomenon, and understanding and modeling the actual processes involved is difficult. Propellants, in their simplest forms, consist of a dispersion of varying sized oxidizer particles within a matrix of fuel/binder. The combustion process involves a number of sub-processes, or steps. In order to begin to understand the burning rate mechanism, it is important to identify the key processes that control the burning. Some of these processes include heating of the solid phase, decomposition of the oxidizer and binder (which burn at different temperatures), possible melting and vaporization, mixing and reactions in the vapor phase, and gas-phase combustion. A number of theoretical models have been proposed to describe the combustion process, including the Beckstead-

Derr-Price (BDP) model and the Petite Ensemble Model (PEM). The BDP model proposes that the flame structure of a composite propellant is not homogeneous, but consists of multiple flames and three combustion regions: two kinetics-dominated (reaction) flames and one diffusion flame. The oxidizer breaks down in one reaction flame and sends oxygen into the diffusion flame. Binder decomposition products pre-react in the other reaction flame then rush into the diffusion flame, where they react further with the oxygen. The influential parameters affecting burning rate in these models include the heat of vaporization, the heat conduction into the solid phase, and the flame standoff distances. One shortcoming of the BDP model is that it considers a single particle size of oxidizer. The PEM model recognizes that most composite propellants contain a wide dispersal of oxidizer particle sizes. Such a scattering is desirable because propellants with a single oxidizer particle diameter are limited to slightly more than an 80% theoretical maximum oxidizer mass fraction. Small oxidizer particles are necessary to fit in between the large ones in order to have a high oxidizer percentage. The combustion process upon which these models are based is shown in Figure A.8.

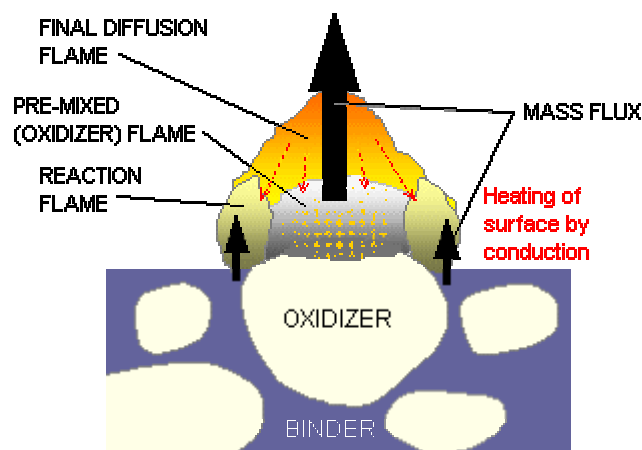


Figure A.8: Simplified model of propellant burning

A key part of the combustion process that determines the burning rate of a propellant is the rate-determining step. As mentioned above, the combustion process is complex and consists of multiple steps. The overall rate at which the burning of a propellant occurs is governed by the slowest step, or rate-determining step. This is usually the decomposition of either the oxidizer or decomposition of the fuel (binder). For ammonium perchlorate (AP) based propellants, it is usually the former. This is why AP particle size plays a big role in burn rate of AP based propellants. For potassium nitrate (KN) based propellants, it would seem to be the latter, or decomposition of the binder that is the rate determining step.

As it is difficult to theoretically predict a propellant's burn rate with sufficient engineering accuracy, the only recourse is to measure burn rate utilizing any number of proven techniques.

A.5 Burn Rate Measurement

There are a number of ways to experimentally determine (or estimate) the burn rate of a particular propellant, and importantly, its relationship to chamber pressure. Three ways will be covered here:

1. Crawford type Strand Burner apparatus
2. Burn rate analysis using the Pressure-Time curve obtained from a motor firing
3. Burn rate Ballistic Evaluation Motor

These methods are discussed below.

A.5-1 Crawford Strand Burner

With the Crawford Strand Burner method of burn rate measurement, a small sample of propellant is burned in a closed firing vessel at a certain constant (or approximately constant) pressure. Each propellant sample, called

a strand, is in the form of a thin stick. The strand is electrically ignited at one end, and the time duration for the strand to burn along its length (cigarette fashion) is measured. The strands are usually inhibited along their whole length to ensure that burning only occurs perpendicular to the surface. Various means are used to measure the time duration, such as lead wires embedded in the strand which melt when contacted by the flame front, or by use of thermocouples. The burn rate is obtained by knowing the burning distance as well as the burning time between the lead wires (or thermocouples). Nitrogen is used to pressurize the firing vessel. To effectively characterize the burn rate versus pressure relationship for a particular propellant, 10 or more tests may be performed, at pressures ranging from a few atmospheres, to 100 atmospheres or more.

A.5-2 Pressure – Time Curve

The instantaneous burning rate of a propellant may be estimated from the pressure-time trace obtained from a motor firing. This method is based on the knowledge that motor chamber pressure and burn rate are directly related in terms of K_n , c^* and the propellant density. The burn rate coefficient and the pressure exponent may also be estimated.

A.5-3 Ballistic Evaluation Motor

The third method of determining burning rate of a propellant is by the use of a Ballistic Evaluation Motor (BEM). Such a motor is illustrated, in concept, in Figure A.9, together with two grain types that may be used in the motor. The principle is simple, with grain ignition occurring on one end (or side, as with the slab grain), and burning along the length of the web. Note that all surfaces are inhibited from burning, except one surface. As the surface area remains constant, the steady-state operating pressure of the motor is

constant, and the burning rate is obtained from the web length (L_{web}) divided by the motor burn time. For a slow burning propellant, the end-burning grain configuration may not be practical (required throat diameter may be too small) to produce the desired pressure. In this case, the slab grain may be the solution, as it allows for a significantly greater burning area.

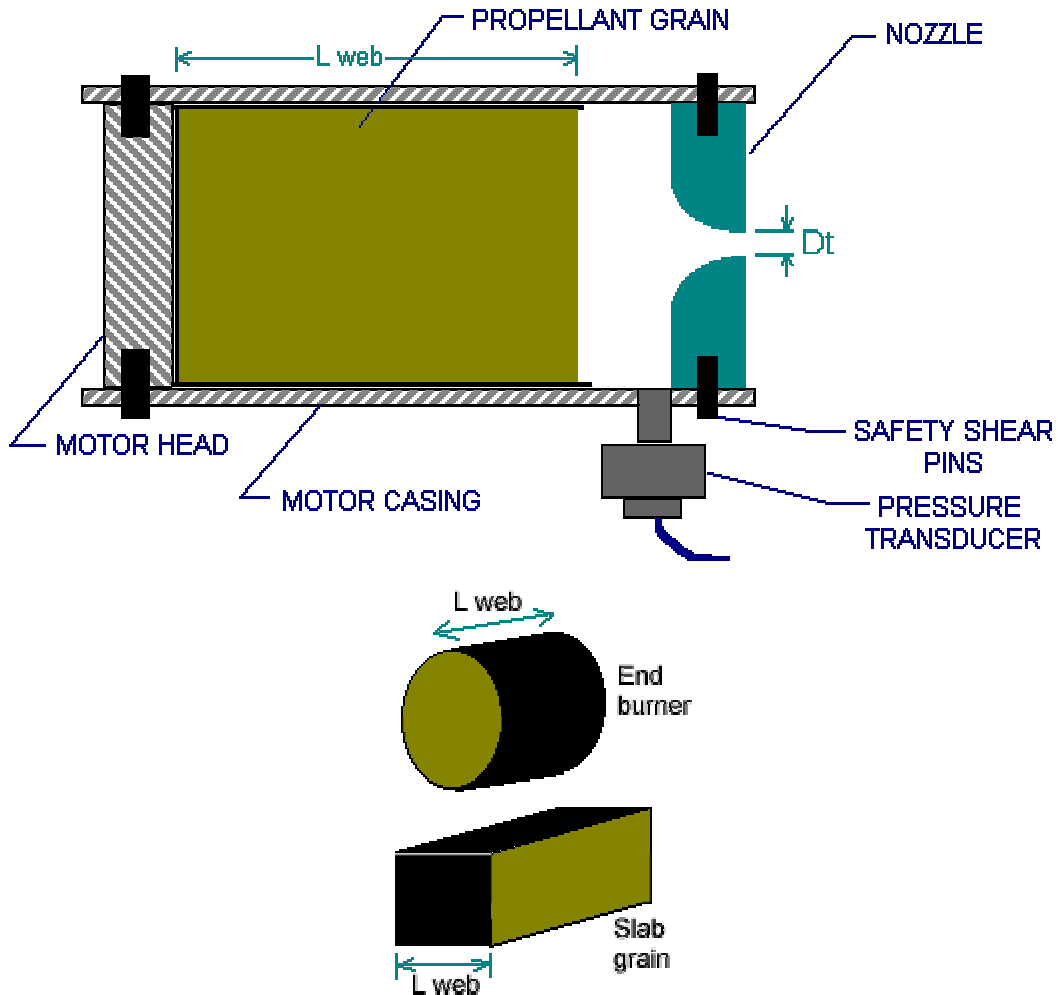


Figure A.9: Burn rate evaluation motor and grain types

For this method, it is important that the entire burning surface of the grain ignites simultaneously. This may be more ensured by use of an ignition aid coating, such as Combustion Primer. One disadvantage of this method is that several motor firings, at various pressures, each requiring a different throat size (D_t), are required to well characterize a propellant.

Appendix B

Species in the Output Data Files

B.1 Species in the Output Data File

The data in this file are based on JANAF thermochemical tables⁽⁷³⁾, and are divided into two types, gaseous species and condensed species.

B.1-1 Gaseous Species

Al	Al ⁺	Al ⁻	AlBO ₂
AlBr	AlBr ₃	AlC	AlCl
AlCl ⁺	AlClF	AlClF ⁺	AlClF ₂
AlCl ₂	AlCl ₂ ⁺	AlCl ₂ ⁻	AlCl ₂ F
AlCl ₃	AlF	AlF ⁺	AlF ₂
AlF ₂ ⁺	AlF ₂ ⁻	AlF ₂ O	AlF ₂ O ⁻
AlF ₃	AlF ₄ ⁻	AlH	AlI
AlI ₃	AlN	AlO	AlO ⁺
AlO ⁻	AlOCl	AlOF	AlOH
AlOH ⁺	AlOH ⁻	AlO ₂	AlO ₂ ⁻
AlO ₂ H	AlS	Al ₂	Al ₂ Br ₆
Al ₂ Cl ₆	Al ₂ F ₆	Al ₂ I ₆	Al ₂ O
Al ₂ O ⁺	Al ₂ O ₂	Al ₂ O ₂ ⁺	Ar
Ar ⁺	B	B ⁺	B ⁻
BCl	BCl ⁺	BClF	BCl ₂
BCl ₂ ⁺	BCl ₂ ⁻	BCl ₃	BF
BF ₂	BF ₂ ⁺	BF ₂ ⁻	BF ₃
BH	BHF ₂	BH ₂	BH ₃
BN	BO	BOCl	BOF
BOF ₂	BO ₂	BO ₂ ⁻	BS
B ₂	B ₂ O	B ₂ O ₂	B ₂ O ₃
B ₃ O ₃ Cl ₃	B ₃ O ₃ F ₃	B ₃ O ₃ H ₃	Ba
BaBr	BaBr ₂	BaCl	BaCl ₂
BaF	BaF ⁺	BaF ₂	BaOH
BaOH ⁺	BaO ₂ H ₂	BaS	Be
Be ⁺	BeBO ₂	BeBr	BeBr ₂
BeCl	BeCl ⁺	BeClF	BeCl ₂
BeF	BeF ₂	BeH	BeH ⁺
BeI	BeI ₂	BeN	BeO
BeOH	BeOH ⁺	BeO ₂ H ₂	BeS

Be ₂ O	Be ₂ OF ₂	Be ₂ O ₂	Be ₃ O ₃
Be ₄ O ₄	Br	Br ₂	C
C ⁺	C ⁻	CCl	CClF ₃
CCl ₂	CCl ₂ F ₂	CCl ₃	CCl ₃ F
CCl ₄	CF	CF ⁺	CF ₂
CF ₂ ⁺	CF ₃	CF ₃ ⁺	CF ₄
CH	CH ⁺	CHCl	CHClF ₂
CHCl ₂ F	CHCl ₃	CHF ₃	CH ₂
CH ₂ ClF	CH ₂ Cl ₂	CH ₂ F ₂	CH ₃
CH ₃ Cl	CH ₃ F	CH ₂ OH	CH ₃ O
CH ₄	CH ₃ OH	CN	CN ⁺
CN ⁻	CN ₂	CO	CO ⁺
COCl	COCIF	COCl ₂	COF
COF ₂	COS	CO ₂	CO ₂ ⁺
COOH	CP	CS	CS ₂
C ₂	C ₂ ⁺	C ₂ ⁻	C ₂ Cl ₂
C ₂ Cl ₄	C ₂ Cl ₆	C ₂ F ₂	C ₂ F ₄
C ₂ H	C ₂ HCl	C ₂ HF	CHCO, ketyl
C ₂ H ₂ , acetylene	C ₂ H ₂ , vinylidene	CH ₂ CO, ketene	C ₂ H ₃ , vinyl
CH ₃ CN	CH ₃ CO, acetyl	C ₂ H ₄	C ₂ H ₄ O, ethylene
C ₂ H ₄ O, ethylene	CH ₃ CHO, ethanal	CH ₃ COOH	(HCOOH) ₂
C ₂ H ₅	C ₂ H ₆	CH ₃ N ₂ CH ₃	CH ₃ OCH ₃
C ₂ H ₅ OH	CCN	CNC	C ₂ N ₂
C ₂ O	C ₃	C ₃ H ₃ , propargyl	C ₃ H ₄ , allene
C ₃ H ₄ , propyne	C ₃ H ₄ , cyclo-	C ₃ H ₅ , allyl	C ₃ H ₆ , propylene
C ₃ H ₆ , cyclo-	C ₃ H ₆ O	C ₃ H ₇ , n-propyl	C ₃ H ₇ , i-propyl
C ₃ H ₈	C ₃ H ₈ O, 1propanol	C ₃ H ₈ O, 2propanol	C ₃ O ₂
C ₄	C ₄ H ₂	C ₄ H ₄ , 1,3-cyclo-	C ₄ H ₆ , butadiene
C ₄ H ₆ , 2-butyne	C ₄ H ₆ , cyclo-	C ₄ H ₈ , 1-butene	C ₄ H ₈ , cis2-buten
C ₄ H ₈ , tr2-butene	C ₄ H ₈ , isobutene	C ₄ H ₈ , cyclo-	(CH ₃ COOH) ₂
C ₄ H ₉ , n-butyl	C ₄ H ₉ , i-butyl	C ₄ H ₉ , s-butyl	C ₄ H ₉ , t-butyl
C ₄ H ₁₀ , isobutene	C ₄ H ₁₀ , n-butane	C ₄ N ₂	C ₅
C ₅ H ₆ , 1,3cyclo-	C ₅ H ₈ , cyclo-	C ₅ H ₁₀ , 1-pentene	C ₅ H ₁₀ , cyclo-
C ₅ H ₁₁ , pentyl	C ₅ H ₁₁ , t-pentyl	C ₅ H ₁₂ , n-pentane	C ₅ H ₁₂ , i-pentane
CH ₃ C(CH ₃) ₂ CH ₃	C ₆ H ₂	C ₆ H ₅ , phenyl	C ₆ H ₅ O, phenoxy
C ₆ H ₆	C ₆ H ₅ OH, phenol	C ₆ H ₁₀ , cyclo-	C ₆ H ₁₂ , 1-hexene
C ₆ H ₁₂ , cyclo-	C ₆ H ₁₃ , n-hexyl	C ₇ H ₇ , benzyl	C ₇ H ₈
C ₇ H ₈ O, cresol	C ₇ H ₁₄ , 1-heptene	C ₇ H ₁₅ , n-heptyl	C ₇ H ₁₆ , n-heptane
C ₈ H ₈ , styrene	C ₈ H ₁₀ , ethylbenz	C ₈ H ₁₆ , 1-octene	C ₈ H ₁₇ , n-octyl
C ₈ H ₁₈ , isooctane	C ₈ H ₁₈ , n-octane	C ₉ H ₁₉ , n-nonyl	C ₁₀ H ₈ , naphthale

C ₁₀ H ₂₁ , n-decyl	C ₁₂ H ₉ , o-bipheny	C ₁₂ H ₁₀ , biphenyl	Ca
Ca ⁺	CaBr	CaBr ₂	CaCl
CaCl ₂	CaF	CaF ₂	CaI
CaI ₂	CaO	CaOH	CaOH ⁺
CaO ₂ H ₂	CaS	Ca ₂	Cl
Cl ⁺	Cl ⁻	ClCN	ClF
ClF ₃	ClO	ClO ₂	Cl ₂
Cl ₂ O	Cr	CrN	CrO
CrO ₂	CrO ₃	Cs	Cs ⁺
CsCl	CsF	CsO	CsOH
CsOH ⁺	Cs ₂	Cs ₂ Cl ₂	Cs ₂ F ₂
Cs ₂ O	Cs ₂ O ₂ H ₂	Cs ₂ SO ₄	Cu
Cu ⁺	CuCl	CuF	CuF ₂
CuO	Cu ₂	Cu ₃ Cl ₃	F
F ⁺	F ⁻	FCN	FO
FO ₂	F ₂	F ₂ O	F ₂ S ₂ , fluorodisu
Fe	Fe ⁺	Fe ⁻	FeC ₅ O ₅
FeCl	FeCl ₂	FeCl ₃	FeO
Fe(OH) ₂	Fe ₂ Cl ₄	Fe ₂ Cl ₆	H
H ⁺	H ⁻	HAIO	HBO
HBO ⁺	HBO ⁻	HBO ₂	HBS
HBS ⁺	HBr	HCN	HCO
HCO ⁺	HC ₂ N	HCl	HF
HI	HNC	HNCO	HNO
HNO ₂	HNO ₃	HOCl	HOF
HO ₂	HSO ₃ F	H ₂	H ₂ ⁺
H ₂ ⁻	H ₂ CO, formaldehy	HCOOH	H ₂ F ₂
H ₂ O	H ₂ O ⁺	H ₂ O ₂	H ₂ S
H ₂ SO ₄	H ₃ B ₃ O ₆	H ₃ F ₃	H ₃ O ⁺
(HCOOH) ₂	H ₄ F ₄	H ₅ F ₅	H ₆ F ₆
H ₇ F ₇	He	He ⁺	Hg
HgBr ₂	I	I ₂	K
K ⁺	KBO ₂	KCN	KCl
KF	KF ₂ ⁻	KH	KO
KO ⁻	KOH	KOH ⁺	K ₂
K ₂ C ₂ N ₂	K ₂ Cl ₂	K ₂ F ₂	K ₂ O ₂ H ₂
K ₂ SO ₄	Kr	Kr ⁺	Li
Li ⁺	LiAlF ₄	LiBO ₂	LiCl
LiF	LiFO	LiF ₂ ⁻	LiH
LiN	LiO	LiO ⁻	LiOH

LiOH ⁺	LiON	Li ₂	Li ₂ Cl ₂
Li ₂ F ₂	Li ₂ O	Li ₂ O ₂	Li ₂ O ₂ H ₂
Li ₂ SO ₄	Li ₃ Cl ₃	Li ₃ F ₃	Mg
Mg ⁺	MgBr	MgBr ₂	MgCl
MgCl ⁺	MgClF	MgCl ₂	MgF
MgF ⁺	MgF ₂	MgF ₂ ⁺	MgH
MgI	MgI ₂	MgN	MgO
MgOH	MgOH ⁺	MgO ₂ H ₂	MgS
Mg ₂	Mg ₂ F ₄	MoO ₃	Mo ₂ O ₆
Mo ₃ O ₉	Mo ₄ O ₁₂	Mo ₅ O ₁₅	N
N ⁺	N ⁻	NCO	NF
NF ₂	NF ₃	NH	NH ⁺
NHF	NHF ₂	NH ₂	NH ₂ F
NH ₃	NH ₂ OH	NH ₄ ⁺	NO
NO ⁺	NOCl	NOF	NOF ₃
NO ₂	NO ₂ ⁻	NO ₂ Cl	NO ₂ F
NO ₃	NO ₃ ⁻	NO ₃ F	N ₂
N ₂ ⁺	N ₂ ⁻	N ₂ C	N ₂ F ₂
N ₂ F ₄	N ₂ H ₂	NH ₂ NO ₂	N ₂ H ₄
N ₂ O	N ₂ O ⁺	N ₂ O ₃	N ₂ O ₄
N ₂ O ₅	N ₃	N ₃ H	Na
Na ⁺	NaAlF ₄	NaBO ₂	NaBr
NaCN	NaCl	NaF	NaF ₂ ⁻
NaH	NaI	NaO	NaO ⁻
NaOH	NaOH ⁺	Na ₂	Na ₂ C ₂ N ₂
Na ₂ Cl ₂	Na ₂ F ₂	Na ₂ O	Na ₂ O ₂ H ₂
Na ₂ SO ₄	Nb	NbO	NbO ₂
Ne	Ne ⁺	Ni	NiCl
NiCl ₂	NiO	NiS	O
O ⁺	O ⁻	OH	OH ⁺
OH ⁻	O ₂	O ₂ ⁺	O ₂ ⁻
O ₃	P	P ⁺	PCl ₃
PF	PF ⁺	PF ⁻	PF ₂
PF ₂ ⁺	PF ₃	PF ₅	PH
PH ₃	PO	PO ₂	P ₂
P ₄	P ₄ O ₁₀	Pb	PbBr
PbBr ₂	PbBr ₄	PbCl	PbCl ⁺
PbCl ₂	PbCl ₂ ⁺	PbCl ₄	PbF
PbF ₂	PbF ₄	PbI	PbI ₂
PbI ₄	PbO	PbS	Pb ₂

S	S ⁺	S ⁻	SCl
SCl ₂	SCl ₂ ⁺	SF	SF ⁺
SF ⁻	SF ₂	SF ₂ ⁺	SF ₂ ⁻
SF ₃	SF ₃ ⁺	SF ₃ ⁻	SF ₄
SF ₄ ⁺	SF ₄ ⁻	SF ₅	SF ₅ ⁺
SF ₅ ⁻	SF ₆	SF ₆ ⁻	SH
SN	SO	SOF ₂	SO ₂
SO ₂ ClF	SO ₂ Cl ₂	SO ₂ F ₂	SO ₃
S ₂	S ₂ Cl	S ₂ Cl ₂	S ₂ F ₂ , thiothiony
S ₂ O	S ₈	Si	Si ⁺
SiBr	SiBr ₂	SiBr ₃	SiBr ₄
SiC	SiC ₂	SiC ₄ H ₁₂	SiCl
SiCl ₂	SiCl ₃	SiCl ₄	SiF
SiF ₂	SiF ₃	SiF ₄	SiH
SiH ⁺	SiHBr ₃	SiHCl ₃	SiHF ₃
SiHI ₃	SiH ₂	SiH ₂ Br ₂	SiH ₂ Cl ₂
SiH ₂ F ₂	SiH ₂ I ₂	SiH ₃	SiH ₃ Br
SiH ₃ Cl	SiH ₃ F	SiH ₃ I	SiH ₄
SiI	SiI ₂	SiN	SiO
SiO ₂	SiS	Si ₂	Si ₂ C
Si ₂ N	Si ₃	Sr	SrBr
SrCl	SrCl ₂	SrF	SrF ⁺
SrF ₂	SrI ₂	SrO	SrOH
SrOH ⁺	SrO ₂ H ₂	SrS	Ta
TaO	TaO ₂	Ti	Ti ⁺
Ti ⁻	TiCl	TiCl ₂	TiCl ₃
TiCl ₄	TiO	TiOCl	TiOCl ₂
TiO ₂	V	VCl ₄	VN
VO	VO ₂	Xe	Xe ⁺
Zn	Zn ⁺	Zn ⁻	Zr
ZrN	ZrO	ZrO ₂	

B.1-2 Condensed Species

Al (<i>s</i>)	Al (<i>l</i>)	AlBr ₃ (<i>s</i>)	AlBr ₃ (<i>l</i>)
AlCl ₃ (<i>s</i>)	AlCl ₃ (<i>l</i>)	AlF ₃ (<i>s</i>)	AlF ₃ (<i>l</i>)
AlI ₃ (<i>s</i>)	AlI ₃ (<i>l</i>)	AlN (<i>s</i>)	Al ₂ O ₃ (<i>s</i>)
Al ₂ O ₃ (<i>l</i>)	Al ₂ SiO ₅ (<i>s</i>)	Al ₆ Si ₂ O ₁₃ (<i>s</i>)	B (<i>s</i>)
B (<i>l</i>)	BN (<i>s</i>)	B ₂ O ₃ (<i>l</i>)	B ₃ O ₃ H ₃ (<i>s</i>)
Ba (<i>s</i>)	Ba (<i>l</i>)	BaBr ₂ (<i>s</i>)	BaBr ₂ (<i>l</i>)

BaCl ₂ (s)	BaCl ₂ (l)	BaF ₂ (s)	BaF ₂ (l)
BaO (s)	BaO (l)	BaO ₂ H ₂ (s)	BaO ₂ H ₂ (l)
BaS (s)	Be (s)	Be (l)	BeAl ₂ O ₄ (s)
BeAl ₂ O ₄ (l)	BeBr ₂ (s)	BeCl ₂ (s)	BeCl ₂ (l)
BeF ₂ (l)	BeF ₂ (s)	BeF ₂ (l)	BeI ₂ (s)
BeI ₂ (l)	BeO (s)	BeO (l)	BeO ₂ H ₂ (s)
BeS (s)	Be ₂ C (s)	Be ₂ C (l)	Br ₂ (s)
Br ₂ (l)	Br ₂ (l)	C (s)	C ₆ H ₆ (l)
C ₇ H ₈ (l)	C ₈ H ₁₈ (l),n-octa	Ca (s)	Ca (l)
CaBr ₂ (s)	CaBr ₂ (l)	CaCO ₃ (s)	CaCl ₂ (s)
CaCl ₂ (l)	CaF ₂ (s)	CaF ₂ (l)	CaO (s)
CaO (l)	CaO ₂ H ₂ (s)	CaS (s)	CaSO ₄ (s)
Cr (s)	Cr (s)	Cr (l)	CrN (s)
Cr ₂ N (s)	Cr ₂ O ₃ (s)	Cr ₂ O ₃ (l)	Cs (s)
Cs (l)	CsCl (s)	CsCl (l)	CsF (s)
CsF (l)	CsOH (s)	CsOH (l)	Cs ₂ SO ₄ (s)
Cs ₂ SO ₄ (l)	Cu (s)	Cu (l)	CuF (s)
CuF ₂ (s)	CuF ₂ (l)	CuO (s)	CuO ₂ H ₂ (s)
CuSO ₄ (s)	Cu ₂ O (s)	Cu ₂ O (l)	Cu ₂ O ₅ S (s)
Fe (s)	Fe (l)	FeC ₅ O ₅ (l)	FeCl ₂ (s)
FeCl ₂ (s)	FeCl ₃ (s)	FeCl ₃ (l)	FeO (s)
FeO(l)	Fe(OH) ₂ (s)	Fe(OH) ₃ (s)	FeS (s)
FeS (l)	FeSO ₄ (s)	FeS ₂ (s)	Fe ₂ O ₃ (s)
Fe ₂ S ₃ O ₁₂ (s)	Fe ₃ O ₄ (s)	H ₂ O (s)	H ₂ O (l)
H ₂ SO ₄ (l)	Hg (s)	Hg (l)	HgBr ₂ (s)
HgBr ₂ (l)	HgO (s)	I ₂ (s)	I ₂ (l)
K (s)	K (l)	KCN (s)	KCN (l)
KCl (s)	KCl (l)	KF (s)	KF (l)
KHF ₂ (s)	KHF ₂ (l)	KOH (s)	KOH (l)
KO ₂ (s)	K ₂ CO ₃ (s)	K ₂ CO ₃ (l)	K ₂ O (s)
K ₂ O ₂ (s)	K ₂ S (s)	K ₂ S (l)	K ₂ SO ₄ (s)
K ₂ SO ₄ (l)	Li (s)	Li (l)	LiAlO ₂ (s)
LiAlO ₂ (l)	LiCl (s)	LiCl (l)	LiF (s)
LiF (l)	LiH (s)	LiH (l)	LiOH (s)
LiOH (l)	Li ₂ O (s)	Li ₂ O (l)	Li ₂ SO ₄ (s)
Li ₂ SO ₄ (l)	Li ₃ N (s)	Mg (s)	Mg (l)
MgAl ₂ O ₄ (s)	MgAl ₂ O ₄ (l)	MgBr ₂ (s)	MgBr ₂ (l)
MgCO ₃ (s)	MgCl ₂ (s)	MgCl ₂ (l)	MgF ₂ (s)
MgF ₂ (l)	MgI ₂ (s)	MgI ₂ (l)	MgO (s)
MgO (l)	MgO ₂ H ₂ (s)	MgS (s)	MgSO ₄ (s)

MgSO ₄ (<i>l</i>)	MgSiO ₃ (<i>s</i>)	MgSiO ₃ (<i>l</i>)	MgTiO ₃ (<i>s</i>)
MgTiO ₃ (<i>l</i>)	MgTi ₂ O ₅ (<i>s</i>)	MgTi ₂ O ₅ (<i>l</i>)	Mg ₂ SiO ₄ (<i>s</i>)
Mg ₂ SiO ₄ (<i>l</i>)	Mg ₂ TiO ₄ (<i>s</i>)	Mg ₂ TiO ₄ (<i>l</i>)	Mo (<i>s</i>)
Mo (<i>l</i>)	NH ₄ Cl (<i>s</i>)	Na (<i>s</i>)	Na (<i>l</i>)
NaAlO ₂ (<i>s</i>)	NaBr (<i>s</i>)	NaBr (<i>l</i>)	NaCN (<i>s</i>)
NaCN (<i>l</i>)	NaCl (<i>s</i>)	NaCl (<i>l</i>)	NaF (<i>s</i>)
NaF (<i>l</i>)	NaI (<i>s</i>)	NaI (<i>l</i>)	NaOH (<i>s</i>)
Na ₂ CO ₃ (<i>s</i>)	Na ₂ CO ₃ (<i>l</i>)	Na ₂ O (<i>s</i>)	Na ₂ O (<i>l</i>)
Na ₂ O ₂ (<i>s</i>)	Na ₂ S (<i>s</i>)	Na ₂ S (<i>l</i>)	Na ₂ SO ₄ (<i>s</i>)
Na ₂ SO ₄ (<i>l</i>)	Na ₃ AlF ₆ (<i>s</i>)	Na ₃ AlF ₆ (<i>l</i>)	Na ₅ Al ₃ F ₁₄ (<i>s</i>)
Na ₅ Al ₃ F ₁₄ (<i>l</i>)	Nb (<i>s</i>)	Nb (<i>l</i>)	NbO (<i>s</i>)
NbO (<i>l</i>)	NbO ₂ (<i>s</i>)	NbO ₂ (<i>l</i>)	Nb ₂ O ₅ (<i>s</i>)
Nb ₂ O ₅ (<i>l</i>)	Ni (<i>s</i>)	Ni (<i>l</i>)	NiS (<i>s</i>)
NiS (<i>l</i>)	NiS ₂ (<i>s</i>)	NiS ₂ (<i>l</i>)	Ni ₃ S ₂ (<i>s</i>)
Ni ₃ S ₂ (<i>l</i>)	Ni ₃ S ₄ (<i>s</i>)	P (<i>s</i>)	P (<i>l</i>)
P ₄ O ₁₀ (<i>s</i>)	Pb (<i>s</i>)	Pb (<i>l</i>)	PbBr ₂ (<i>s</i>)
PbBr ₂ (<i>l</i>)	PbCl ₂ (<i>s</i>)	PbCl ₂ (<i>l</i>)	PbF ₂ (<i>s</i>)
PbF ₂ (<i>l</i>)	PbI ₂ (<i>s</i>)	PbI ₂ (<i>l</i>)	PbO (<i>s</i>)
PbO (<i>l</i>)	PbO ₂ (<i>s</i>)	PbS (<i>s</i>)	PbS (<i>l</i>)
Pb ₃ O ₄ (<i>s</i>)	S (<i>s</i>)	S (<i>l</i>)	SCl ₂ (<i>l</i>)
S ₂ Cl ₂ (<i>l</i>)	Si (<i>s</i>)	Si (<i>l</i>)	SiC (<i>s</i>)
SiO ₂ (<i>l</i>)	SiO ₂ (<i>s</i>)	SiO ₂ (<i>l</i>)	Si ₂ N ₂ O (<i>s</i>)
Si ₃ N ₄ (<i>s</i>)	Sr (<i>s</i>)	Sr(<i>l</i>)	SrCl ₂ (<i>s</i>)
SrCl ₂ (<i>l</i>)	SrF ₂ (<i>s</i>)	SrF ₂ (<i>l</i>)	SrO (<i>s</i>)
SrO (<i>l</i>)	SrO ₂ H ₂ (<i>s</i>)	SrO ₂ H ₂ (<i>l</i>)	SrS (<i>s</i>)
Ta (<i>s</i>)	Ta (<i>l</i>)	TaC (<i>s</i>)	TaC (<i>l</i>)
Ta ₂ O ₅ (<i>s</i>)	Ta ₂ O ₅ (<i>l</i>)	Ti (<i>s</i>)	Ti (<i>l</i>)
TiC (<i>s</i>)	TiC(<i>l</i>)	TiCl ₂ (<i>s</i>)	TiCl ₃ (<i>s</i>)
TiCl ₄ (<i>l</i>)	TiN (<i>s</i>)	TiN (<i>l</i>)	TiO (<i>s</i>)
TiO(<i>l</i>)	TiO ₂ (<i>s</i>)	TiO ₂ (<i>l</i>)	Ti ₂ O ₃ (<i>s</i>)
Ti ₂ O ₃ (<i>l</i>)	Ti ₃ O ₅ (<i>s</i>)	Ti ₃ O ₅ (<i>l</i>)	Ti ₄ O ₇ (<i>s</i>)
Ti ₄ O ₇ (<i>l</i>)	V (<i>s</i>)	V (<i>l</i>)	VCl ₂ (<i>s</i>)
VCl ₃ (<i>s</i>)	VCl ₄ (<i>l</i>)	VN (<i>s</i>)	VO (<i>s</i>)
VO (<i>l</i>)	V ₂ O ₃ (<i>s</i>)	V ₂ O ₃ (<i>l</i>)	V ₂ O ₄ (<i>s</i>)
V ₂ O ₄ (<i>l</i>)	V ₂ O ₅ (<i>s</i>)	V ₂ O ₅ (<i>l</i>)	Zn (<i>s</i>)
Zn (<i>l</i>)	ZnSO ₄ (<i>s</i>)	Zr (<i>s</i>)	Zr (<i>l</i>)
ZrN (<i>s</i>)	ZrN (<i>l</i>)	ZrO ₂ (<i>s</i>)	ZrO ₂ (<i>l</i>)

تحريي لدراسة التوازنات الكيمياءوية المعقدة لخليط غازات نواتج الإحتراق

رسالة

مقدمة إلى كلية الهندسة في جامعة النهريين وهي جزء من
متطلبات نيل درجة دكتوراه فلسفة في الهندسة الكيمياءوية

من قبل

فائق حسام سري

بكالوريوس ١٩٩٧

ماجستير ٢٠٠٠

وذلك في

١٤٢٥ هـ

٢٠٠٤ م

شهر جمادى الأولى

الموافق حزيران

.

)

.

.(

%ì

%í

.